Université de Lomé

Universität Rostock

DRP-CCDRM

INTERNATIONAL MASTER PROGRAMME IN ENERGY AND GREEN HYDROGEN

SPECIALITY: Bioenergy, Biofuels and Green Hydrogen Technology

MASTER THESIS

Subject/Topic:

Biochar production from palm kernel shell as alternative catalyst for thermochemical hydrogen production

2023-2025

Presented on the 30th Day of September 2025

by:

Isaac S. WHULING, III

Exam Committee members:

Chair: Tizane DAHO, Professor, Université Joseph KI-ZERBO, Burkina Faso

Examiner/judge: Komlan Segbéya GADEDJISSO-TOSSOU, Associate Professor, Université de Lomé - Togo

Main Supervisor: Damgou MANI KONGNINE, Associate Professor, Université de Lomé – Togo

Co-Supervisor: Satyanarayana NARRA, Professor, University of Rostock - Germany

WASCAL West African Science Service Centre on Climate Change and Adapted Land Use

Federal Ministry of Research, Technology and Space

Dedication

This work is dedicated to my beloved mom, whose unwavering love, support, and encouragement have been my greatest inspiration. Thank you for believing in me.

Acknowledgements

I am sincerely grateful to the Funders – the Federal Ministry of Education and Research (BMBF) and WASCAL — for awarding me the scholarship that enabled this study. My heartfelt appreciation goes to the President of the University of Abdou Moumouni, Niamey, for their unwavering support throughout the first and second semesters, and for their continued commitment to academic excellence and institutional growth.

I also extend my sincere thanks to the Vice Chancellor of the University of Lomé, Prof. Adama Mawulé KPODAR, for providing a conducive academic environment during my third semester. The research stays in Germany were useful to my research and personal development. I am deeply thankful to the Rector of the University of Rostock, Prof. Dr. Elizabeth Prommer for offering such a valuable opportunity.

I wish to acknowledge Prof. Adamou Rabbani, WASCAL Director at the University of Abdou Moumouni, as well as Dr. Komi AGBOKA, WASCAL Director, and Dr. Komi BEGEDOU, WASCAL Deputy Director at the Université de Lomé, for their mentorship and guidance, which have played a vital role in shaping my academic path.

My deepest gratitude goes to my major supervisor, Dr. Damgou MANI KONGNINE, my co-supervisor, Prof. Dr. habil Satyanarayana Narra, and my daily supervisor Mr. Isaac Mensah (MSc) for their expert guidance, continuous encouragement, and unwavering support throughout my studies and research.

I am also thankful to the esteemed members of the jury for their time, feedback, and expertise during my defense, which greatly contributed to the enhancement of my work. I extend special thanks to the Director and the research team of the Department of Waste and Resource Management, University of Rostock, for providing a nurturing and collaborative learning environment.

Furthermore, I appreciate the hardworking team at AdFIS Product GmBH for the technical support and guidance in making my experiment a success. My special appreciation to Dr. Yoshiteru Nakawaga for giving me all the technical and expert advice during my experiment. A big thank you to the Board of the Fr. Thomas Hayden Liberia Scholarship Fund for the unwavering support during my stay in Germany.

Lastly, I would like to express my deep gratitude to my colleague, Faustina Asiedu for her immense support and to everyone who supported, encouraged, and inspired me throughout this journey. Your contributions have been invaluable. I am truly honored to have had your support and belief in me. You have been a driving force in my academic and personal growth, and I am eager to apply the knowledge and experiences gained to make a positive impact.

Thank you all.

Abstract

Palm kernel shell (PKS), an abundant agro-industrial residue, represents a largely underutilized biomass resource in West Africa despite its high fixed carbon content and structural properties that make it suitable for energy applications. While PKS has been studied for adsorbents, biofuels, and composites, its potential as a renewable catalyst in thermochemical hydrogen production remains underexplored. This study aimed to develop PKS-derived biochar and activated carbon as sustainable and cost-effective catalytic precursors for biomass gasification. The methodology adopted a two-stage approach: first, Box–Behnken Design (BBD) under Response Surface Methodology (RSM) was employed to optimize pyrolysis parameters (temperature, heating rate, and residence time) for biochar production. Then, the optimum biochar underwent steam activation under controlled conditions to enhance microporosity and catalytic properties. Proximate, elemental, physicochemical, and structural analyses were performed, including determination of fixed carbon, volatile matter, density, ash content, and iodine number. Results revealed that pyrolysis at 500 °C and 15 °C/min with a residence time of 60 min produced the optimum biochar (PKS-OP1) with high fixed carbon (77.1 wt%) and moderate porosity (iodine number: 155 mg/g). Subsequent steam activation transformed this biochar into a highly microporous activated carbon (PKS-Akt 280) with enhanced properties: iodine number of 885 mg/g, low volatile matter (~4 wt%), high fixed carbon (90 wt%), and pH ~10, demonstrating superior porosity, surface area, and thermal stability. Comparative analysis showed PKS-Akt 280 matches or outperforms some conventional catalysts, positioning it as a viable catalyst precursor. The study concludes that PKS-derived activated carbon offers an efficient, low-cost, and sustainable alternative to traditional metal-based catalysts for hydrogen production via gasification. It is recommended that further pilot-scale testing and industrial-scale process development be investigated to integrate PKS-biochar as a renewable catalyst pathway, contributing to waste valorization, cleaner hydrogen production, and the circular bioeconomy in palm-growing regions.

Key words: Palm kernel shell; biochar; activated carbon; catalyst; biomass gasification.

Résumé

La coque de palmiste (PKS), un résidu agro-industriel abondant, représente une ressource de biomasse largement sous-exploitée en Afrique de l'Ouest, malgré sa teneur élevée en carbone fixe et ses propriétés structurales qui la rendent adaptée aux applications énergétiques. Bien que la PKS ait été étudiée pour les adsorbants, les biocarburants et les composites, son potentiel comme catalyseur renouvelable pour la production thermochimique d'hydrogène reste sous-exploré. Cette étude a visé l'élaboration du biochar et du charbon actif dérivés de la PKS comme précurseurs catalytiques durables et rentables pour la gazéification de la biomasse. La méthodologie a adopté une approche en deux étapes: tout d'abord, la conception Box-Behnken (BBD) sous la méthodologie des surfaces de réponse (RSM) a été utilisée pour optimiser les paramètres de pyrolyse (température, vitesse de chauffe et temps de séjour) pour la production de biochar. Ensuite, le biochar optimal a été soumis à une activation à la vapeur dans des conditions contrôlées afin d'améliorer sa microporosité et ses propriétés catalytiques. Des analyses approximatives, élémentaires, physico-chimiques et structurales ont été réalisées, notamment la détermination du carbone fixe, des matières volatiles, de la masse volumique, de la teneur en cendres et de l'indice d'iode. Les résultats ont révélé que la pyrolyse à 500 °C à une cinétique de chauffage de 15 °C/min pour un temps de séjour de 60 min a produit le biochar optimal (PKS-OP1) avec un carbone fixé élevé (77,1 % en poids) et une porosité modérée (indice d'iode: 155 mg/g). Une activation ultérieure à la vapeur l'a transformé en un charbon actif hautement microporeux (PKS-Akt 280) avec des propriétés améliorées: indice d'iode de 885 mg/g, faible teneur en matières volatiles (~ 4 % en poids), carbone fixé élevé (90 % en poids) et pH ~ 10, démontrant une porosité, une surface spécifique et une stabilité thermique supérieures. Une analyse comparative a montré que le PKS-Akt 280 égale ou surpasse certains catalyseurs conventionnels, le positionnant comme un précurseur de catalyseur viable. L'étude conclut que le charbon actif dérivé du PKS offre une alternative efficace, économique et durable aux catalyseurs traditionnels à base de métaux pour la production d'hydrogène par gazéification. Il est recommandé d'étudier d'autres essais à l'échelle pilote et le développement de procédés à l'échelle industrielle afin d'intégrer le biochar PKS comme voie de catalyseur renouvelable, contribuant ainsi à la valorisation des déchets, à la production d'hydrogène plus propre et à la bioéconomie circulaire dans les régions productrices de palmiers à huile.

Mots clés: Coque de palmiste; biochar; charbon actif; catalyseur; gazéification de la biomasse.

Acronyms and abbreviations

ANOVA:	Analysis of Variance
APR:	Aqueous-Phase Reforming
APSR:	African Periwinkle Shell Residue
ASTM:	American Society for Testing and Materials
ATR:	Autothermal reforming
BET:	Brunauer-Emmett-Teller
BBD:	Box-Behnken Design
CEFIC:	European Chemical Industry Council
CPO:	Crude Palm Oil
DF:	Dilution Factor
DIN:	German Institute for Standardization (German: Deutsches Institut für Normung)
DOE:	Design of Experiment
EFB:	Empty Fruit Branches
EJ:	Exajoule
FC:	Fixed Carbon
HHV:	Higher Heating Value
HTL:	Hydrothermal Liquefaction
IEA:	International Energy Agency
ISO:	International Organization for Standardization
MC:	Moisture Content
MJ:	Mega Joule
MT:	Million Tons
NCG:	Non-Condensable Gases
NL:	Normal Liter
OSC:	Oxygen Storage Capacity
PET:	Polyethylene Terephthalate
PKS:	Palm Kernel Shell
PMF:	Palm Mesoderm Fibers
PP:	Polypropylene
PVC:	Polyvinyl Chloride
RSM:	Response Surface Methodology
SCWG:	Supercritical Water Gasification
SD:	Standard Deviation
SMR:	Steam Methane Reforming
SMSI:	Strong Metal-Support Interactions
SRF:	Solid Recovered Fuels

TGA:	Thermogravimetric Analysis
TOF:	Turn over frequency
USDA:	United States Department of Agriculture
VM:	Volatile Matter
VOC:	Volatile Organic Compounds
WGS:	Water-Gas Shift

List of tables

List of figures

Table of Contents

Introduction

Background of the Study

Biochar, a carbon-rich solid material (Kong et al., 2019) is produced via thermochemical conversion of biomass. Thermochemical conversion of biomass (pyrolysis, gasification, hydrothermal carbonization and torrefaction) refers to the process by which organic material is decomposed into different energy carriers or products such as biochar, biooil or syngas (Wang et al., 2023) by applying high temperature without the presence of oxygen or under oxygen limited environment (Iwuozor et al., 2023). Of these thermochemical pathways, pyrolysis is a promising process for optimizing biochar yield (Ahiekpor et al., 2023) while gasification for enhance syngas production, a hydrogen-rich gas (Rubinsin et al., 2024). The pyrolysis process is interesting for optimum biochar production because operational parameters like temperature, retention time and heating rate can be manipulated while subjecting biomass to high temperature in an oxygen-free environment to inhibit full combustion (Saleh et al., 2024).

Biochar has several environmental benefits and applications. One of the applications of biochar is its use as sorbent in biorefineries for gas cleaning (Shen et al., 2018). Moreover, biochar's environmental benefits include application in soil remediation and carbon capture and storage (Gui et al., 2025). Furthermore, recent studies have investigated the use of biochar as catalysts for biodiesel production (Akpasi, 2016) and catalysts support (Yao et al., 2016) in energy industries. Biochar is regarded as a key element in the energy transition by offering a way to decarbonize various sectors and reduce reliance on fossil fuels. According to Pelkmans (Pelkmans et al. 2024) the International Energy Agency (IEA) had speculated that a total of 100 EJ (exajoule) in energy would be provided in 2050 by biomass of which 60% would be obtained from biochar.

Consequently, the shift in paradigm towards global sustainable energy presents emerging challenges and diverse opportunities. Catalysts could serve as a key enabler in this transition by influencing process efficiency across the entire energy life cycle (Levin, 2023). Therefore, leveraging the diverse nature and application of biochar in the field of catalysis is essential in solving this puzzle. It is important to note that catalysts as a substance increase the rate at which a chemical reaction approaches equilibrium without being consumed permanently. Today, there are several types of catalysts used in energy industries to enhance production and to curtail environmental pollution. Study from Nwachukwu (Nwachukwu, 2024) categorized these catalysts to include homogenous catalysts (acid and base catalysts), heterogenous catalysts (metal-based catalysts, activated carbon), nanostructured catalysts (metal nanoparticle catalysts, carbon-based nanostructured catalysts) and biocatalysts (enzymes).

Biochar-based catalysts are heterogeneous catalysts derived from biomass sources, such as agricultural residues and municipal solid waste, through pyrolysis and subsequent activation via gasification using steam or CO_2. Palm kernel shell (PKS) is an abundant agricultural residual biomass of palm oil processing which can be converted into biochar via pyrolysis and activated for use as catalysts. Nowadays, almost all energy industrial applications ranging from petroleum refinery to thermochemical conversion predominantly rely on traditional catalysts

like metal-based materials. However, these catalysts are expensive, non-regenerative, and susceptible to deactivation due to tar formation (Hussain et al., 2023). In contrast, biochar-based catalysts derived from PKS offer a sustainable (Shakir et al., 2024), renewable, efficient and cost-effective alternative (Jagadale et al., 2025).

Using PKS as feedstock in a pilot gasification system (Pranolo et al. 2023), Pranolo demonstrated that produce fuel gas show combustible content which can be used to supply heat via direct combustion or generate electricity for fossil fuel substitution in internal combustion engine. Kostić studied the catalytic activities of PKS in biodiesel production using sunflower oil (Kostić et al. 2016). With 3 wt% deposition of the PKS catalysts in the reaction, the production of fatty acid methyl esters was 99% at 65ºC. The utilization of PKS was done by Yeboah (Yeboah et al., 2020) to fabricate Magnesium-biochar composites for hydrogen storage. The result of their study shows that when the palm kernel shell biochar concentration was increased from 5 wt% to 20 wt%, it improves the hydrogen sorption performance by converting Mg into MgH_2 roughly from 83% to 93%. Additionally, other studies show PKS used as feedstock can serve as a viable sustainable energy source. Kongto investigated pyrolysis and co-pyrolysis processes using PKS, PMF (palm mesoderm fibers) and empty fruit bunches (EFB) as feedstocks (Kongto et al., 2024). The results show that biochar derived from PKS proved to have higher energy content, larger porosity and higher surface area than the other feedstocks. These properties are interesting for making biochar from PKS not only as energy source but also as a strong catalysts support for metals. While PKS have been studied for fuels applications, absorption materials for hydrogen storage and catalyst for biodiesel production, its role in thermochemical hydrogen production remains underexplored. Therefore, this study addresses this gap by developing PKS biochar as a renewable catalyst to enhance hydrogen yield, reduce tar formation, and improve process sustainability. The novelty lies in leveraging PKS, an underutilized agro-industrial waste as a feedstock, optimizing pyrolysis conditions for catalytic performance, and integrating biochar catalyst into hydrogen production systems to advance waste-to-energy strategies.

Statement of the problem

The oil palm industry around the world generates a substantial amount of solid waste that relatively affect the environment due to lack of waste management strategies (Hosseini et al., 2015). Studies have shown that about 90% of biomass from palm trees is wasted while only 10% oil palm is converted to CPO (Babatunde et al., 2025; Hosseini et al., 2015; Nabila et al., 2023). The biomass composition breaks down as follows: 7% PKS residue, 23% EFB, 15% mesocarp fiber, and 45% combined oil palm fronds and trunks (Nabila et al., 2023).

Based on its high energy content and environmental sustainability, PKS is the most sorted out among all oil palm biomasses yet remained highly underutilized especially in West Africa. Countries like Indonesia and Malaysia as well as other semi industrialized countries utilized more than 80% of PKS biomass as industrial fuel in power plants and other industrial

applications (Pranolo et al., 2023; Zafar, 2024) while the remaining 20% are either dispose of in landfills or burned openly in air (Uchegbulam et al., 2022). Unlike these industrialized countries, almost all PKS biomass generated in CPO top producing countries in Africa (e.g. Nigeria, Ghana, Côte d'Ivoire) is not valorized. Despite its availability, a substantial fraction of this biomass is disposed in landfills or left in open fields, exacerbating environmental pollution. For instance, more than 2.5 million tonnes (MT) of PKS are generated annually in Nigeria and about 95% of this fraction is not utilized (Uchegbulam et al., 2022) thereby posing substantial threat to the environment through methane emission, a greenhouse gas.

Basically, applications of PKS from recent studies focus on its use as a feedstock for energy generation (Kongto et al., 2024), a low-cost adsorbent for wastewater treatment (Uchegbulam et al., 2022), and absorption material for hydrogen storage (Yeboah et al., 2020). However, its potential as a catalytic agent in thermochemical hydrogen production remains largely unexplored. Therefore, biochar-derived catalysts from PKS generated from CPO top producing countries as used in this study could probably help in mitigating biomass waste challenges, advancing cost-effective and sustainable alternatives to conventional fossil-based catalysts like nickel and platinum.

Objective of the study

The main aim of the study is to produce biochar using PKS as feedstock via pyrolysis and activate the PKS-derived biochar as precursor for hydrogen production.

The Specific objectives are:

i. To produce biochar from PKS via pyrolysis;
ii. To optimize PKS biochar production by investigating the effects of temperature, heating rate, and residence time;
iii. To activate the optimum biochar product;
iv. To characterize the physicochemical properties of produced PKS-biochar and PKS-activated carbon;
v. To study the use of PKS-biochar and PKS-activated carbon as precursor for hydrogen production via biomass gasification and evaluate its catalytic efficiency.

Research questions

i. How can biochar be produced from PKS via pyrolysis?
ii. What are the effects of temperature, heating rate, and residence time on the yield and quality of PKS-biochar?
iii. What activation parameters are most effective for enhancing the properties of PKS biochar?
iv. What are the key physicochemical properties of PKS-biochar and PKS-activated carbon, and how do these properties relate to potential catalytic performance?
v. How do the properties of PKS-biochar compare with those of PKS-activated carbon?

vi. Can PKS-biochar and PKS-activated carbon serve as effective precursors for hydrogen production through biomass gasification?
vii. What is the catalytic efficiency of PKS-derived biochar and activated carbon in enhancing hydrogen yield during gasification?

Significance of the study

The significance of this study is pillared on the investigation of the potential for PKS-derived biochar and PKS-activated carbon to serve as sustainable, and cost-effective catalysts in biomass gasification processes. These bio-based catalysts can improve syngas yield, reduce tar formation, and promote cleaner energy production, thereby contributing to more efficient and environmentally friendly biomass conversion technologies. Furthermore, utilizing PKS, an abundant agricultural residue, aligns with circular economy principles by valorizing waste materials into valuable energy catalysts. This approach not only reduces reliance on expensive and sometimes less sustainable metal catalysts but also offers a renewable alternative that supports energy transition goals. The application of these bio-derived catalysts has the potential to advance decentralized energy systems, promote sustainable biomass utilization, and reduce greenhouse gas emissions associated with traditional fossil fuel-based processes.

Research hypothesis

The research hypothesis is pillared on these principles:

I. The use of biochar produce from palm kernel shell as catalyst for biomass gasification will enhance hydrogen production.
II. PKS biochar catalyst is viable and efficient for thermochemical hydrogen production than metal-based catalysts.

Scope of the study

The scope of this present study encompasses a comprehensive investigation of PKS as a raw material for producing biochar and activated carbon through controlled pyrolysis and activation processes. It includes the optimization of pyrolysis conditions using statistical design methods, characterization of physicochemical properties such as moisture, volatility, pH, fixed carbon content, densities and iodine number, and evaluation of the resulting materials' catalytic potential in biomass gasification. The study further compares the performance and stability of PKS-activated carbon with conventional catalysts such as nickel-based catalysts, exploring their applicability as sustainable alternatives for tar cracking and syngas enhancement in energy conversion processes like gasification. Overall, the research aims to develop and validate bio-based catalyst materials that are economically viable, environmentally sustainable, and suitable for scalable biomass gasification applications.

Limitation of the study

This present study primarily focuses on PKS as feedstock without extensively investigating other biomass types or feedstock variations, which may influence the generalization of the findings. Additionally, the experimental conditions for pyrolysis and activation are conducted at laboratory scale, and challenges related to scaling up these processes for industrial applications remain unaddressed. For instance, the optimization and activation processes were conducted under controlled conditions that might differ from real-world operational environments. Characterization methods focused primarily on physicochemical properties; advanced catalytic testing under continuous gasification systems was outside the scope. Comparative analysis with conventional catalysts was based on literature data rather than direct experimentation. Finally, feedstock variability such as differences in PKS source and composition, which may impact the contextualize findings to other regions or processing plants. Furthermore, pilot-scale experimental application of biochar and activated as catalysts in biomass gasification was not performed. Additionally, the potential environmental impacts and lifecycle assessments of the biochar and activated carbon production processes are limited, necessitating further investigation for practical deployment.

Structure of the thesis

This current study is organized into three chapters and a preface. The preface highlights the background and context of the study. In this section, the research problems, research questions, objectives and hypothesis are well-defined and elaborated. Chapter 1 explored related literature focusing on PKS-derived biochar catalysts for thermochemical hydrogen production. It details the role of hydrogen in global energy transition, the various thermochemical pathways for hydrogen production like pyrolysis and gasification as well as the role of catalysts in these processes. Furthermore, PKS as a feedstock will be evaluated within this chapter and comparative efficiency of PKS biochar to traditional catalyst will be explored. Chapter 2 explored the materials and methods: feedstock collection, the technique of PKS biochar production through pyrolysis under varying conditions, how the characterization of the produced PKS biochar is performed, how activation and characterization of the biochar precursor and propose use of the PKS-biochar and PKS-activated carbon for biomass gasification. The last chapter (3) highlighted the results, the correlation between cause and effect, conclusion, and recommendation.

Chapter 1

Brief overview on catalysts and thermochemical conversion process of biomass

1.1 Introduction

This section offers an overview of the existing body of research and fundamental developments relevant to catalysis, biochar production through pyrolysis, and subsequent activation as a precursor for thermochemical hydrogen generation. It begins with an exposition of the broader context of catalysis, including an exposition of catalyst types, their applications within thermochemical processes for hydrogen production, along with an investigation of prevailing challenges and limitations, as well as recent advancements and knowledge gaps in the field.
Special emphasis is placed on the strategic utilization of PKS as a valuable feedstock for biochar synthesis, exploring relevant technologies and the critical process parameters influencing yield and quality. The primary aim of this review is to systematically survey, analyze, and synthesize scholarly sources to recognize relatable theories, methodologies, and research gaps.
Furthermore, the review systematically organizes and evaluates studies regarding catalyst types, process parameters such as temperature, heating rate, and residence time as well as activation techniques. It emphasizes the physicochemical characteristics of biochar-based catalysts, including surface area, porosity, and functional groups, and how these properties influence catalytic performance. Finally, this literature review contextualizes the current study by illustrating how it builds upon, diverges from, and contributes to the existing knowledge base. It underscores the research's motivation, outlining how it aims to address identified gaps and to advance understanding within this research domain.

1.2 Catalysts

1.2.1 Definition and Role in energy conversion

Catalysts are substances that increase the rate of a chemical reaction without being consumed in the process. This is possible when they act by lowering the activation energy, a barrier for reaction to proceed, thereby making the reaction faster and more efficient under favorable thermodynamics conditions (Kakaei et al., 2019). The reaction in which catalysts are used for chemical transformation is considered catalysis. During catalysis, the catalyst directs chemical reaction pathways with high selectivity ensuring that specific desired products are formed over unwanted byproducts, which is crucial for any chemical conversion process. Their unique ability to influence reaction pathways makes them vital in various energy conversion processes, ranging from fuel production to environmental remediation (Conceicao, 2024; Fornasiero, 2021). In modern energy systems, catalysts remain indispensable not only to refining conventional fossil fuels but also enabling the next generation of renewable energy technologies such as sustainable hydrogen production. For instance, conventional processes like catalytic cracking, hydrocracking, and reforming rely on solid acid catalysts and metal catalysts to break down large hydrocarbon molecules from crude oil into high-value products such as gasoline, diesel and jet fuel (Sadeghbeigi, 2020). As seen in the energy provide diagram (Fig. 1.1), a catalyst helps to open new reaction pathways by lowering the activation energy; hence,

efficiently converting reactants (X and Y) into suitable products (Z) which account for lower energy utilization than an uncatalyzed reaction.

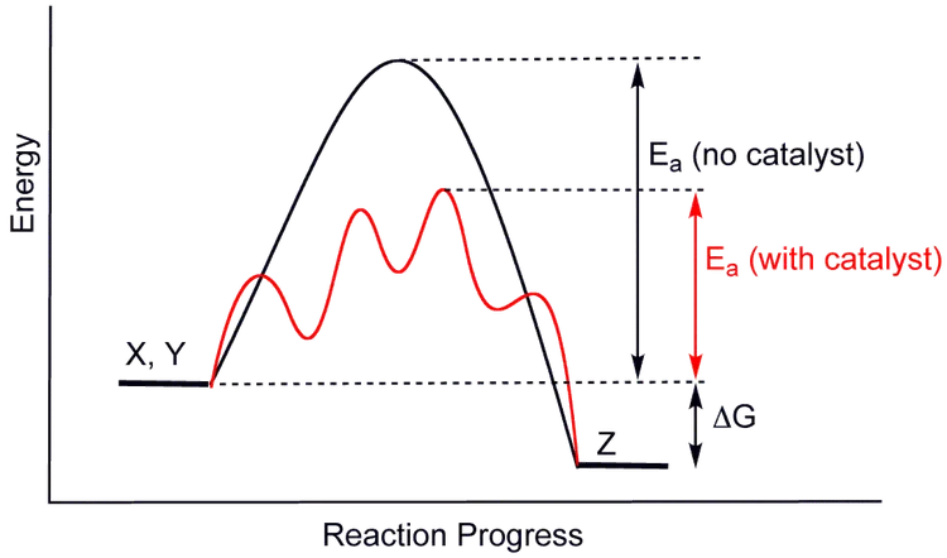

Figure 1.1: Energy profile diagram with catalyst; adapted from (Marras, 2010)

It is important to note that these processes would not have been possible without catalysts as they would require prohibitively high temperature and pressures thereby making them economically and environmentally unviable. Furthermore, catalytic converters in vehicles, containing platinum group metals, perform oxidation and reduction reactions to convert harmful exhaust pollutants such as CO, NO_x and unburnt hydrocarbons into less toxic gases like N_2 and H_2O (Della et al., 2011). As indicated, the importance of catalysts extends far beyond fossil fuels and is arguably even more critical for sustainable energy and the green energy transition.

Accordingly, catalysts are the enablers of the hydrogen economy. For example, on one hand, proton exchange membrane (PEM) electrolyzer requires traditional catalysts like iridium and platinum to efficiently split water into hydrogen and oxygen (Wei et al., 2017). The reverse process also utilizes platinum-based catalysts in Hydrogen Fuel Cells by combining hydrogen and oxygen to generate electricity with water as the only emission source (Debe, 2012). On the other hand, thermochemical processes like gasification and pyrolysis use catalysts for converting biomass or waste into syngas, bio-oil or biochar. During these processes, raw material like biomass or waste requires extensive catalytic upgrading for valorizing via reforming, water-gas shift reactions and deoxygenation. Nowadays, most hydrogen production methods or upgrading steps for chemicals and biofuels via thermochemical processes in large-scale industries utilize nickel-based and zeolite catalysts (Huber et al., 2006).

1.2.2 Types and classification of catalysts

Catalysts are universally classified based on their physical state and their relationship to the reaction phase they accelerate. This fundamental classification is critical as it dictates the catalyst's mechanism of action, its application, and the engineering design of the reactors that contain them. The selection and optimization of catalysts play a pivotal role in determining the efficiency and product distribution of thermochemical processes like pyrolysis and gasification or in biochemical conversion processes such as fermentation and anerobic digestion. Catalysts in biomass conversion are broadly categorized into three types: homogeneous, heterogeneous, and biocatalysts (Diallo et al., 2025), each with distinct mechanisms and applications. However, and due to the nature of the study, the discussion in this chapter will focus solely on homogenous and heterogeneous catalysts.

1.2.2.1 Homogenous catalysts

Homogeneous catalysts are typically molecular organometallic complexes or acids/bases dissolved in a solvent whereas the substrates for a reaction and the catalyst components are brought together in the same phase (van Leeuwen, 2003). In a well-defined solution, every catalyst molecule is identical and fully accessible to reactants, leading to exceptionally high selectivity and activity, often under milder reaction conditions (Kumar et al., 2022). In so doing, the process eliminates common issues like pore diffusion limitations, inactive internal sites, and catalyst sintering. The mechanism often involves the formation of a soluble intermediate complex, where the catalyst coordinates with the reactant, facilitates the reaction like C-C bond cleavage and water gas shift (WGS) reaction, and then regenerates itself (Crabtree, 2005). As stated, homogeneous catalysts can operate efficiently at relatively lower temperatures (65-100 °C), with remarkable catalytic turnover frequency (TOF), and can minimize production of catalyst poisoning and formation of impurities like CO; thereby, facilitating purer hydrogen streams critical diverse applications (Kumar et al., 2022).

1.2.2.1.1 Applications in Thermochemical Hydrogen Production

Recent advances extend to hydrogen production from biomass-derived substrates like glycerol and monosaccharides using homogeneous catalysis under relatively low temperature and pressure, expanding the feedstock base for renewable hydrogen (Cheng et al., 2022). These catalysts enable reforming reactions and hydrogen liberation via dehydrogenative transformations with high efficiency and selectivity. Electrochemical homogeneous catalysis represents an emerging approach combining redox catalysis with thermochemical pathways, potentially enabling energy-efficient hydrogen production integrated with renewable electricity sources (Cheng et al., 2022). Contemporary technologies include aqueous-phase reforming (APR), supercritical water gasification (SCWG) and liquid-phase reforming and dehydrogenation.

1.2.2.1.1.1 Aqueous-Phase Reforming (APR)

Homogeneous catalysts play a significant role in APR process for generating hydrogen from biomass-derived compounds (glycerol and sugars) via low temperatures and pressures. The mechanism involves two main reactions: reforming the substrate to produce CO and H_2, followed by WGS reaction converting CO and water into additional H_2 and CO_2 with minimization of methanation as side reactions due to controlled lower temperatures (Lakhtaria et al., 2023). Water soluble transitional metal complexes belonging to homogenous catalysis, have demonstrated high activity for the cleavage of C-C bonds and the promotion of WGS reaction which are critical for maximizing H_2 yield and minimizing CO production (King et al., 2010). Ciftci investigated APR of glycerol as a model compound for biobased feedstock using rhenium (Re) promotion for carbon-supported platinum (Pt) and rhodium (Rh) nanoparticles via homogenous catalysis (Ciftci et al. 2014). The findings indicate that the overall APR catalytic performance strongly correlates with the activity trend for the gas-phase WGS reaction whereas RhRe/C exhibited the highest activity for glycerol conversion rate and increased renewable hydrogen yield. Therefore, it is important to note that the homogeneous nature of the catalyst allows for efficient interaction with the aqueous feedstock to promote rapid reforming.

1.2.2.1.1.2 Supercritical Water Gasification (SCWG)

In SCWG, biomass is processed in water above its critical point using about temperature, 374 °C and pressure, 22.1 MPa (Demirel et al., 2021; Pinkard et al., 2019). Under these conditions, water becomes a unique solvent with high diffusivity and the ability to dissolve organic compounds and gases. Homogeneous alkali catalysts, such as potassium hydroxide (KOH), sodium carbonate (Na_2CO_3), and sodium hydroxide (NaOH), are highly effective in this environment. They effectively catalyze the reaction through ionic mechanisms, promoting the WGS reaction ($CO + H_2O \leftrightarrow CO_2 + H_2$) and enhancing the gasification rate, leading to higher hydrogen yields and lower char and tar formation (Pinkard et al., 2019). The catalyst is dissolved and uniformly distributed, ensuring excellent contact with the reacting species throughout the supercritical medium.

1.2.2.1.1.3 Liquid-Phase Reforming and Dehydrogenation

Certain homogeneous organometallic catalysts are exceptionally suitable for selective dehydrogenation reactions. Liquid-phase reforming and dehydrogenation are important catalytic processes for hydrogen production, particularly from oxygenated hydrocarbons derived from biomass and organic liquids. Pioneering work by Wang on so-called pincer complex considered as liquid organic hydrogen carriers often employs homogeneous iridium (Ir), or iron (Fe) complexes to catalytically release hydrogen from molecules like perhydro-dibenzofuran, perhydro-indole, N-methyl perhydro-indole among other molecules at moderate temperatures (Wang et al. 2011). These complexes show high activity for the release of hydrogen molecules within these compounds. While not a primary production method from raw

biomass, this application highlights the precise control that homogeneous catalysts offer for hydrogen release in integrated storage and production systems.

1.2.2.1.2 Challenges and Limitations of homogeneous catalysts

Despite their superior selectivity and activity, the industrial application of homogeneous catalysts in thermochemical processes faces series of challenges. One major drawback is catalyst separation and regeneration. Separating dissolved molecular catalysts from the complex product mixture often containing water, gases, and residual organics is energy-intensive and costly. Processes like distillation, extraction, or membrane filtration are required, which can degrade the catalyst or lead to irreversible loss (Cole-Hamilton, 2003; Marras, 2010). Another challenge falls in their thermal stability. For instance, many sophisticated organometallic complexes decompose at the high temperatures typical of conventional gasification (>700 °C), limiting their application to lower-temperature processes like APR and SCWG (Britovsek, 2012; Moccia et al., 2021). This issue makes homogenous catalyst unsuitable for precursors in thermochemical processes like biomass gasification or pyrolysis. Furthermore, the catalyst is sensitive to poisoning due to presence of uniform active sites. For example, sulfur, chlorine and other heteroatoms common in biomass feedstocks can coordinate strongly with the metal centers and permanently deactivate the catalyst (Crabtree, 2014). Finally, homogenous catalysts are cost intensive, making them economically unviable for large industrial applications. The most active catalysts often rely on expensive noble metals (Ru, Rh, Ir, Pt). Combined with potential loss during recovery, the overall process economics can become prohibitive for large-scale fuel production (Çapa et al., 2023).

1.2.2.1.3 Recent Advances and Strategies for application of homogenous catalysts

Research has focused on mitigating these challenges. A key strategy for mitigation is the devising of heterogenization of homogenous catalysts. This is a process whereby the molecule active site or complexes are anchored into solid supports like polymers, silica or carbon (T. Chen et al., 2023). The objective is to preserve the high selectivity of the molecular site while gaining the easy separability of a heterogeneous system (Lille-uccs et al., 2022). Furthermore, there is a drive to develop more robust and abundant non-noble metal catalysts, such as those based on iron or manganese, though their activities currently lag noble metal systems.

Future breakthroughs in catalyst control techniques and the development of cheap, stable, and poison-resistant molecular catalysts are essential to unlock the full potential homogenous catalysts. For now, their role remains confined to niche applications such as those of low temperature and pressure as well as where their superior performance can justify the added complexity and cost.

1.2.2.2 Heterogenous catalysts

Heterogenous catalysts are solid catalysts that exist in a phase separate from the reactants; hence, making their separation process easily from the reaction medium by filtration or centrifugation for regeneration or recycled (Çapa et al., 2023; Lille-uccs et al., 2022). Heterogeneous catalysts remain the cornerstone of large-scale thermochemical hydrogen production. Their inherent advantages range from ease in separation, robustness under high operating conditions to potential for regeneration thereby making them suitable for industrial applications. In the context of the green energy transition, developing efficient, stable, and cost-effective heterogeneous catalysts is paramount for solving sustainable hydrogen production from biomass and waste feedstock via processes like steam reforming and gasification. For instance, hydrogen production via thermochemical processes is a key route toward a sustainable hydrogen economy and heterogenous catalysis will play a central role in hydrogen generation from renewable resources like biomass.

1.2.2.2.1 Design and types of heterogenous catalysts

The efficient production of hydrogen via thermochemical pathways like steam reforming, gasification, and tar cracking is intrinsically linked to the performance of heterogeneous catalysts. These solid materials accelerate key reactions without being consumed, serving as the molecular engines that order process efficiency, product selectivity, and operational durability. The design of these catalysts is a sophisticated multi-scale endeavor, moving from the atomic-level composition of active sites to the macro-scale geometry structure. The types of heterogeneous catalysts discussed under this section focused on application in SMR and biomass gasification, the two dominant thermochemical routes to produce H_2. A modern heterogeneous catalyst is a composite material typically consisting of three key elements, active site, support and promoter (Santamaria et al., 2021). The active site is basically the component where the catalytic reaction occurs. This is typically a metal (Ni, Rh, Fe) or metal oxide responsible for bond breaking and formation (C-C cleavage, water dissociation). As it relates to the support, it is a high surface area material that anchors and disperses the active, preventing its sintering. Examples of common supports include γ-Al_2O_3, SiO_2, CeO_2 and activated carbon. The promoters are substances or additives release in trace quantities that enhance the performance, or selectivity of the catalysts. Examples of promoters include BaO in Ni/Al_2O_3 that improve the mechanical strength and thermal stability of the support, or chemical promoters (K, Ce) that modify the electronic structure of the active metal, suppressing carbon deposition or enhancing specific reaction pathways (Hutchings, 2001).

1.2.2.2.1.1 Nickel-Based Catalysts

Nickel-based catalysts are common industrial heterogeneous catalysts utilize for large-scale thermochemical hydrogen production, primarily due to their high activity for C-C and C-H bond cleavage and their favorable cost compared to noble metals (Helena et al., 2014). They

are the catalyst of choice for SMR, the dominant route for industrial H_2 production, and are extensively researched for biomass gasification and tar reforming.

The typical design consists of nickel nanoparticles (10-25 wt%) dispersed on a refractory oxide support, most commonly γ-Al_2O_3, chosen for its high surface area (Loviat et al., 2009). However, a major drawback of this combination is the formation of an inactive nickel aluminate spinel ($NiAl_2O_4$) at high temperatures and the acidic nature of Al_2O_3, which promotes carbon deposition (coking) through cracking reactions (Mohammad et al., 2010). To mitigate this, basic promoters like magnesium (MgO) or potassium (K) are added to neutralize acid sites and facilitate the gasification of surface carbon (Franz et al., 2021). A more advanced strategy involves using supports with high oxygen mobility, such as Ceria (CeO_2) or Ceria-Zirconia (CeO_2-ZrO_x) (Chaudhary et al., 2022). These materials provide lattice oxygen to actively remove carbon precursors from the nickel surface, creating a self-cleaning mechanism that improves catalyst, selectivity, longevity and activity (Siakavelas et al., 2021).

Despite these improvements, Ni catalysts remain highly susceptible to deactivation as a primary mechanism that challenges most industrial applications. Ongoing research focuses on designing more robust catalysts through alloying Ni with a second metal (Sn, Co) to geometrically dilute surface Ni sites and suppress coke formation or utilizing perovskite-type oxides such as $LaNiO_3$ as precursors that, upon reduction, yield highly dispersed and stable Ni nanoparticles anchored within a protective oxide matrix (Neagu et al., 2013).

1.2.2.2.1.2 Noble Metal Catalysts

Noble metal catalysts, primarily based on ruthenium (Ru), rhodium (Rh), platinum (Pt), and palladium (Pd), represent the high-performance scale in thermochemical hydrogen production. Despite their high cost, they are the subject of intense research due to their high activity, and selectivity for desired reactions, and remarkable resistance to deactivation mechanisms, a challenge for non-noble alternatives like nickel (Manfro et al., 2023; Santana Maldonado et al., 2023). Rhodium is often regarded as the most effective noble metal, particularly for steam reforming and tar cracking reactions. Roychowdhury (Roychowdhury et al. 2021) demonstrates that Rh as catalyst has an incomparable ability to cleave C-C bonds while minimizing the competitive methanation reaction ($CO + 3H_2 \rightarrow CH_4 + H_2O$), thereby maximizing yield. Furthermore, Rh exhibits a strong inherent resistance to carbon deposition (coking), as it is less prone to the formation of carbon filaments that encapsulate active sites. This is an important advantage when processing complex feeds like biomass-derived syngas, which is rich in tars and coke precursors (Ocsachoque et al., 2011). Ruthenium also shows excellent activity, especially for methane reforming, but can suffer from volatility under high-temperature oxidizing conditions (Su et al., 2024).

The high cost and low abundance of these metals require highly efficient designs. Research focuses on using very low loadings (<1 wt%) on advanced supports that provide strong metal-support interactions (SMSI). Reducible oxides like CeO_2 and CeO_2-ZrO_x are preferred supports.

They not only stabilize small metal nanoparticles against sintering but also actively participate in the reaction via their oxygen storage capacity (OSC), enabling the removal of carbonaceous deposits from the metal surface and thus enhancing stability (Navarro et al., 2007). While their expense currently impedes widespread industrial use in massive gasifiers, their superior performance makes them the catalyst of choice for applications where reliability and compactness are paramount over raw cost, such as in small-scale and distributed reforming units for fuel cell systems. Their role is also indispensable in fundamental research, where they serve as a model system to understand reaction mechanisms and to set performance targets for developing cheaper, non-noble catalysts (Ruocco et al., 2020).

1.2.2.2.1.3 Non-Nickel and Non-Noble Metal Catalysts

The search for cost-effective and abundant alternatives to nickel and noble metals has driven significant research into non-nickel, non-noble metal catalysts for thermochemical hydrogen production. This category primarily encompasses catalysts based on iron (Fe), cobalt (Co), copper (Cu), and molybdenum (Mo), often derived from inexpensive minerals or waste streams, aligning with the economic and sustainability goals of biomass conversion (Dong et al., 2025; Kumar et al., 2025). Among these, cobalt-based catalysts are the most prominent, offering a balance between activity and stability. Cobalt shares many catalytic properties with Ni, demonstrating high activity for tar reforming and the WGS reaction. Furthermore, Co often exhibits a lower tendency for carbon filament growth compared to nickel, as it has a lower solubility for carbon, making it more resistant to deactivation by coking (Bahari et al., 2022). However, its higher cost and tendency to oxidize under certain conditions remain challenges.
Furthermore, Iron-based catalysts are another major focus due to their extreme low cost and natural abundance. Iron is highly active for the WGS reaction and can be effective for tar cracking, particularly when promoted with other metals. Its primary drawback is a lower overall reforming activity compared to Ni or Co and a susceptibility to oxidation, which can deactivate the metallic phase essential for catalysis (Pinilla et al., 2011).
Other metals like copper are primarily important for their excellent activity in the low-temperature WGS reaction but lack the stability for high-temperature reforming due to severe sintering. Molybdenum and tungsten carbides are also investigated as platinum-like catalysts due to their ability to facilitate similar reactions, though they can be sensitive to oxidation (Y. Zhao et al., 2025). The performance of all these catalysts is greatly enhanced by strategic formulation, including using basic supports such as MgO and CaO to adsorb CO_2 and suppress coke, or combining them in bimetallic systems (Fe-Co) to synergistically improve activity and stability. Some inexpensive natural minerals like dolomite ($CaMg(CO_3)_2$) and olivine ($(Mg,Fe)_2SiO_4$) are widely used as primary bed materials for initial cracking. These materials are normally prepared through calcination to convert carbonates to active oxides (CaO, MgO). While these materials are cost-effective and easily disposable, their activity is moderate, and they usually suffer from rapid attrition or physical breakdown (Devi et al., 2003).

1.2.2.2.1.4 Carbonaceous catalysts

Carbonaceous catalysts specifically refer to carbon-based solid materials used as catalysts or catalysts support in heterogeneous catalysis. Examples include activated carbon, carbon nanotubes, graphene, carbon black, and biochar (Lam & Luong, 2014; Serra et al., 1997). These carbon materials are often used to support metal nanoparticles (Ni, Co, Fe) or act as catalysts due to their unique surface properties, high surface area, and chemical stability (Bitter, 2023). They promote reactions such as hydrogenation, reforming, and oxidation by providing active sites and facilitating electron transfer. The focus of this paper will be placed on biochar and activated carbon as sustainable carbonaceous catalysts for thermochemical processes.

Biochar-based catalyst and activated carbon

Biochar can be modified or combined with catalytic active species and can serve as an effective catalyst or catalyst support for various environmental and chemical processes, including pollutant degradation, biomass conversion, and energy production (Cao et al., 2017). The catalytic performance of biochar is largely influenced by its surface chemistry, porosity, and the presence of specific functional groups, which can be enhanced through various activation methods. Activation methods for biochar can be broadly categorized into physical and chemical approaches. Physical activation involves treatments such as steam or carbon dioxide activation at high temperatures, which enhance surface area, develop pore structures, and generate oxygen-containing functional groups (Sakhiya et al., 2020). This process though does not pose any environmental risk, but associated issues is its energy intensity since the process occur within higher temperature range (Shahcheragh et al., 2023). Chemical activation, on the other hand, employs activating agents like potassium hydroxide (KOH), phosphoric acid (H_3PO_4), or zinc chloride ($ZnCl_2$), which not only increase porosity but also introduce active sites conducive to catalytic reactions (Molina-Sabio et al., 2004). For instance, KOH activation typically results in biochar with a high surface area and enhanced microporosity, beneficial for adsorption and catalytic applications. However, the main drawbacks of chemical activation of biochar include environmental and health concerns associated with the use of activating agents such as KOH, H_3PO_4, and $ZnCl_2$, which can produce hazardous waste residues requiring proper disposal (Debbache et al., 2024). Additionally, chemical activation often involves the use of concentrated acids or bases, which pose safety risks during handling and processing. The process can also be more costly due to the need for chemical reagents and subsequent washing or neutralization steps to remove residual chemicals, potentially leading to higher operational expenses and environmental impacts (Sajjadi et al., 2019). Moreover, residues of activating agents may interfere with subsequent applications of the biochar, such as in catalytic activities or soil amendment, if not thoroughly removed.

In contrast, biochar-based catalysts are gaining interest owing to their renewable nature, high surface area, porosity, and functional groups conducive to catalytic activity (Daabo et al., 2022). Several studies demonstrate that biochar derived from biomass can serve as a catalyst or catalyst

support in hydrogen production. For instance, Frainetti found that nickel-loaded biochar showed comparable activity to conventional Ni-based catalysts in dry reforming of methane (59% yield), with the added benefit of enhanced stability due to biochar's porous structure and surface functionalities (Frainetti et al. 2024). This suggests biochar can act as a sustainable support material, reducing catalyst deactivation. Moreover, biochar's inherent properties, such as high thermal stability and potential for functionalization, enable its application directly as an active catalyst or as a support modified with metal nanoparticles. Huang reported that biochar supported Ni catalysts exhibited improved performance and durability in thermochemical water splitting compared to unmodified biochar, emphasizing its potential as a cost-effective and environmentally friendly alternative (Huang et al. 2023). However, challenges remain in optimizing biochar's catalytic activity, durability, and scalability. Unlike traditional catalysts, biochar's properties depend heavily on feedstock type and pyrolysis conditions, leading to variability in catalyst performance (Amalina et al., 2022). Furthermore, biochar's catalytic mechanisms are less understood and require further research to improve activity, selectivity, and lifespan in industrial applications.

Surface area

Surface area is a critical parameter determining the adsorption capacity and reactivity of biochar and activated carbon. Both materials are porous carbons with high surface areas, but their preparation methods significantly influence these properties (Rostamian et al., 2015). Typically, the surface area is measured using nitrogen adsorption-desorption isotherms and calculated via BET theory (Zulkania et al., 2018). Activated carbon generally exhibits higher surface areas often exceeding 1000 m^2/g due to chemical or physical activation processes that develop porosity (G. Li et al., 2023). Biochar, produced under pyrolysis conditions with less intensive activation, typically has lower surface areas, usually between 50 and 500 m^2/g (McLaughlin et al., 2012). Despite the importance of surface area, there are notable gaps in standardization and understanding. Variability in measurement conditions such as adsorption temperature, gas adsorption time, and the type of adsorbate can lead to inconsistent results (Sabitha et al., 2025). Furthermore, surface area alone does not fully explain adsorption performance; pore size distribution and surface chemistry also play pivotal roles. For instance, micropores are primarily responsible for low-molecular-weight compound adsorption, while mesopores assist in the transport of larger molecules. Additionally, surface functional groups influence adsorption affinities, which surface area measurements do not capture comprehensively.

Porosity

Porosity is a vital characteristic that determines the adsorption capacity and reactivity of biochar and activated carbon, influencing their effectiveness in environmental remediation and energy storage applications as well as catalysis (Choi et al., 2023). Both materials possess classified

porous structures, including micropores (<2nm), mesopores (2-50 nm), and macropores (>50 nm), which collectively influence their performance (Yalçin & Sevinç, 2000). Activated carbon typically exhibits a higher degree of porosity and a greater proportion of micropores due to chemical or physical activation processes designed to develop internal pore networks (P. Kumar et al., 2022; Ogungbenro et al., 2018; W. Shen et al., 2003). In contrast, biochar's porosity largely depends on feedstock type and pyrolysis conditions, leading to variability in pore size distribution and volume (Muzyka et al., 2023). Despite its significance, a key gap in current knowledge involves the precise control and quantification of pore structure during biochar production, which affects its adsorption efficiency and functional applications (Leng et al., 2021).

Functional groups

The surface chemistry of biochar and activated carbon is characterized primarily by the presence of various functional groups, which significantly influence their adsorption properties and reactivity. Both materials typically contain oxygen and hydrogen containing groups such as hydroxyl (-OH), carbonyl (C=O), carboxyl (-COOH), and phenolic groups (Dong et al., 2024), which can interact with contaminants through various mechanisms, including hydrogen bonding, electrostatic attraction, and chemical reactions (Chen et al., 2024). The abundance and types of functional groups are highly dependent on pyrolysis and activation conditions; for instance, higher pyrolysis temperatures tend to decrease oxygen-containing groups, leading to a more hydrophobic surface (Adhikari et al., 2022; M. Zhang et al., 2022). Conversely, activation methods can introduce or enhance specific functional groups to improve adsorption capacity for pollutants such as heavy metals or organic compounds (Dong et al., 2024). The presence of acidic functional groups like carboxyl and phenolic groups is particularly relevant for metal binding (Ilić et al., 2022), while hydroxyl groups can facilitate interactions with organic molecules (S. Zhang et al., 2022).

1.2.2.2.2 Applications of heterogenous catalysts in thermochemical hydrogen production

Heterogeneous catalysts play a crucial role in thermochemical processes aimed at sustainable hydrogen production, such as steam reforming, gasification, and pyrolysis. These catalysts, typically solid materials like nickel, noble metals, nonnoble metals and carbonaceous supported on carriers such as alumina or biochar, facilitate key reactions by providing active sites that lower activation energies and improve reaction rates (Akhtar et al., 2025; Kakaei et al., 2019; Niu et al., 2023). Primary thermochemical methods for hydrogen production include SMR, autothermal reforming (ATR) and biomass gasification. Each process involves catalyzed reactions involving heterogeneous catalysis to convert hydrocarbons or biomass-derived oxygenates into hydrogen-rich syngas or pure hydrogen streams. Among these processes, SMR is the most established method which typically utilizes natural gas (CH_4) as feedstock. The reaction involving steam reforming is highly endothermic and requires a catalyst to proceed at

viable rates and temperatures. Also, the catalysts will facilitate the subsequent WGS reaction to maximize hydrogen yield and reduce CO content (Szablowski et al., 2025).

Thus, SMR technologies utilize nickel-based catalysts as predominantly material to convert methane into hydrogen and carbon monoxide; however, their susceptibility to sintering and coke deposition challenges long-term stability (Ochoa et al., 2018). Recent studies focus on developing robust biochar-supported nickel or iron catalysts derived from agricultural residues, offering cost-effective and sustainable alternatives with enhanced stability and activity (Cheng et al., 2018).

On the other hand, biomass gasification remains another important technology for converting solid biomass into syngas by reacting it with a controlled amount of oxygen and/or steam at high temperature (800 – 1000 ℃). The raw syngas contains significant quantities of tar which is a complex hydrocarbons; hence, the process normally requires catalytic reforming to crack them for enhancing syngas yield and preventing downstream operational issues (Sutton et al., 2001). To this effect, catalysts such as nickel, cobalt, and noble metals are employed to facilitate the reforming of volatile compounds released during thermal decomposition of biomass (Niu et al., 2024). Furthermore, innovations include doped or nanostructured catalysts to improve resilience against thermal and coking deactivation. Despite their advantages, catalyst deactivation remains a key challenge, necessitating ongoing research into regeneration strategies and durable catalyst formulations to enable scalable hydrogen production via thermochemical pathways.

1.2.2.2.3 Challenges and Limitations of heterogenous catalysts

Heterogeneous catalysts are vital for numerous industrial processes, including energy conversion and environmental remediation; however, their application is often hindered by several significant challenges. One primary concern is catalyst deactivation, which can occur via sintering, coking, poisoning, or surface corrosion, leading to loss of active surface area and reduced activity over time (Naji et al., 2021). Sintering, driven by high operational temperatures, causes particle agglomeration, diminishing catalytic sites. Coking and poisoning from sulfur, nitrogen, or other contaminants result in surface fouling, necessitating regeneration or replacement strategies that increase operational costs (Lin et al., 2022).

Another limitation involves the complex synthesis and stability of nanostructured or doped catalysts designed for enhanced activity, which can be sensitive to process conditions and difficult to scale up. Additionally, the selectivity of heterogeneous catalysts can be challenging to control, potentially leading to undesired by-products or incomplete conversions. Mass transfer limitations hinder optimal contact between reactants and active sites, especially in thick catalyst beds or when dealing with viscous feeds, thereby reducing efficiency (Wu et al., 2019). Addressing these challenges requires ongoing research into catalyst stability, regeneration techniques, and design innovations to develop durable, cost-effective catalysts suitable for long-term industrial operation.

1.2.2.2.4 Recent Advances and Strategies for application of heterogenous catalysts

Recent developments in heterogeneous catalysis have focused on enhancing catalytic activity, stability, and selectivity to meet the demands of contemporary industries basically involving sustainable energy and environmental applications. For instance, the development of nano-structural catalysts have emerged as a key strategy, enabling high surface area and tailored active sites that improve reaction efficiency, as exemplified by the deployment of metal nanoparticles supported on various substrates (Cheng et al., 2018). Surface modification techniques, such as doping with heteroatoms or functional groups, have been used to fix acidity, basicity, and electronic properties, thereby optimizing catalytic performance in processes like biomass conversion and carbon dioxide reduction (Venezia et al., 2022).

Another notable development involves fabrication of bifunctional and multifunctional catalysts that can facilitate multi-step reactions, reducing operational complexity and costs. The integration of catalysts within flow microreactors, coupled with in situ spectroscopic techniques, allows for real-time monitoring and improved process control, leading to process intensification (Gross et al., 2014). Furthermore, strategies to improve catalyst durability such as sintering resistance and facile regeneration are being actively pursued through novel supports and core-shell architectures. These innovations collectively push the limit toward more efficient, cost-effective, and environmentally benign catalytic systems for applications ranging from clean energy production to pollutant reduction.

1.3 Biochar production technologies

Biochar production technologies encompass various methods aimed at converting biomass into stable carbon-rich materials with enhanced physicochemical properties (Phadtare et al., 2022). These technologies typically involve thermal processes such as pyrolysis slow, carbonization, gasification, and torrefaction each influencing the characteristics of the resulting biochar (Zhu et al., 2025). Recent advancements include microwave-assisted pyrolysis, which promotes uniform heating and efficient energy utilization (Zulkornain et al., 2021), and co-pyrolysis with different feedstocks to improve biochar quality (Faris et al., 2023). The selection of feedstock, temperature, heating rate, and residence time critically influence the biochar's chemical, physical, and functional properties such as surface area, porosity, and carbon stability (Sharma et al., 2024). Biochar production technologies continue to evolve toward more efficient, scalable, and environmentally sustainable methods, addressing waste management and contributing to carbon sequestration and soil enhancement in circular bioeconomy frameworks.

1.3.1 Pyrolysis (slow pyrolysis)

Slow pyrolysis is a thermal decomposition process of biomass conducted at relatively low heating rates, typically between 1 to 10°C per minute, and at moderate temperatures ranging from 400 to 700°C (Cai et al., 2020). This method emphasizes maximizing char production while minimizing gaseous and liquid yields (J. Li et al., 2024), making it particularly suitable

for biochar generation. The process occurs under limited or oxygen-free conditions, leading to thermal stability and enhancing carbon features characteristic of biochar.

Research indicates that slow pyrolysis parameters such as temperature, residence time, feedstock type, and moisture content substantially influence the physicochemical properties of the resulting biochar (Sakhiya et al., 2020). Higher pyrolysis temperatures generally increase fixed carbon content and aromaticity, enhance surface area, and improve stability, making biochar more effective for soil amendment and carbon sequestration applications (Shyam et al., 2025). Conversely, lower temperatures tend to retain more volatile matter (VM) and functional groups beneficial for nutrient retention and microbial activity.

Moreover, the composition and structure of biochar produced by slow pyrolysis are highly dependent on feedstock properties, including lignocellulosic content, ash, and elemental composition. For instance, woody biomass tends to yield biochar with higher carbon content and porosity compared to agricultural residues or manure. The slow pyrolysis process also allows for greater control over biochar characteristics, which can be tailored for specific purposes such as pollutant adsorption, soil fertility enhancement, or energy recovery.

Research advances focus on optimizing process conditions to maximize desirable biochar properties while minimizing environmental impacts. Techniques such as precursor pretreatment and post-pyrolysis activation are also explored to enhance surface functionalities and porosity. Overall, slow pyrolysis remains a versatile and widely studied technology for sustainable biomass utilization, particularly in producing stable biochar for climate change mitigation and soil improvement.

1.3.2 Carbonization

Carbonization is a thermochemical process that transforms organic material, such as biomass, into carbon-rich products like biochar, charcoal, or activated carbon (Chiaramonti et al., 2014; Rima et al., 2013). This process typically involves heating the feedstock in an oxygen-limited environment, leading to the thermal decomposition of volatile components and the concentration of fixed carbon content in the remaining solid material (Chiaramonti et al., 2014). The primary motivation for carbonization includes soil amendment, carbon sequestration, and the production of activated carbon for adsorption applications (Karume et al., 2023) and important energy source in Sub-Saharan Africa (Schure et al., 2019). Key parameters influencing carbonization efficiency and product quality include temperature, residence time, feedstock type, and moisture content (Köhler et al., 2017). Feedstock properties such as lignin, cellulose, and hemicellulose content affect the quality and characteristics of the resulting char, emphasizing the importance of feedstock selection and pre-treatment (Lu et al., 2014).

While carbonization is a promising technology for biomass valorization and climate mitigation, a deeper understanding of process parameters, feedstock variability, emission controls, and long-term impacts is essential for broader application and optimization.

1.3.3 Gasification

Gasification is a thermochemical process that converts carbonaceous feedstocks, such as biomass and coal, into syngas (H_2, CO, CO_2, CH_4) by reacting the material at high temperatures under controlled oxygen or air supply (Jafri et al., 2020). This technology is recognized for its potential in producing renewable energy, chemicals, and liquid fuels, contributing sustainable process and waste valorization (Hrbek et al., 2021).

Several critical parameters influence gasification efficiency and syngas quality. Key among these are temperature, pressure, and the equivalence ratio – the ratio of oxygen supplied to the stoichiometric requirement (Ammar et al., 2016). Higher temperatures, typically exceeding 800°C, favor complete carbon conversion and influence the proportions of syngas constituents, especially enhancing hydrogen and carbon monoxide production (Kalivodová et al., 2022). Operating pressure impacts residence time and gas flow dynamics, with elevated pressures generally improving throughput and conversion efficiency (Q. Wang et al., 2023).

Moreover, feedstock properties, including moisture content, particle size, and ash content, significantly affect the gasification process. High moisture content can lead to lower thermal efficiency due to energy consumption in moisture evaporation (C. Lin et al., 2023), while ash can cause slagging and fouling (Moilanen et al., 2011), impacting reactor integrity and operational stability. Understanding and controlling these parameters are essential for optimizing process performance.

Furthermore, environmental impacts, such as emissions from tars and particulates (Preetha Devi et al., 2017), remain areas of concern, highlighting the need for improved emissions control technologies. In conclusion, while gasification holds promise as a sustainable energy pathway, addressing key gaps related to process parameters, feedstock variability, and by-product management is essential for enhancing efficiency and commercial viability.

1.3.4 Torrefaction

Torrefaction is a thermal treatment process use to produce solid biofuels occurring at temperature range 200 – 300°C and resident time of 15 – 60 mins (Miguel et al., 2018; Ong et al., 2019). Torrefaction is usually deployed as a treatment technique to promote the energy quality (Miguel et al., 2018) and remove moisture and volatiles matter (Ong et al., 2019) from organic material which makes it suitable for combustion in energy generating industries. Recent studies have revealed that biochar resulting from torrefaction contain high heating value and energy yield (Chen et al., 2015).

1.4 Conclusion

Catalysts, in general, are essential materials that accelerate chemical reactions without being consumed, and they are vital across a wide range of industrial and environmental applications. These can be broadly categorized into homogeneous and heterogeneous catalysts, with the latter being more favored in thermochemical processes due to their ease of separation and recyclability. Common types include metal-based (such as nickel, platinum, and iron), metal oxide, and biochar-supported catalysts. In thermochemical processes like pyrolysis, gasification and reforming, catalysts facilitate conversion reactions by enhancing efficiency, selectivity, and process sustainability. Recent advances emphasize the development of biochar-based catalysts, which leverage the structural properties of biochar derived from biomass sources. These catalysts exhibit high surface area, porosity, and functional groups conducive to catalytic activity, especially when supporting active metals like nickel. When used in reforming processes, biochar-supported catalysts demonstrate performance and stability comparable to or exceeding that of conventional metal catalysts, partly due to their resistance to sintering, poisoning, and deactivation mechanisms.

Despite promising results, significant challenges remain. Variability in biochar properties which can be affected by feedstock type and pyrolysis conditions pose scalability issues. Furthermore, limited understanding of the detailed catalytic mechanisms can hinder further optimization. Additional limitations include mechanical durability, thermal stability, and the economic feasibility of large-scale deployment. Overall, the literature suggests that biochar-derived catalysts have substantial potential to support sustainable hydrogen production and other thermochemical conversions, but addressing these challenges through comprehensive research, process integration, and technological innovation is vital for their broader adoption in industry. This evolving field signals a transition toward environmentally friendly, cost-effective catalytic systems aligned with the global pursuit of clean energy solutions.

Chapter 2

Methodology and experimental techniques

2.1 Introduction

The characterization of biochar and biochar-based catalysts is essential to understand their physicochemical properties, which directly influence their performance in environmental and catalytic applications. Common analytical techniques include proximate and ultimate analyses, Brunauer-Emmett-Teller (BET) surface area measurement and porosity, Fourier-transform infrared spectroscopy (FTIR), etc. BET analysis or iodine number provides insights into surface area and porosity, critical factors for catalytic activity, while SEM reveals morphological features. Also, FTIR detects functional groups that influence reactivity and adsorption capacity. In this study, the methodology outlines a systematic approach to optimizing the preparation of activated carbon from PKS via a two-stage experimentation. Initially, PKS underwent slow pyrolysis under varying conditions (temperature, heating rate, and residence time) using a Box-Behnken Design (BBD) to identify optimal pyrolysis parameters that yield high-quality biochar. The process parameters were experimentally varied at predetermined levels to evaluate their effects on biochar properties. Subsequently, the obtained biochar was subjected to steam activation at high temperatures (800 - 900°C) to enhance porosity and surface characteristics. This step aimed to produce a highly microporous activated carbon with improved physicochemical properties suitable for catalytic applications. The characterized materials were then analyzed using techniques such as iodine adsorption number, and other physicochemical assessments (volatile matter, ash content, fixed carbon, densities, and pH) to determine their suitability as catalyst precursors in biomass gasification processes.

2.2 Materials

2.2.1 PKS as Feedstock

Palm Kernel Shell (PKS), a byproduct of oil palm processing, has gained significant attention as a sustainable and economical feedstock to produce various solid biofuels (biochar and activated carbon). Its abundance, high carbon content, and favorable physicochemical properties make it an attractive material for various environmental and energy applications. The increase of oil palm plantations, particularly in Southeast Asia and parts of Africa, has resulted in large quantities of PKS as agro-industrial waste. For instance, the total plantation area in Indonesia has grown from 8.4 million hectares in 2010 to over 12 million hectares by 2017 resulting in substantial biomass residues such as PKS in major producing provinces like Riau and North Sumatra (Rahayu et al., 2018). Similarly, expansion of industrial oil palm plantations in Africa similarly contributes to significant agro-industrial waste generation (Carrere, 2013), including PKS. PKS is characterized by high lignocellulosic content, with considerable amounts of cellulose, hemicellulose, and lignin, which influence its thermal decomposition and carbonization behavior (Boonsombuti et al., 2023; Rashid et al., 2018). Its relatively high fixed carbon and low or no sulfur content (Kpelou et al., 2018) also reduce the risk of undesirable emissions during thermal processing. Biochar derived from PKS has been extensively studied

due to its potential for soil amendment, carbon sequestration, energy production and waste management (Mohammed et al., 2024). The pyrolysis process (thermal decomposition in limited oxygen) transforms PKS into biochar with properties that depend heavily on pyrolysis conditions such as temperature, heating rate, and residence time (Hasan et al., 2019).

Studies show that increasing pyrolysis temperature enhances the aromaticity and surface area of the biochar, which improves its capacity for nutrient retention and pollutant adsorption (Li et., 2023). Aman et al. (2024) demonstrated that PKS biochar produced at 400–700 °C exhibits high stability and porosity, making it suitable for environmental remediation and soil improvement. Activation processes (physical or chemical) are employed to enhance the porosity and surface heterogeneity of biochar, transforming it into activated carbon with higher adsorption capacities (Hernandez et al., 2007). Physical activation typically involves steam or carbon dioxide at high temperatures, while chemical activation employs activating agents such as KOH, $ZnCl_2$, or H_3PO_4 (Yuliusman et al., 2021).

Therefore, using PKS as feedstock for biochar and activated carbon is environmentally advantageous due to the valorization of an otherwise renewable waste, reducing open field burning and associated emissions (Setiawan et al., 2025). Additionally, utilizing PKS supports circular economy principles by converting waste into value-added products for energy and environmental remediation sectors. While many studies underscore PKS's potential, challenges remain in optimizing process parameters for optimum biochar production and further activation for enhance surface and structural porosity as well as cost-effective production as large-scale catalyst precursor.

The PKS sample used for this study was provided by AdFis products GmBH, Teterow, Germany. The sample contain PKS from Malaysia, Nigeria and Ghana. The reagents used included iodine, hydrochloric acid (HCl) and sodium thiosulphate ($Na_2S_2O_3$), all analytical-grade. Other reagents like acetone and deionized water were used for cleaning purposes. Experimental analyses for biochar production via pyrolysis and activated carbon production via steam activation were conducted at AdFis Lab in Teterow, Germany.

2.2.2 Material preparation

The PKS was ground using a Ceccato Tritone 130 grinder to reduce the particle size. The grinding process was followed by two-stage sieving with a sieve stack, 2 – 4mm of 240 mesh size. This was done to obtain homogeneity of the sample and fine particle size distribution during the experiment. To remove impurities and reduce the ash content of the PKS, the sample was rinse with tap water then placed in a container and washed with deionized water several times for 3 hours. The sample was placed in an oven at 80°C and allowed to dry for 24 hours. Fig. 2.1 shows a PKS sample before washing (a) and after washing (b).

(a) (b)

Figure 2.1: Fine PKS sample before (a) and after (b) washing

2.3 Experimental design

For optimum PKS-biochar yield, three key independent factors, temperature, heating rate and residence time were studied. These factors were coded $(-1, 0, +1)$ for low, middle point and high. The temperature (℃), heating rate (℃/min) and residence time (min) were represented by A, B, C. The temperature was varied from 300 to 500 ℃ at 100 ℃ interval; heating rate from 5 to 15 ℃/min at 5 ℃/min interval; and residence time from 60 to 120 mins at 30 mins interval. The Design of Experiment (DOE) was based on Box-Behnken Design (BBD) to evaluate the influence of the 3 factors using Response Surface Methodology (RSM). RSM is a mathematical and statistical method widely used to model and analyze various processes where the desired response is influenced by various variables with the aim of optimizing the response. RSM usually utilizes multivariate techniques that mathematically and statistically fit the experimental range under consideration; for instance, employing regression analysis and causal relationship between factors and responses (Nor & Wan, 2015; Szpisják-Gulyás et al., 2023). BBD is an effective and widely used RSM design for establishing cause-and-effect relationships usually between three-levels with coded factors. Moreover, the BBD was chosen due to its flexibility in reducing experimental time and cost (Nor & Wan, 2015). The DOE was done using Minitab Statistical Software version 22 (Minitab, 2025). This software followed a second-order regression model to estimate the optimum biochar yield as a function of the independent variables: temperature, heating rate and residence time. The model as shown in Eq. (1) is a quadratic model based on Taylor series used for the biochar yield.

$$y = \beta_0 + \sum_{p=1}^{k} \beta_p x_{ip} + \sum_{p=1}^{k} \beta_{pp} x_{ip}^2 + \sum_{p=1}^{k-1} \sum_{p'>1}^{k} \beta'_{pp} x_{ip} x'_{ip} + \varepsilon_i \quad (1)$$

were y is the response variable (biochar yield), β_0 is the constant, $\beta_p x_{ip}$ is the linear effect coefficient, $\beta_{pp} x_{ip}^2$ is the quadratic effects or square term, $\beta'_{pp} x_{ip} x'_{ip}$ is the interaction

effects of the various coefficients and ε_i indicates the random error term. The subscripts $p, i\ k$ shows the variable, pyrolysis parameters and number of variables respectively.

Table 2.1 presents the experimental design matrix for a Box-Behnken Design (BBD) used to optimize the pyrolysis process of Palm Kernel Shells (PKS). The design investigates the influence of three key independent variables, or factors: pyrolysis temperature (A), heating rate (B), and residence time (C). Each factor is tested at three levels: a low level (-1), a central point (0), and a high level (+1). The table lists the 15 experimental runs, showing both the coded factor levels used for statistical modeling and the corresponding actual, real-world values for each condition. The inclusion of three repeated runs at the central point allows for the estimation of experimental error and model adequacy.

Table 2.1: BBD matrix for pyrolysis of PKS with three levels (temperature, heating rate and residence time)

Run order	A	B	C	Temperature (°C)	Heating rate (°C/min)	Residence time (min)
1.	-1	-1	0	300	5	90
2.	$+1$	-1	0	500	5	90
3.	-1	$+1$	0	300	15	90
4.	$+1$	$+1$	0	500	15	90
5.	-1	0	-1	300	10	60
6.	$+1$	0	-1	500	10	60
7.	-1	0	$+$	300	10	120
8.	$+1$	0	$+1$	500	10	120
9.	0	-1	-1	400	5	60
10.	0	$+1$	-1	400	15	60
11.	0	-1	$+1$	400	5	120
12.	0	$+1$	$+1$	400	15	120
13.	0	0	0	400	10	90
14.	0	0	0	400	10	90
15.	0	0	0	400	10	90

2.3 Experimental set-up and procedures

2.3.1 Pyrolysis of PKS

Figure 2.2 shows the schematic of a three-step laboratory process for converting PKS into biochar. The process begins with preparing the raw material by grinding and sieving it to a specific particle size (2-4mm) and washing it with deionized water. The cleaned biomass is then completely dried in an oven before undergoing the key transformation step.

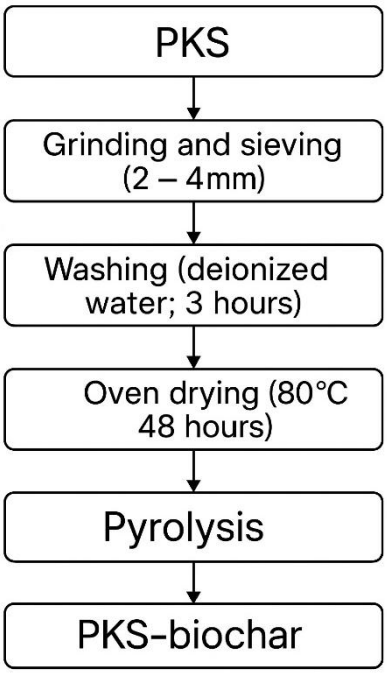

Figure 2.2: Schematic diagram of the preparation and pyrolysis process for producing biochar from PKS

The pyrolysis of PKS was carried out using two horizontal tubular furnaces (RT 50–250/11 Nabertherm) equipped with two temperature-controller (B 180 and P330). For each run, the sample was first dried overnight, and the moisture content was recorded before carbonization using an A&D MF50 Moisture Analyzer. To analyze the moisture content of the raw PKS sample, 5 g is placed in a plate-like holder within a rotating ramp. The sample is heated at 106°C for 5-10 minutes, after which the moisture content is determined and recorded. Then, 210 g of PKS sample was placed in a quartz tube with length, 600 mm and inner dimensions (diameter) 45mm. Using glass-wool, one end of the tube is closed, and the sample (batch process) is fed at the inlet using a funnel. The quartz tube is mounted in a horizontal position in the furnace. Then nitrogen flushes into the reactor at a rate of 10 NL/min for 15 min as a waiting time before the carbonization process. This nitrogen flow rate is maintained for the remainder of the reaction cycle. For each run, the temperature and residence time was set using the controller and the heating rate was determined by Eq. (2).

$$\text{Heating rate} = \frac{\text{Desired temperature} - \text{Room temperature}}{\text{Heating time}} \quad (2)$$

Once the holding time is reached, the machine is turned off under a constant nitrogen flow allowing it to cool to room temperature overnight. The carbonized PKS sample was collected and weighed and the biochar yield (wt%) was calculated using Eq. (3).

$$\text{Biochar yield (wt\%)} = \frac{\text{Mass of biochar sample}}{\text{Mass of sample before pyrolysis}} \text{ x } 100 \quad (3)$$

Other pyrolysis products such as bio-oil and tar were condensed and collected in a jar. The PKS-biochar sample for each process was stored in an airtight container for further analysis. Fig. 2.3 shows a schematic of a fixed-bed pyrolysis reactor system. A sample is heated in a quartz tube under an inert nitrogen (N_2) atmosphere. The resulting gases and vapors exit the tube and are condensed into bio-oil in a container, while non-condensable gases (NCGs) are vented. Fig. 2.4 illustrates the laboratory-scale production of biochar from PKS feedstock.

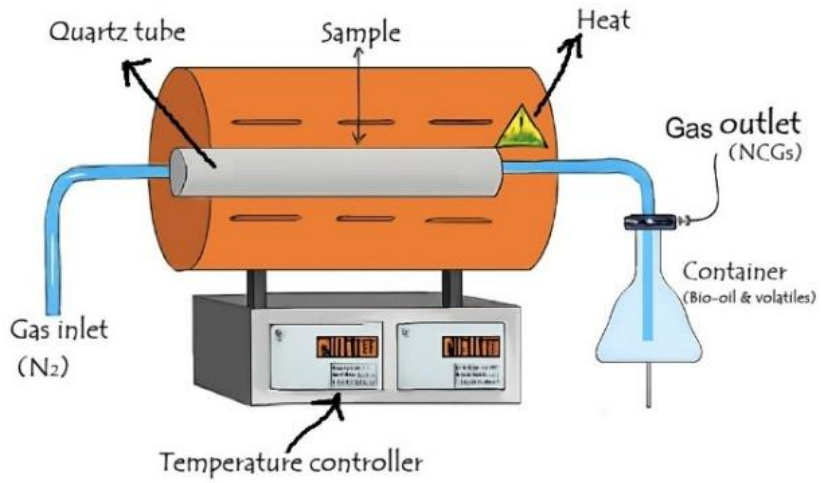

Figure 2.3: Schematic diagram of the laboratory-scale fixed-bed pyrolysis reactor system

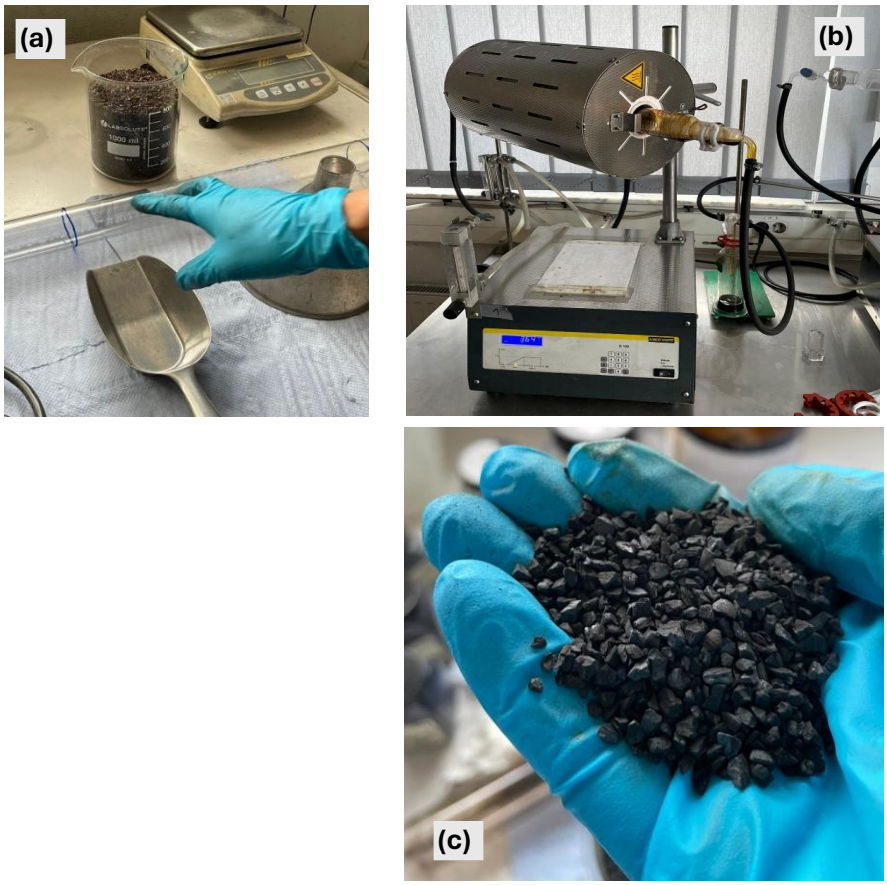

Figure 2.4: Laboratory-scale conversion of biomass into biochar: (a) Feedstock preparation, (b) pyrolysis using a tubular furnace, and (c) harvested biochar

2.3.2 Steam Activation of PKS-Biochar

To improve the microporosity of the PKS-carbonized material, physical activation using steam was performed on the optimum biochar. Studies have shown that activated carbon tend to have larger surface area (Fu et al., 2020), wide range of functional groups and more uniform size distribution suitable for absorption, catalytic application and pollutant removal in wastewater (Ozdemir et al., 2014). 200 g of the optimum PKS-Biochar (PKS-OP1) was first dried overnight at 80 ℃ to obtain a dry mass less than 2 wt%. The sample was placed in a rotary kiln in the form of a quartz tube with a length of 510 mm and diameter of 158 mm. The reactor for activation was a horizontal tube furnace (Xerion rotation reactor 2159/201, Xerion Advanced Heating Ofentechnik, Freiberg, Germany) equipped with a temperature controller and with two thermocouples for measuring the outer surface temperature of the reactor and the furnace. The reactor was also mounted with a diaphragm metering pump (Simdos 10, KNF flodos, Switerland) for liquid injection during activation. To determine the amount of water reacting with the carbon material, 3 bottles were set up with distilled water measuring 200, 120, and 120 g. Basically, the primary reaction involves the gasification of carbon material at high temperature follow by a WGS reaction where the water vapor is broken down to CO_2. During the WGS reaction, water vapor is broken down to CO_2 and H_2 thereby activating the surface

structure of the carbon material. The reactions occurring during steam activation (Sajjadi et al., 2019) are shown below:

$$C + H_2O \rightarrow CO + H_2 \quad (4)$$

$$CO + H_2O \rightarrow CO_2 + H_2 \quad (5)$$

$$C + 2H_2O \rightarrow CO_2 + 2H_2 \quad (6)$$

After the setup, the sample reactor was flushed with a nitrogen flow of 1 NL/min while rotating at 3 rpm for 15 min wait time. Then the sample was heated to the desired temperature (800, 850 and 900 °C) while maintaining the constant nitrogen flow with heating rate of 15 °C/min. Reaching the desired activation temperature, the diaphragm metering pump was used to inject the liquid water into the reactor with flow rate 3 mL/min for two activation time (60 and 120 min). When the desired activation time was completed, the reactor was allowed to cool to room temperature under a constant nitrogen flow and the activated sample was weight to determine the yield, amount of water that reacted with the sample and PKS carbon conversion (X_c) using Eq (7) modified from Müller, (2021).

$$X_c = \left\{ \frac{m_0 \times \frac{C(fix)_0}{100} - m_f \times \frac{C(fix)_f}{100}}{m_0 \times \frac{C(fix)_0}{100}} \right\} \times 100 \quad (7)$$

This Fig. 2.5 illustrates a three-stage process for producing activated carbon from palm kernel shell (PKS). Stage 1: Carbonized PKS, which has a mesoporous structure, is shown in the initial stage after being heated in the absence of air. Stage 2: The carbonized material undergoes steam activation in a specialized furnace to develop enhanced porosity. Stage 3: The end-product is PKS-activated carbon with a microporous structure, suitable for adsorption applications.

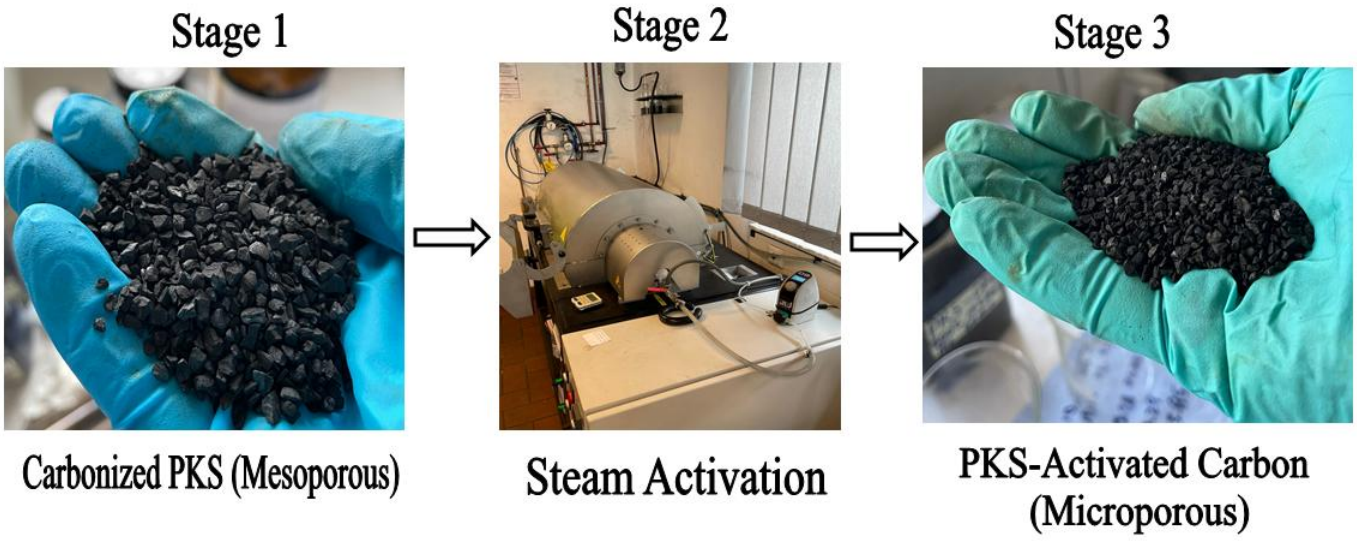

Figure 2.5: Three-stage preparation of activated carbon from palm kernel shell (PKS): (1) Carbonization of PKS produces mesoporous char, (2) Steam activation increases porosity, (3) Final PKS-activated carbon exhibits a microporous structure

2.4 Methods

2.4.1 Proximate Analysis of PKS-biochar

Sequential determination of the moisture, ash, and volatile matter of PKS-biochar and PKS-activated carbon was done according to DIN 51718, (2015), DIN 51719, (2015) and DIN 51720, (2015), respectively. The procedure for determining the proximate composition begin with grinding (powdered) 5 grams of the sample using an Ultra Centrifugal Mill (Retsch ZM 300) containing high speed rotor and a ring sieve of mesh size 500 µm. All procedures were performed in duplicate, and the average value was used for further analysis.

2.4.1.1 Moisture content

One gram of the powdered sample was placed in a crucible uncovered and heated in furnace (Nabertherm, B 180) to a temperature of 106 ± 4℃ at nitrogen flow rate of 0.7 to 1.4 NL/min for 1 hour. After heating, the sample was placed in a desiccator and allowed to cool to room temperature. The moisture content was calculated from mass loss relative to the initial sample mass using the Eq. (8).

$$MC = [(W - B)/W] \times 100 \quad (8)$$

Where: MC = moisture content (wt%), W = mass of the sample used, (g) and B = mass of the sample after drying in moisture test, (g). Similar procedure was performed on the raw PKS except for the powdering or grinding process.

2.4.1.2 Volatile matter

The sample containing the crucible as used for the determination moisture content was covered and reweighed to determine volatile content. The sample was placed in the furnace with a nitrogen flow rate between 0.7 to 1.4 NL/min to sweep away the volatile components. The furnace temperature was raised from 107 ℃ to 800 ± 20 ℃ for 30 min. This temperature was maintained at a holding time of 7 min. The weights of the crucibles and covers at the end of the holding time were used to calculate the volatile matter using Eq. (9)

$$VM = [(B - C)/W] \times 100 \quad (9)$$

where C = mass of the sample after heating in volatile matter test, (g).

2.4.1.3 Ash content

Following the volatile matter test, the furnace was programmed to cool from 800 ℃ to 650 ℃ while removing the cover of the crucible containing sample. The furnace with the sample then was heated from 650 ℃ to 815 ± 20℃ in an open environment for 1 h. After such time, the required temperature is maintained at a holding time of about 2 h to ensure complete oxidation of organic matter and decomposition of carbonates. After the holding, the crucible containing as was cooled in a desiccator to room temperature and the ash content was calculated using Eq. (10)

$$AC = [(F - G)/W] \times 100 \quad (10)$$

where F = mass of crucible and ash residue, (g); G = mass of empty crucible

2.4.1.3 Fixed Carbon

The fixed carbon was determined by difference using equation (11).

$$FC = 100 - (MC + AC + VM) \quad (11)$$

2.4.2 Elemental composition

The elemental composition, C, H, N, S of the raw PKS was determined by using the DIN-EN ISO-21663 (2021) and Oxygen (O) was found by difference. This method basically utilizes instrumental techniques like combustion analysis at a very high temperature to convert these components in connection with gas detection level or infrared spectroscopy. This technique is mostly applied on biomass materials considered as solid recovered fuels (SRF) for applications in energy recovery systems such as power plants or large processing industry. The elemental composition of the carbonized PKS and the PKS activated carbon was determined from different literature using extrapolation.

2.4.3 pH determination

The pH of the samples (biochar and activated carbon) was determined using the CEFIC 3.6 method. The procedure followed by adding 4 g of powdered PKS-biochar to a beaker containing 100 mL distilled water and placed on a hot plate. The distilled water used for this experiment was CO_2 free. The sample containing material was allowed to boil for 5 minutes and cooled to room temperature. Then, a pH electrode (Thermo Scientific, Orion Star A221) was immersed within the suspension after decantation to measure the pH.

2.4.4 Determination of bulk density

The bulk density or apparent density is the mass under specified conditions (dry-weight) of a unit volume of a solid sorbent including its pore volume and inter-particle voids (D2652-11, 2015). The bulk density of the PKS-biochar and PKS-activated carbon was determined by this procedure: the sample containing PKS-biochar was first dried overnight at 80 °C to obtain a dry-weight by mass. The moisture content of the sample was obtained using a moisture analyzer. It is important to consider a total dried weight of less than 2 wt% before measuring the bulk density as the mass of the sample must be determined on a dry-weight basis. Then up to 200 mL of the sample was added to a graduated cylinder (250 mL) through a funnel while maintaining a uniform rate under free fall condition. The weight (mass) of the sample within the 250 mL graduated cylinder was measured. The volume of the sample within the graduated cylinder was observed using a meniscus and recorded. Then the bulk density of the sample was determined using equation (12).

$$\rho = \frac{m}{v} \quad (12)$$

Where $m =$ mass of the sample (g) and $v =$ its correspondent volume (mL).

2.4.5 Determination of Compact density

Compact density like bulk density is essential to the physical, chemical and functional properties of biochar. The sample after free fall within the graduated cylinder was tamp using a Jolting Volumeter STAV II. Using the DIN-ISO-787 (2015) method, the sample was tamped 1250 swings with height fall of 3 mm. The volume was observed using meniscus until the difference between two single results were less than 2 mL. The compact density was measured using equation (12) above.

2.4.6 Determination of Iodine number

The determination of the iodine was done using volumetric ASTM D4607-94, (2005) method; basically to estimate the pore structure and surface characteristics (P. Kumar et al., 2022) of the PKS-activated carbon and the carbonized PKS sample. To determine the iodine number, 1.3 ± 0.2 g of dried powdered sample was placed in an Erlenmeyer flask and 10 ml of HCl (5 wt%) was added to the sample. The suspension was then placed on a hot plate and heating till boiled for exactly 30 seconds. This process was closely monitored using a stopwatch. After the boiling process, the sample was allowed to cool down to room temperature between 15 – 30 minutes. Then, 100 ml of 0.1 N iodine solution was added to the suspension and then shake vigorously for exactly 30 seconds. The suspension was filtered off using a filter paper and the aliquote part of the filtrate (50 ml) was titrated with 0.1 N $Na_2S_2O_3$ by using starch as an indicator. The result expressed in mg/g was calculated using equation (13).

$$X/M = [A - (DF)(B)(S)]/M \quad (13)$$

where is X/M = iodine absorbed per gram of carbon, mg/g, A = blank factor, DF = dilution factor, B = near endpoint factor, S = sodium thiosulfate, mL, and M = mass of carbon used, g. It is important to note that factors such as A and B were predetermined.

2.5 Conclusion

In this study, a systematic experimental methodology was employed to investigate the production, characterization, and activation of PKS-biochar as a sustainable alternative catalyst for hydrogen production via biomass gasification. Pretreated PKS feedstock underwent controlled slow pyrolysis (300-500℃) using a BBD, varying temperature, heating rate, and residence time to optimize biochar yield and properties. Detailed proximate and physicochemical analyses including volatile matter, ash content, fixed carbon, pH, and density were carried out on both raw and processed materials. Subsequent steam activation experiments examined the influence of activation temperature (800-900°C) and holding time (60-120min) on the properties of PKS-activated carbon (PKS-Akt). Key performance indicators such as yield, iodine number (micropore development), and fixed carbon content were systematically examined, providing a better framework for the identification of optimum activation conditions tailored to catalytic applications, especially for hydrogen production.

Chapter 3

Results and Discussion

3.1 Introduction

This section presents the outcomes of the optimization and characterization of biochar and activated carbon derived from PKS. Firstly, the results of the various processes (pyrolysis, activation and characterization) are presented in tables and figures followed by brief description of each result. Then the discussion details how pyrolysis parameters influenced biochar properties, identifying optimal conditions (500°C temperature and 15°C/min heating rate) that produced biochar with favorable fixed carbon content and porosity. This is followed by discussion on steam activation and how it significantly enhanced the materials' surface area and microporosity, yielding activated carbon (labelled PKS Akt 274 – 281 based on process conditions) with high iodine number and excellent physicochemical characteristics. Lastly, a conclusion and perspective based on the results in this study is presented. The section highlights the relationship between activation conditions, material properties, and catalytic performance, underlining the potential application of PKS-derived activated carbon in renewable energy technologies.

3.2 Results

3.2.1 BBD experimental design with biochar yield

Table 3.1 summarizes a series of experimental runs for producing PKS-biochar using different pyrolysis conditions. Each run investigates how temperature, heating rate and residence time affect the resulting biochar yield (%).

Table 3.1: BBD experimental design showing influence of temperature, heating rate and residence time on biochar yield

Run order	A	B	C	Temperature (°C)	Heating rate (°C/min)	Residence time (min)	PKS-biochar yield (%)
1.	−1	−1	0	300	5	90	59.40
2.	+1	−1	0	500	5	90	37.47
3.	−1	+1	0	300	15	90	59.85
4.	+1	+1	0	500	15	90	35.30
5.	−1	0	−1	300	10	60	58.29
6.	+1	0	−1	500	10	60	36.31
7.	−1	0	+	300	10	120	58.22
8.	+1	0	+1	500	10	120	36.35
9.	0	−1	−1	400	5	60	44.28
10.	0	+1	−1	400	15	60	40.57
11.	0	−1	+1	400	5	120	43.44
12.	0	+1	+1	400	15	120	39.41

13.	0	0	0	400	10	90	39.95
14.	0	0	0	400	10	90	40.13
15.	0	0	0	400	10	90	38.61

Lower temperatures (300°C) consistently give higher biochar yields (~58–59%), while higher temperatures (500°C) result in significantly lower yields (~35–37%) under similar conditions. Increasing the heating rate and residence time at a fixed temperature typically has a modest effect on biochar yield. Runs at 400°C show intermediate yields (~39–44%), with slight variations based on heating rate and residence time.

3.2.2 Biochar yield model

The Analysis of Variance (ANOVA) presented in Table 3.2 was conducted to assess the effects of three factors (A, B, and C) and their interactions on a response variable, related to biochar yield. The model includes linear terms, quadratic (square) terms, and two-way interaction effects. The model explains over 99% of the variance with significant contributions from factor A and its quadratic term. Interaction terms are non-significant, and the model shows good fit for experimental data.

Table 3.2: ANOVA summary table evaluating the effects of factors A, B, and C, including their quadratic and interaction terms, on the response variable with 95% confidence level

Source	DF	Adj SS	Adj MS	F-Value	P-Value
Model	9	1213.35	134.82	92.86	0.000[a]
Linear	3	1031.64	343.88	236.86	0.000[a]
A	1	1019.94	1019.94	702.51	0.000[a]
B	1	11.19	11.19	7.70	0.039[a]
C	1	0.52	0.52	0.35	0.577
Square	3	179.97	59.99	41.32	0.001[a]
A^2	1	176.02	176.02	41.32	0.000[a]
B^2	1	8.72	8.72	6.01	0.058
C^2	1	2.51	2.51	1.73	0.246
2 – Way interaction	3	1.74	0.58	0.40	0.759
AB	1	1.72	1.72	1.18	0.327
AC	1	0.00	0.00	0.00	0.965
BC	1	0.03	0.03	0.02	0.900
Error	5	7.26	1.45		
Lack-of-Fit	3	5.88	1.96	2.84	0.271
Pure Error	2	1.38	0.69		
Total	14	1220.61			
Model summary					
	S	R-sq		R-sq (adj)	R-sq(pred)

	1.20493	99.41%	98.33%	92.04%

DF: Degree of freedom, Adj SS: Adjusted sum of squares, Adj MS: Adjusted mean squares, [a] significant term, S: standard error

A Pareto chart of standardized effects for PKS-biochar yield (Figure 3.1), indicates the influence of different process factors. The chart shows that temperature (A) has the most significant impact on biochar yield, followed by the quadratic effect of temperature (AA). Heating rate (B), residence time (C), and their interactions contribute less substantially, as their standardized effects fall below the significance threshold (2.57).

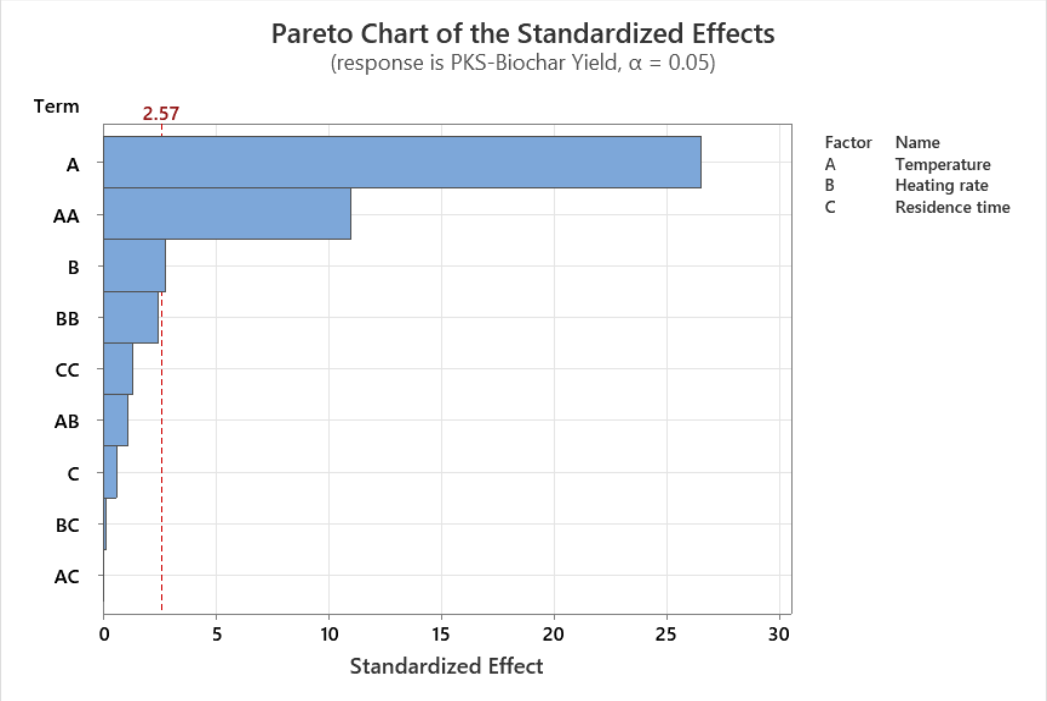

Figure 3.1: Pareto chart revealing the dominant effect of temperature on palm kernel shell biochar yield, with other factors and interactions with less or no significant influence

3.2.3 Selection of optimum biochar

This 3D surface plot in figure 3.2 shows how the yield of PKS-Biochar is simultaneously influenced by pyrolysis temperature and heating rate. The residence time is held constant at 90 minutes. The graph shows that biochar yield (z-axis) decreases as temperature (x-axis) increases, forming a downward-sloping surface. The yield also appears to decrease with increasing heating rate (y-axis), though this effect is less pronounced than that of temperature. The peaks and valleys on the surface help identify optimal combinations of parameters for maximizing yield.

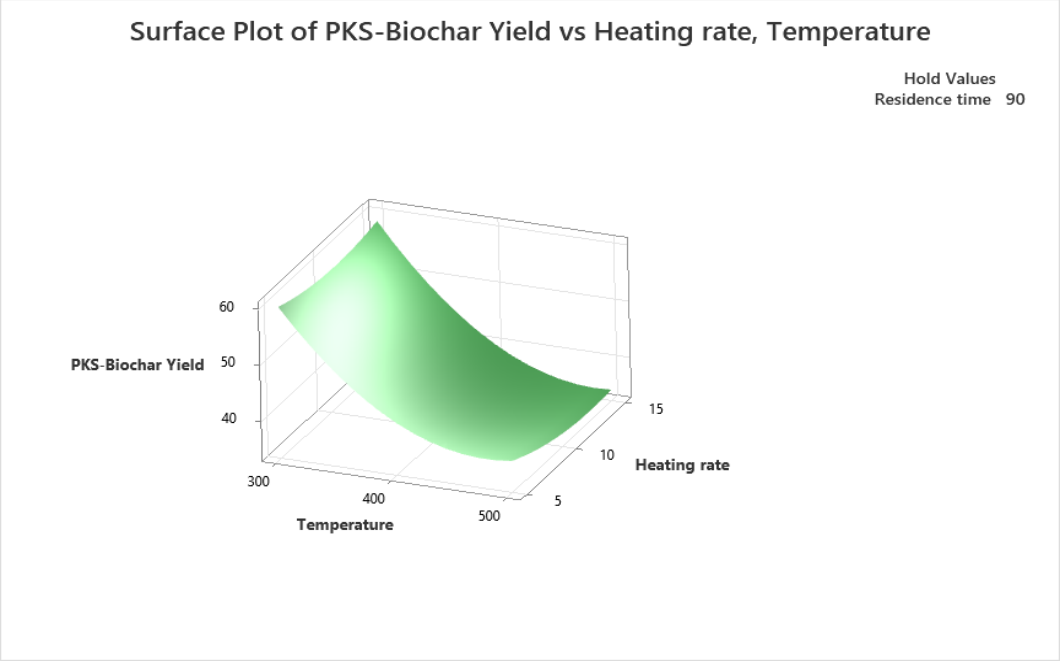

Figure 3.2: Three-dimensional surface plot depicting the relationship between PKS-Biochar yield, pyrolysis temperature, and heating rate at a constant residence time of 90 minutes

For maximizing biochar yield, the two-dimensional contour plot (Figure 3.3) was used. The colored bands represent specific ranges of biochar yield (< 35%, 35-40%, > 55%). Lines of constant yield (contours) can be assumed between these bands. It clearly shows that the highest yields (> 55%) are achieved at the lowest temperatures and heating rates (bottom-left corner), while the lowest yields (< 35%) occur at the highest temperatures and heating rates (top-right corner). This type of plot is important for precisely reading the approximate yield expected for any given pair of temperature and heating rate values why at constant residence time.

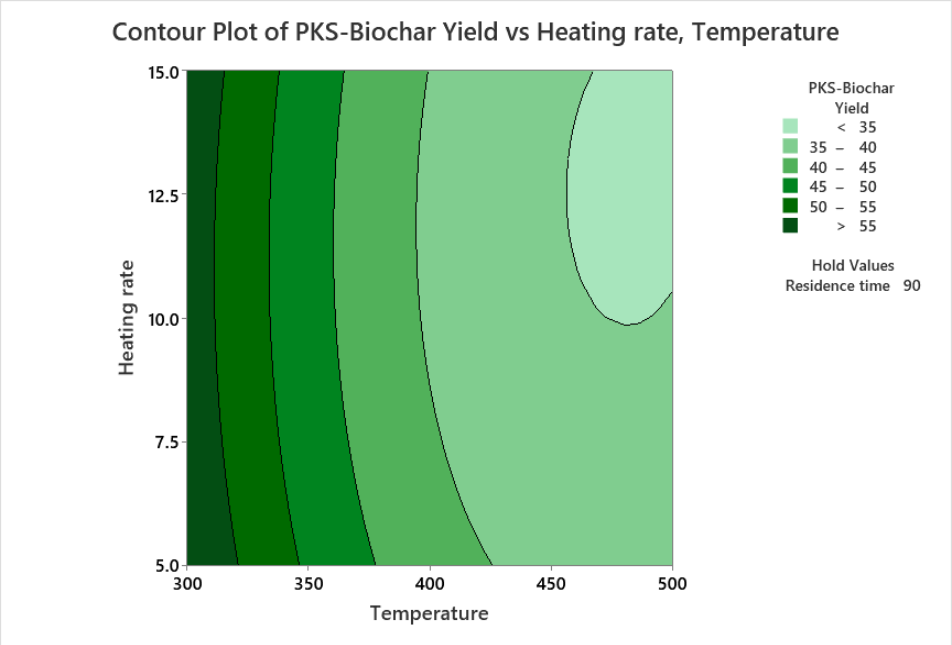

Figure 3.3: Contour plot of PKS-Biochar yield as a function of heating rate and temperature, with yield values categorized into discrete bands and a residence time fixed at 90 minutes

3.2.4 Steam activation

This line graph (Figure 3.4) shows the effect of activation temperature and process time on the final yield of activated carbon produced from optimal PKS-biochar. The yield percentage decreases significantly as the activation temperature increases from 800°C to 900°C for both hold times. Furthermore, the longer activation hold time of 120 minutes consistently results in a lower yield compared to the 60-minute process at the same temperature. This inverse relationship between yield and both temperature and time is a well-established trend in the activation process.

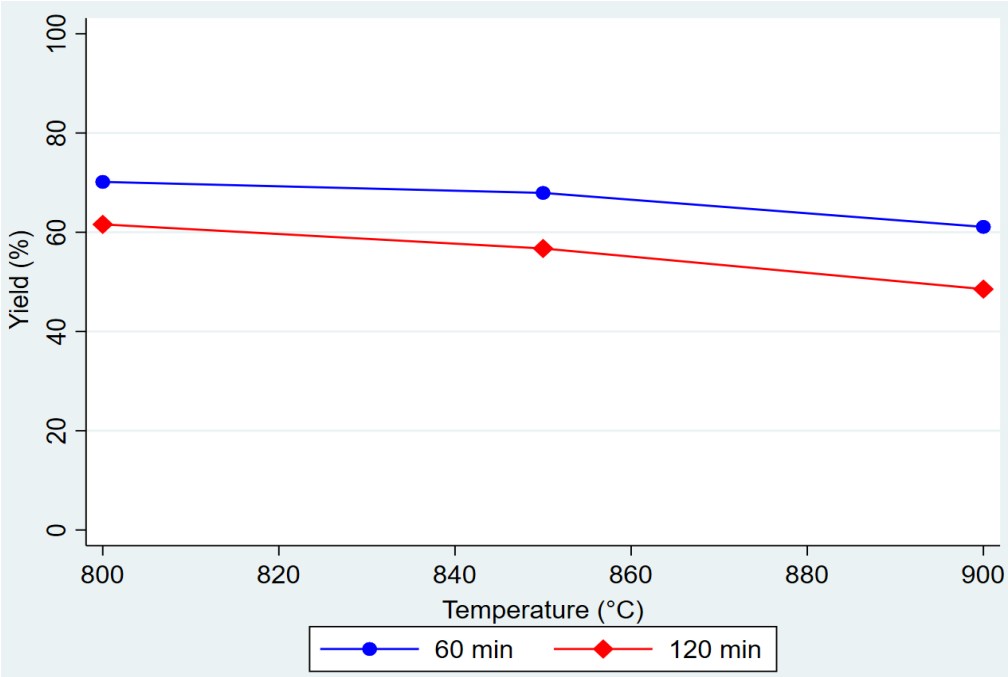

Figure 3.4: Yield of PKS-derived activated carbon as a function of activation temperature for two different hold times (60 and 120 minutes)

3.2.5 Characterization

3.2.5.1 PKS characterization

Table 3.4 compares the proximate composition of PKS before and after a pre-treatment process while Table 3.5 gives the elemental composition of PKS. The pre-treatment significantly reduced the moisture content and ash content while increasing the fixed carbon. The volatile matter remained relatively unchanged. It is important to note that most biomass contains inorganic minerals (K, Cl, Ca); hence, by washing with deionize water, these minerals tend to dissolve and leach out of the biomass thereby significantly improving ash-related characteristics of the biomass (Lebendig et al., 2022).

Table 3.2: Proximate analysis of raw and pre-treated PKS samples

Sample	Moisture (wt%)	Volatile matter (wt%)	Ash content (wt%)	Fixed carbon (wt%)
Raw PKS (before pretreatment)	8.15 ± 0.00	70 ± 0.07	1.14 ± 0.04	20.71 ± 0.05
Raw PKS 2 -4mm (after pretreatment)	0.45 ± 0.10	70.69 ± 0.07	0.65 ± 0.16	28.21 ± 0.11

Mean ± SD; N=2

Table 3.3: Elemental composition of PKS sample

Carbon	Hydrogen	Oxygen	Nitrogen	Sulfur
48.05 ± 2.9	5.20 ± 0.32	45.34 ± 3.24	0.25 ± 0.01	0.03 ± 0.01

3.2.5.2 PKS-biochar characterization

Table 3.6 presents the characterized properties of 15 different treated PKS biochar samples (T1-T15) as representative run based on the BBD order while Table 3.7 gives the characterization of the optimum biochar. The data shows significant variation in key quality parameters, including volatile matter, ash content, fixed carbon, pH, and bulk densities. The samples are categorized in distinct groups, particularly between high volatile matter/low fixed carbon (T1, T3, T5, T7) and low volatile matter/high fixed carbon (T2, T4, T6, T8) biochar, suggesting different process conditions (temperature, heating rate and residence time).

Table 3.4: Proximate analysis, pH, and density properties of various PKS-biochar samples

Sample	Volatile matter[a] (wt%)	Ash content[a] (wt%)	Fixed carbon[d] (wt%)	pH	Bulk Density (g/L)	Compact density (g/L)
PKS-T1	49.16 ± 0.05	1.64 ± 0.14	49.20 ± 0.12	6.8	717 ± 0.70	724 ± 0.00
PKS-T2	18.67 ± 0.23	2.54 ± 0.34	78.79 ± 0.11	7.6	678 ± 0.00	683 ± 2.83
PKS-T3	49.02 ± 0.56	1.09 ± 0.14	49.96 ± 0.12	5.9	682 ± 0.00	690 ± 2.83
PKS-T4	19.88 ± 0.02	2.42 ± 0.05	77.7 ± 0.22	8.3	577 ± 0.00	583 ± 0.00
PKS-T5	43.83 ± 0.01	2.85 ± 0.05	53.32 ± 0.12	6.4	679 ± 2.83	688 ± 0.00
PKS-T6	19.57 ± 0.03	2.85 ± 0.03	77.58 ± 0.11	8	600 ± 0.00	608 ± 2.12
PKS-T7	48.20 ± 0.02	1.44 ± 0.03	50.36 ± 0.21	6.3	679 + 0.00	688 ± 2.12
PKS-T8	18.18 ± 0.02	3.05 ± 0.02	78.77 ± 0.12	7.8	608 ± 0.00	615 ± 4.95
PKS-T9	31.88 ± 0.01	2.06 ± 0.04	66.06 ± 0.21	7	652 ± 2.12	661 ± 2.12
PKS-T10	27.18 ± 0.12	2.79 ± 0.01	70.03 ± 0.22	7.2	604 ± 2.83	608 ± 2.83
PKS-T11	31.03 ± 0.11	2.38 ± 0.01	66.59 ± 0.11	7.0	607 ± 4.24	615 ± 0.00
PKS-T12	24.24 ± 0.21	2.51 ± 0.11	73.25 ± 0.10	9.1	602 ± 0.00	608 ± 0.00
PKS-T13	26.61 ± 0.03	3.04 ± 0.00	70.35 ± 0.11	7.2	600 ± 0.00	659 ± 4.00
PKS-T14	26.63 ± 0.01	2.42 ± 0.02	70.95 ± 0.11	7.5	597 ± 4.00	608 ± 4.00

PKS-T15	24.07 ± 0.03	2.72 ± 0.03	73.21 ± 0.12	7.7	586 ± 4.00	591 ± 4.00

[a]water free (values on dry weight basis); Mean ± SD, N=3; [d]By difference FC=100-(AC+VM)

Table 3.5: Yield, Iodine number, proximate analysis, pH, and density properties of optimum PKS biochar (PKS-OP1)

Sample	Yield (wt%)	Iodine n° (mg/g)	Volatile matter (wt%)	Ash content (wt%)	Fixed Carbon (wt%)	pH	Density (g/L)
PKS-OP1	36.26 ± 1.12	155	20.01 ± 0.15	2.87 ± 0.03	77.12 ± 0.15	7.9	566 ± 2.24

Table 3.6: Elemental composition of PKS-biochar at 500°C

Carbon	Hydrogen	Oxygen	Nitrogen
72.2	5.0	22.1	0.7

(Kong et al., 2022)

Figure 3.5 visually represents the results of the proximate analysis for a biochar sample, displaying its composition in terms of key quality parameters. The chart shows the relative percentages of volatile matter, fixed carbon, and ash content.

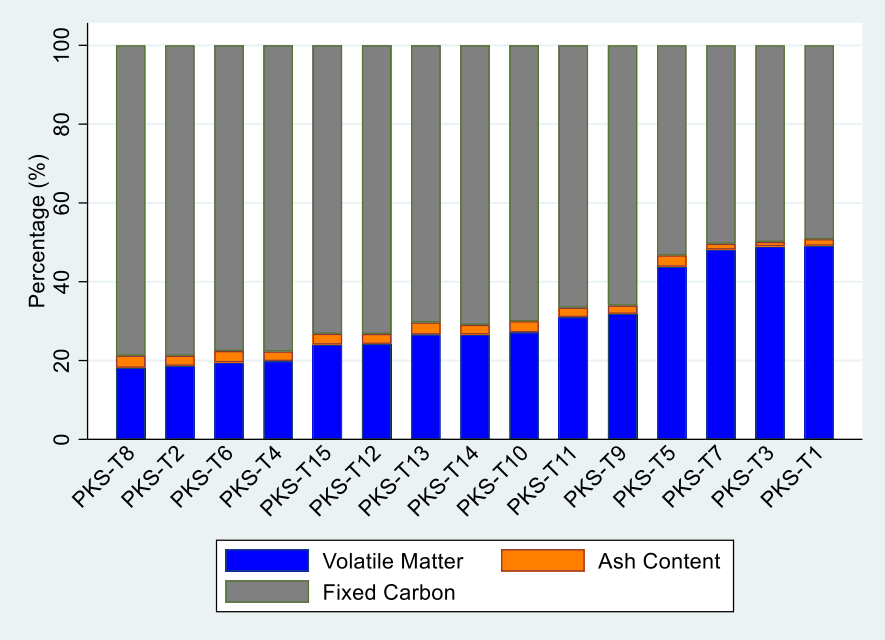

Figure 3.5: Proximate composition (volatile matter, fixed carbon, and ash content) of PKS-biochar

3.2.5.3 PKS-activated carbon (PKS-Akt) characterization

The characterization of PKS-activated carbon (PKS-Akt) is shown in Table 3.9 with key indicators such iodine number, fixed carbon, pH and densities. The number code represents each process condition for steam activation (temperature and holding time). The first three samples (274, 275 and 278) were produced via temperature 800, 850 and 900 ℃ respectively with constant holding time, 60 min. Samples (279, 280 and 281) were synthesized under constant temperature as the previous three samples but different holding time of 120 min. The increase in iodine number with increase in temperature and holding time and decrease in density with increase in temperature and holding time. The fixed carbon of all samples was significantly high (> 90 wt%).

Table 3.7: Properties of PKS-activated carbon under steam activation, including crystallinity (carbon conversion), adsorption capacity, proximate analysis, pH, and density

Sample	X_c (wt%)	Iodine number (mg/g)	Volatile[a] matter (wt%)	Ash[a] content (wt%)	Fixed[d] Carbon (wt%)	pH	Density (g/L)
PKS-Akt 274	15.33	582	2.57	4.35	93.08	9.9	602 ± 0.00
PKS-Akt 275	58.96	704	2.71	4.10	93.19	9.8	589 ± 0.00
PKS-Akt 278	63.40	768	3.01	4.59	92.40	9.8	561 ± 1.00
PKS-Akt 279	63.81	758	5.08	4.28	90.64	9.9	533 ± 0.00
PKS-Akt 280	66.79	885	4.46	5.24	90.30	10.1	508 ± 0.00
PKS-Akt 281	70.86	970	1.95	5.45	92.60	10.3	501 ± 1.00

[a]Water free (value on dried weight basis); [d]Fixed carbon by difference: FC=100-(VM+AC)

3.2.5.4 Comparative analysis of PKS-Akt and PKS-OP1 (proximate composition)

A comparative analysis of the proximate composition is provided in figure. 3.6 below. The comparison highlights volatile matter, fixed carbon, and ash content across several steam-activated carbon samples (PKS-Akt 274, 275, 278, 279, 280, 281) and one optimum biochar sample (PKS-OP1). It is interesting to note that all PKS-Akt shows high fixed carbon over 90% as compared to the PKS-OP1. As a result, we can underscore that a high carbon-rich material, which is the primary aim of steam activation, was produced from a moderate carbon rich material.

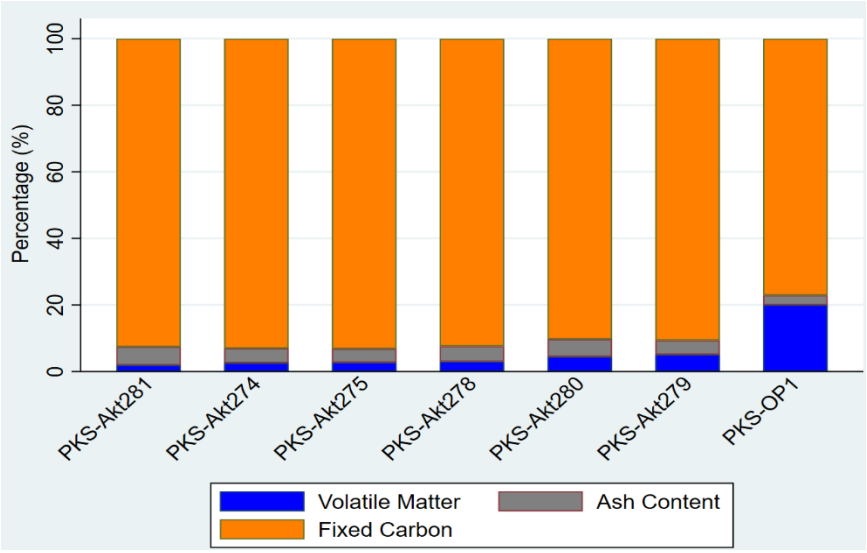

Figure 3.6: Comparative proximate analysis composition of steam-activated carbons (PKS-Akt series) and an optimum biochar (PKS-OP1)

3.2.5.5 Effect of activation temperature and time on Iodine number

Figure 3.7 shows how the iodine number (a measure of micropore volume and surface area) changes with both activation temperature and activation time. The data suggests that the Iodine Number increases significantly with rising temperature, reaching a peak around 800-900°C, and is also influenced by the duration of the activation process, with 120 minutes being a key holding point.

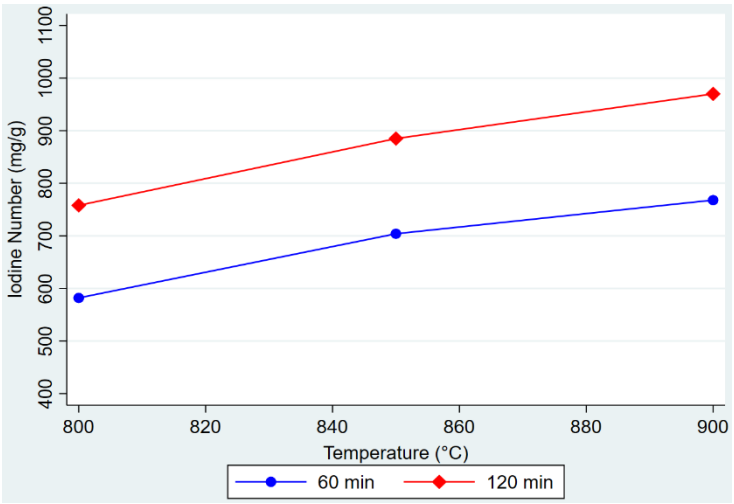

Figure 3.7: Effect of activation temperature and holding time on iodine number

3.3 Discussion

3.3.1 PKS-biochar yield

The PKS-biochar yield under varying pyrolysis conditions is presented in Table 3.1 Prior to the pyrolysis process, the average moisture content of the dried PKS sample was 1.05 ± 0.36 wt%, confirming that the feedstock was adequately pre-treated and sufficiently dried for thermal conversion. During the initial stage of pyrolysis (200 - 290 ℃), vapors from the reactor tube condensed visibly on the quartz wall, whereas more intense volatile matter release and non-condensable gases were observed in the range of 300 to 400 ℃. This behavior is consistent with earlier thermogravimetric analysis findings reported by Rashidi (Rashidi et al. 2019) and Shoaib (Shoaib et al. 2015), where the decomposition of hemicellulose and cellulose leads to significant volatile release at this temperature range. From the experimental results, biochar yield exhibited a dependence on pyrolysis temperature, heating rate, and residence time. In general, yield decreased with increasing temperature. At 300 ℃, relatively high yields were recorded (~58-60%), regardless of heating rate or residence time. For example, the highest yield (59.85%) was obtained at 300 ℃, 15 ℃/min, and 90 min. However, such high values at low temperatures suggest incomplete carbonization, as lignocellulosic components are not fully degraded below 350 ℃ (Kok et al., 2017).

When the temperature was raised to 400 ℃, yields dropped to 38-44%, depending on the heating rate. Notably, trials conducted at 400 ℃ and 90 min residence time (Runs 13 to 15) consistently produced yields around 39-40%, indicating that prolonged residence at this temperature did not result in significant yield. Instead, this suggests stabilization of the thermal degradation process, where secondary decomposition reactions consume more biomass material, producing higher amounts of volatiles and tar rather than solid carbonaceous residue (Balat, 2008). At 500 ℃, the lowest yields (35-37%) were observed across all runs, confirming that higher pyrolysis temperatures favor devolatilization and gas release over char formation (Qureshi et al., 2021). Heating rate and residence time influenced the yield marginally at this point, as the extent of carbonization was already maximized by the elevated temperature. Importantly, lower temperatures (around 300 ℃) retain a greater solid fraction (biochar) but may indicate incomplete carbonization. Conversely, higher temperatures (500 ℃) promote complete decomposition but at the expense of yield.

3.3.2 Biochar model

The ANOVA results (Table 3.2) clearly indicate that the overall regression model was statistically significant (p-value < 0.05), with no significant lack-of-fit (p-value = 0.271), confirming that the model was a reasonable representation of the experimental data. The model yielded a very high coefficient of determination (R^2 = 99.41%), while the adjusted R^2 (98.33%) and predicted R^2 (92.04%) remained close in value. This consistency suggests excellent model reliability and predictive capability, making it suitable for future forecasting of PKS-biochar

yield. Similar justification was made by Ahiekpor (Ahiekpor et al. 2023); and Sopandi (Sopandi et al. 2025). Moreover, the low standard error (S = 1.20) indicates that the predicted values are very close to the actual experimental results.

The factor effects reveal that temperature (factor A) was the most significant variable, both in its linear and quadratic forms, with an F-value of 702.51 and $p < 0.005$. This confirms that temperature is the dominant determinant of biochar yield. Heating rate (factor B) also had a statistically significant value though weaker linear effect (F-value = 7.70, p = 0.039), while residence time (factor C) did not significantly affect yield (p-value > 0.05). Among the quadratic terms, only temperature (A^2) was significantly important ($p < 0.05$), further reinforcing its dominant influence. In contrast, the quadratic contributions of heating rate (B^2) and residence time (C^2) were not statistically significant ($p > 0.05$). Importantly, none of the two-way interactions (AB, AC, BC) influenced biochar yield (all $p > 0.05$), suggesting that each parameter acts independently within the studied ranges. The regression coefficients (Equation. 14) also provide useful interpretation. The negative coefficient for temperature indicates that higher pyrolysis temperatures reduce biochar yield due to enhanced volatilization and decomposition of the biomass matrix. Similarly, the negative coefficients for heating rate and residence time reflect the general trend of reduced yield with glaring processing conditions, though their effects are not statistically strong compared to temperature.

$$\text{Biochar yield} = 206.5 - 0.6530A - 0.894B - 0.172C + 0.0006905A^2 + 0.0615B^2 + 0.000916C^2 - 0.00131AB + 0.000009AC + 0.00053BC \quad (14)$$

Collectively, the statistical analysis demonstrates that temperature is the sole factor of primary importance for yield optimization, while heating rate exerts only a minor influence, and residence time can be considered negligible. These findings align with the experimental results where maximum yields occurred at 300 °C across different runs, but such high-yielding conditions may correspond to incomplete carbonization. Therefore, for selecting an optimum PKS-biochar for subsequent direct activation, emphasis should be placed not only on yield but also on physicochemical properties. Biochar derived at intermediate conditions (around 400 - 500 °C) is expected to offer balanced yield, reduced volatile matter, higher fixed carbon, and greater structural stability, all of which are promising for activation processes.

To further validate the process conditions (temperature, heating rate and residence) and to determine which factor had significant influence on the biochar yield, the standardized effects based on Pareto chart (Figure 3.1) were utilized. At a 95% confidence level ($\alpha = 0.05$), the threshold line for statistical significance was determined to be approximately 2.57. Among the studied variables, the chart confirms that temperature (factor A) exhibited the strongest and most significant influence on biochar yield, which is consistent with the ANOVA results (Table 3.2). Increasing temperature led to a marked decrease in biochar yield, reflecting enhanced

devolatilization and secondary decomposition of organic matter, while simultaneously promoting the formation of a more carbon, stable biochar (Mariyam et al., 2024).

The heating rate (factor B) was the next factor approaching the significance threshold. Although its effect was weaker than that of temperature, and only marginally above the threshold line, it can still be considered slightly influential on yield. In contrast, residence time (factor C) did not exhibit any statistically significant effect. Its standardized effect fell below the Pareto threshold, reaffirming that variations in residence time, within the tested range, had negligible impact on PKS-biochar yield (Figure 3.1).

3.3.3 Selection of optimum biochar

3.3.3.1 Effects of temperature and heating rate

To achieve optimal PKS-biochar yield and quality, the effects of temperature and heating rate were thoroughly analyzed, holding residence time constant at 90 min. The 3D surface plot (Figure 3.2) and contour plot (Figure 3.3) illustrate the response of biochar yield to these primary process variables. From both plots, biochar yield declines steadily as temperature increases from 300°C to 500°C, particularly at higher heating rates. This trend supports the understanding that elevated temperatures result in greater devolatilization and the onset of secondary reactions such as cracking and reforming thereby leading to increased gaseous and tar products at the expense of solid biochar. Higher temperatures also facilitate the removal of coke precursors (heavy oxygenated and phenolic compounds), promoting further carbonization and improving the physicochemical properties (e.g., carbon content and porosity), even as yield decreases. This observation is in line with earlier reports on the pyrolysis of lignocellulosic materials (Ahiekpor et al., 2023; Zeng, 2015).

The heating rate further modulates these effects. At lower heating rates, devolatilization proceeds gradually, favoring higher solid biochar yields, though with higher volatile content. In contrast, higher heating rates (15°C/min) accelerate bond-scission reactions and vapor-phase cracking, sharply reducing the biochar yield, as seen in both figures. These rapid conditions limit heat and mass transfer, increase secondary reactions, and therefore encourage conversion to gases and bio-oil (Salehi et al., 2009).

The combined effect (synergy) of high temperature and high heating rate yields the lowest biochar throughput (~35% at 500°C and 15°C/min; Figure 3.3), while low temperature and low heating rate maximize biochar yield (>55%). Both factors (higher temperature and heating rate) account for maximum biomass decomposition resulting in enhanced biochar with low volatile and mesopore. These effect are validated from experimental works and studies done by (Ahiekpor et al., 2023; Chatterjee et al., 2020; Salehi et al., 2009; Zeng, 2015).

The contour plot (Figure 3.3) further highlights this relationship by showing gradient zones: the darkest regions (>55 wt% yield) correspond to low temperature and low heating rate. The lightest regions (<35 wt%) occur at high temperature and high heating rate. Experimental results confirm that primary decomposition (mainly breakdown of hemicellulose and cellulose)

primarily occurs between 300-400°C, whereas above 450°C, further thermal cracking drives the conversion of solid biomass to gaseous products like CO, CO_2, CH_4 as well as bio-oil with lower biochar (Chen et al., 2022).

For practical optimization, while maximum yield is attractive, enhanced carbonization and desired physicochemical properties are achieved at higher temperatures, even though yield is lower. The model and validation run indicate that the optimum conditions for producing high-quality, carbon-rich PKS-biochar (suitable for further activation) are 500°C, a heating rate of 15°C/min, and a residence time of 60 min. At these settings, the predicted yield (36.02 ± 1.5 wt%) matches closely with experimental results (36.26 ± 1.12 wt%, N=4), affirming the model's robustness. Finally, residence time does not have a significant effect ($p > 0.05$) on yield within the tested range. Extending residence time above 60 min, neither enhances yield nor substantially alters physicochemical properties, making longer durations unnecessary from both an economic and energy perspective.

3.3.4 Steam Activation

The result of the steam activation examines the impact on activation temperature (800–900°C) and residence time (60-120 min) on steam-activated PKS (PKS-Akt). Key parameters include yield and water consumption on direct activation. This is followed by analysis on physicochemical parameters such as carbon conversion iodine number (micropore capacity), volatile matter, ash content, fixed carbon, pH, and density.

3.3.4.1 Effects of activation temperature and holding time on yield

The findings presented in Figure 3.4 9 demonstrate a clear linear decrease in PKS-Akt yield as both temperature and residence time are increased. Specifically, the yield declines from 70.15 wt% to 61.08 wt% as the temperature increases from 800 to 900°C at a constant residence time of 60 min. A similar trend is observed with longer residence times: the yield drops from 61.59 wt% to 48.54 wt% when the holding time increases from 60 min to 120 min across the same temperature range. This negative correlation underscores the impact of elevated thermal conditions on the gasification or activation process. As temperature rises, the extent of thermal decomposition and volatilization intensifies, promoting the release of volatile components (P. Kumar et al., 2022) and reducing solid yield. The effect is compounded by longer residence times, which allow for prolonged exposure to high temperatures and further removal of mass due to continued devolatilization and, at the highest temperature (900°C), accelerated carbon burn-off (Chang et al., 2000; Drobíková et al., 2012).

Such trends are consistent with those observed during primary carbonization, where higher process temperatures favor secondary reactions, greater conversion of biomass to gases, and reduced solid fraction. The pronounced yield losses at 900°C reflect rapid carbon consumption and burn-off, as previously reported by Chang (Chang et al., 2000) and more recently by Kumar (Kumar et al. 2022), further validating the experimentally observed behavior. Both increased

temperature and extended residence time are important to the yield of PKS-Akt samples, driven principally by enhanced volatilization and carbon burn-off mechanisms at higher thermal intensities.

3.3.4.2 Effects of activation temperature and holding time on water consumption

The reaction ($C + H_2O \rightarrow CO + H_2$) that involves the carbonized material and water to form carbon monoxide and hydrogen is done solely to increase the surface structure of a carbonize material from mesopore to enhance micropore. During steam activation, increase in activation temperature resulted to increase in H_2O consumption on weight basis from 64.2 g to 108.9 g at 800 ℃ to 900 ℃ and constant holding time, 60 min. This follows the rate at which the carbon material diffuses water molecules during activation. The rate of water consumption per hour increased with increase in temperature and holding time from 0.321 to 0.473 g/g/h under these conditions (temperature 800 to 900 ℃) and at rate 60 min and from 0.272 g/g/h to 0.585 g/g/h at 120 min. (see app. Table A)

3.3.5 Characterization

3.3.5.1 PKS (proximate and elemental)

The proximate characterization of the raw palm kernel shell (PKS) prior to carbonization (Table 3.3) highlights the necessity and effectiveness of pretreatment for efficient biochar production. Pretreatment is an essential step in biomass utilization, as it not only enhances process efficiency during pyrolysis but also improves the physicochemical attributes of the feedstock for downstream applications, including combustion, gasification, catalytic support, and activated carbon production (Koppejan et al., 2019).

A consistent particle size distribution (2-4 mm) achieved through crushing and sieving ensured uniformity in heat transfer during pyrolysis, thereby facilitating stable carbonization. The raw PKS exhibited a relatively high moisture content (8.15 wt%), attributed both to the intrinsic structure of lignocellulosic biomass. High moisture content is undesirable as it reduces thermal efficiency, increases energy demand for drying, and inhibits stable pyrolysis (Orang et al., 2015). After oven-drying at 105 °C, the moisture content decreased significantly to 0.45 wt%, representing a near-complete removal of residual water. This optimized moisture range is crucial, as it ensures enhanced carbonization efficiency and reproducibility. Comparable results have been observed in PKS and other biomass studies, where oven drying typically reduces moisture to below 5 wt% (Haryati et al., 2018).

The volatile matter content (>50 wt%) remained largely unchanged before and after pretreatment, indicating that mechanical and thermal pretreatment had minimal effect on inherent volatiles. The ash content of the PKS biomass was reduced after washing to 0.65 wt%, reflecting the removal of surface dust and extrinsic inorganic impurities such as silicates, nitrates, hydroxides, and trace minerals (Vassilev et al., 2013). Although moderate ash can provide catalytic benefits in gasification or as in-situ mineral activators, high ash generally

reduces yields and modifies pore development due to the deposition of inorganics on biochar surfaces (Abioye et al., 2024). Hence, minimizing ash through pretreatment was crucial for preserving pore structure and ensuring improved textural properties during carbonization and subsequent activation. The fixed carbon content by difference was relatively low (<30 wt%), which is characteristic of fresh lignocellulosic biomass. However, this fraction contributes substantially to biochar stability and is expected to be enriched after devolatilization.

The elemental (ultimate) composition of raw PKS (Table 3.4) further confirms its excellent suitability as pyrolytic feedstock. The high carbon content (~48 wt%) combined with balanced oxygen (~46 wt%) and hydrogen (~5 wt%) signifies the dominance of lignin, which is thermally stable and contributes to higher solid yield (Baffour-Awuah et al., 2021). The trace nitrogen (<1 wt%) and sulfur (<0.5 wt%) contents are advantageous as they minimize potential secondary emissions during thermal treatment and improve the environmental compatibility of the resultant biochar. Importantly, the relatively high C/O ratio of the PKS favors the production of biochar yields greater than 35 wt%, with improved aromatization and surface area development (Chen, 2020).

3.3.5.2 PKS-biochar (proximate)

The proximate composition of PKS-biochar samples (T1-T15) provides critical insights into the effect of pyrolysis conditions on biochar physicochemical properties (Table 3.5). Variations in volatile matter, ash content, fixed carbon, pH, and bulk/compact densities reflect the gradual transformation of biomass with increasing pyrolysis severity, primarily influenced by temperature.

3.3.5.2.1 Volatile matter

Volatile matter (VM) varied widely, from 18.18 wt% (T8) to 49.16 wt% (T1). As expected, samples produced at the lowest temperature (300 °C: T1, T3, T5, T7) retained the highest volatile fractions (> 43 wt%); Figure 3.5 10, representing incomplete devolatilization and partial breakdown of biomass components such as cellulose and hemicellulose as previous indicated. By contrast, biochar obtained at 500 °C (T2, T4, T6, T8) contained very low VM (18–20 wt%), consistent with advanced devolatilization and secondary decomposition processes. These results confirm the general trend that increasing pyrolysis temperature leads to a significant reduction in volatile matter, which is desirable for enhancing thermal stability and producing more carbonized material.

3.3.5.2.2 Ash content

Across all samples show low ash (1.09-3.05 wt%), indicative of the naturally low inorganic fraction in PKS. Nevertheless, differences were observed depending on carbonization conditions. Low-temperature samples (T1, T3, T5, T7) exhibited the lowest ash values (1.09-2.85 wt%), while higher-temperature biochar, especially T8 and T13-T15, showed slightly

elevated ash levels (up to 3.05 wt%). This increase in ash at higher temperatures results from progressive volatilization of the organic matrix, concentrating the mineral fraction (Noor et al., 2019). While moderate ash levels may serve as intrinsic activating agents during pyrolysis, excessive ash deposition can interfere with pore development and reduce textural quality (Biedermann et al., 2005).

3.3.5.2.3 Fixed Carbon

The fixed carbon (FC) was determined by difference, and it showed the inverse relationship to VM. The maximum FC contents were observed in samples produced at 500 °C (T2, T4, T6, T8), with values between 77.6-78.8 wt%, reflecting extensive conversion of organics to stable carbon structure. Conversely, low-temperature samples (T1, T3, T5, T7) recorded lower FC contents (49-53 wt%), further confirming incomplete carbonization. These trends suggest that higher temperature biochar possess superior aromatic stabilization and long-term persistence, which are advantageous for adsorption processes and soil amendment applications (Deshmukh et al., 2023). These findings indicate that temperature is the most dominant factor shaping proximate properties, in agreement with ANOVA and surface plot analyses. For applications requiring high fixed carbon, enhanced stability, and alkaline surface chemistry, biochar produced at 500 °C and higher heating rates (e.g., T2, T4, T6, T8) are more suitable for direct activation. Conversely, when maximizing yield is the primary aim, lower-temperature chars (T1, T3, T5, T7) are more favorable, albeit less carbonized.

3.3.5.3 pH of PKS-biochar

The pH demonstrated a clear dependence on carbonization. Biochar obtained at 300 °C were slightly acidic to near-neutral (5.9 - 6.8), attributed to retained acidic surface functional groups and volatile organics (Janu et al., 2021). In contrast, 500 °C pyrolysis produced alkaline chars (7.6-8.3), resulting from the accumulation of alkali and alkaline earth metals in the ash fraction and the progressive loss of oxygenated acidic groups (Fidel et al., 2017). The remaining samples carbonized at ~ 400 °C (T9 - T15) had near-neutral to mildly alkaline pH (7.0-7.7), representing an intermediate state of carbonization. Thus, pH evolution reflects the transition from oxygen-rich, acidic chars at low temperature to alkaline, mineral-rich chars at higher temperature.

3.3.5.4 Densities of PKS-biochar

The bulk (577-717 g/L) and compact densities (583-724 g/L) were also affected by carbonization intensity. The densest char was obtained from T1 (300 °C, bulk 717 g/L), consistent with the high volatile fraction retained within the structure. As carbonization intensified, bulk density generally decreased, reaching a minimum in T4 (577 g/L) and T15 (586 g/L). This reduction can be attributed to structural rearrangements, pore formation, and mass loss induced by devolatilization (Brewer et al., 2014). Lower density biochar tends to

exhibit improved textural characteristics, including greater specific surface area, at the expense of yield (Walters et al., 2018).

3.3.5.5 PKS-Akt (proximate composition)

The volatile matter content of the PKS-Akt samples exhibits contrasting trends depending on the temperature and residence time. At a residence time of 60 min, volatile matter slightly increases from 2.57 wt% to 3.01 wt% as the temperature rises from 800 to 900°C. However, at a longer residence time of 120 minutes, volatile matter decreases from 5.01 wt% to 4.08 wt% over the temperature range of 800 to 850°C, followed by a further decline to 1.95 wt% at 900°C. This progressive reduction in volatile content at elevated temperature and prolonged holding time is indicative of more complete gasification, resulting in enhanced removal of volatiles and a more thermally stable carbonaceous matrix.

The observed initial increase in volatile matter at shorter residence time may be attributed to the diffusion and retention of water molecules or partially decomposed volatile compounds within the carbon structure, which can temporarily enhance porosity and stability. This phenomenon aligns with findings from some authors (Ogungbenro et al., 2018), who reported that increased temperature facilitates the evolution of volatile compounds and tar deposits during biochar activation, temporarily affecting measured volatile content.

Significantly, the volatile matter content decreases substantially from the original PKS material to the final activated precursor. For example, the reduction from approximately 20 wt% volatile matter in the original PKS-OP1 (shown in Figure 3.6) to around 2 wt% in the activated material highlights the development of enhanced porosity and greater thermal stability in the activated carbon.

Similarly, the ash content exhibits a moderate increase with rising activation temperature, increasing from approximately 2.85 wt% in the carbonized material to nearly 5 wt% in the activated carbon. This increase is likely due to the concentration of inorganic constituents within the material as organics volatilize and burn off during activation (Lesaoana et al., 2019). The fixed carbon content of all activated carbon samples exceeds 90 wt%, demonstrating the formation of a strong carbon matrix with high carbon content and superior adsorption potential. Figure 3.6 11 illustrates these trends clearly that the increase in fixed carbon and ash content, coupled with the decrease in volatile matter, when comparing PKS-Akt samples (PKS-Akt 274 to 281) against the original PKS precursor (PKS-OP1).

It is important to note that these properties suggest that the PKS-Akt materials produced exhibit excellent performance attributes for environmental remediation, such as gas cleaning, tar adsorption as well as application in wastewater treatment. This is consistent with experimental results reported by Frilund based on these properties where activated carbons effectively removed acidic gases, including H_2S, from syngas streams and enhance hydrogen production (Frilund et al., 2023).

3.3.5.6 PKS-Akt iodine number and carbon conversion (effects of temperature and holding time)

The characterization of the PKS-activated carbon (PKS-Akt – temperature variation) shown in Table 3.7 demonstrates significant trends in physiochemical properties relevant for catalytic application via different absorption medium. The results show that there is a linear correlation between carbon conversion (X_c) and iodine numbers. This means that as the X_c increases the iodine number increases due to enhanced micropore formation and increased surface area of the material. This also correlates with rising activation temperature and holding time. The iodine number of PKS-Akt 274 (800℃) is 582 mg/g at a lower X_c (15.33) for 60 min. At the same holding time, the iodine number of PKS-Akt 275 (704 mg/g) increase by more than 20% when the temperature increases, 850℃. This remains vividly clear for all the materials at increasing X_c. The highest seen is PKS-Akt 281 with X_c = 70.86 wt% which displayed iodine number of 970 mg/g (Figure 3.7. 12).

3.3.5.7 Selection of optimum PKS-Akt

The selection of the optimum PKS-Akt precursor was based on a comprehensive evaluation of key parameters including biochar yield, iodine number, fixed carbon content, ash content, and activation temperature, all of which critically influence its performance potential for hydrogen production and catalytic applications.

The iodine number, a widely accepted indicator of micropore volume (pores < 2 nm), generally increases with activation temperature due to enhanced development of surface area and porosity. However, empirical evidence from PKS-Akt samples demonstrates that excessively high activation temperatures, particularly near or above 900°C (e.g., PKS-Akt 281), can lead to micropore widening or pore wall burn-off. This phenomenon causes a reduction in micropore volume, often converting micropores into mesopores, thereby adversely affecting the specific surface area relevant to adsorption and catalytic function (Roncancio & Gore, 2021). These transformations also correlate with significant yield reductions, driven by gasification reactions:

$C + H_2O \rightarrow CO + H_2$ and

$C + CO_2 \rightarrow 2CO$ thereby promoting carbon burn-off and mass loss.

Examining the dataset, PKS-Akt 281, produced at approximately 900°C with 120 min residence time, exhibited the highest iodine number (970 mg/g) indicative of well-developed porosity, and a fixed carbon content of 92.6 wt%. However, this sample registered the lowest yield (~48 wt%), reflecting the trade-off of enhanced pore development against substantial material consumption through carbon burn-off.

Equally, PKS-Akt 274, activated at a lower temperature (800°C) with 60 minutes residence time, demonstrated the highest yield (~70 wt%) but the lowest iodine number (582 mg/g), indicating a less developed microporous structure and, potentially, reduced adsorption capacity. Notably, PKS-Akt 280, activated at an intermediate temperature (850 °C) and intermediate residence time, achieved a balanced performance profile with a substantial yield (~57 wt%) and

a high iodine number (885 mg/g). This suggests optimal micropore development without excessive pore widening or burn-off, resulting in enhanced thermal stability and surface area preservation. From an economic and practical perspective, maintaining higher yields is crucial for process viability, as excessive burn-off at higher temperatures increases raw material consumption and operational costs. Moreover, the slightly lower iodine number of PKS-Akt 280 relative to PKS-Akt 281 implies more controlled pore growth, which may reduce sintering and catalyst deactivation risks during gasification and catalytic reactions (Ochoa et al., 2018). The higher pH (~10.1) and fixed carbon content (~90.3 wt%) of PKS-Akt 280 further support its chemical stability and adsorption capacity. Industrial-scale activated carbon production typically occurs between 700–1100 °C with activation times ranging from 30 to 120 minutes (Skoczko et al., 2024; Zhao et al., 2023). Within this context, PKS-Akt 280's activation conditions are commercially relevant and energy-efficient, offering a pragmatic balance between enhanced porosity and yield preservation. Therefore, considering both physicochemical properties and process economics, PKS-Akt 280 is identified as the optimum precursor for hydrogen production via catalytic gasification. It offers adequate microporosity for adsorption and catalytic activity while maintaining economically viable yield and structural stability under operational conditions.

3.3.5.7.1 Comparison analysis of PKS-Akt 280 with lignocellulosic feedstocks (iodine analysis)

Table 3.9 provides a comprehensive comparison of the activation conditions and physicochemical properties of activated carbon derived from a range of agricultural waste feedstocks, with particular focus on the iodine number as an indicator of micropore surface area and adsorption capacity. This analysis underscores the inherent variability in performance outcomes that are driven by differences in precursor material, activation parameters, and process conditions.

Table 3.9: Comparative analysis of iodine from data found in literature with this current study

Feedstocks	Tempera-ture (°C)	Time (min)	Iodine n° (mg/g)	Yield (%)	Reference
Coconut shell	800	60	821	26.3	(P. Kumar et al., 2022)
Cotton gin trash (CGT)	700	45	429	35.0	(Hernandez et al., 2007)
Rubber seed shell	880	60	1326	30.5	(Sun & Jiang, 2010)
Apricot stone	800	240	1057	9.4	(Şentorun-Shalaby et al., 2006)
Date stones	800	60	814	-	(Akila et al., 2019)
Palm oil shell	759	120	620	19.66	(Vitidsant et al., 1999)
Eupatorium adenophorum	950	60	1031	25	(Zheng et al., 2014)

Palm kernel shell (PKS)	850	120	885	56.73	This study

Notably, the rubber seed shell demonstrated an exceptionally high iodine number of 1326 mg/g at elevated activation temperatures (~880°C), highlighting its potential for applications demanding high surface area materials. Conversely, in this study, PKS-based activated carbon (PKS-Akt 280), achieved under optimized conditions (850°C, 120min), exhibited a commendable iodine number of 885 mg/g while maintaining a significant process yield of approximately 56.7%. This balance indicates not only the material's high micropore development but also a favorable compromise between surface area enhancement and process efficiency. The significance of this finding cannot be overstated: while some feedstocks like rubber seed shell can produce materials with superior adsorption capacity, their process yields tend to be lower, and the activation conditions are often more energy intensive. PKS, by contrast, is an abundant, low-cost, and readily available agricultural residue. The ability to produce a high-quality, high-yield activated carbon at relatively moderate activation temperatures (850°C) positions PKS-Akt 280 as a commercially viable and sustainable alternative for applications such as tar removal, catalyst support, and gas purification within bioenergy systems. Furthermore, this comparative analysis highlights the importance of process optimization specifically, the calibration of activation temperature and time, to balance micropore development and material yield. Activation at excessively high temperatures (~900°C and above) tends to favor pore widening or burn-off, which can reduce micropore volume and adversely impact adsorption capacity. In addition, the observed physicochemical properties such as high fixed carbon content, alkaline pH, and low volatile matter are consistent with enhanced sorption properties and stability, further supporting its suitability for catalytic applications. The superior performance of PKS-Akt 280 in this context demonstrates its potential as a cost-effective and sustainable precursor for activated carbon in advanced bioenergy and catalytic processes. Possibly, this comparative analysis validates the position of PKS-derived activated carbon, particularly PKS-Akt 280, as a promising candidate for scalable production. Its favorable combination of high iodine number, process efficiency, and physicochemical robustness aligns well with industrial requirements, underscoring the importance of activation parameters to optimize material properties for targeted applications in biomass gasification.

3.3.5.8 Study of PKS-OP1 as catalyst for biomass gasification

This PKS-OP1 (Table 3.6) biochar exhibits characteristics that influence its potential catalytic performance in biomass gasification. The relatively high fixed carbon content (77.12 wt%) indicates a carbon-rich material with a significant fraction of carbon remaining after volatile compounds are released during pyrolysis. Such high fixed carbon is interesting in catalytic applications as it provides a stable carbon matrix for active sites and enhances carbon conversion efficiency during gasification, providing a longer catalyst lifetime during

gasification. For instance, the carbon itself can participate in the reactions ($C + H_2O \rightarrow CO + H_2$) which is crucial for in-situ catalyst regeneration and thermal activity (Zhang et al., 2023). The low ash content (2.87 wt%) is advantageous since excessive ash can lead to fouling, slagging, and reduced catalyst performance by coating active sites (Lin et al., 2022). Ash components can also alter catalytic pathways, notwithstanding, the low ash content suggests minimum negative impact on catalyst activity and durability, supporting stability and durability (Puri et al., 2024). Furthermore, the volatile matter content of 20.01 wt% is relatively low, indicating effective devolatilization during pyrolysis and a stable char structure (Foong et al., 2020). This reduces reactivity loss due to volatile release during catalytic gasification. Additionally, the neutral pH (7.9) supports less corrosive behavior and compatibility within normal gasification environments.

The density of approximately 566 g/L denotes a moderately dense biochar, which can influence the packing and flow dynamics when used as catalyst in fixed-bed or fluidized-bed gasifiers (Pfeifer et al., 2004). Moreover, the iodine number value of 155 mg/g reflects the adsorptive quality and microporous surface area of the biochar. Although lower than highly PKS-activated carbons (above 500 mg/g), this moderate value suggests the PKS-OP1 biochar has considerable microporosity important for enabling gas-solid interactions and enhancing adsorption of tar and other organics during gasification (Yang et al., 2023). Improved tar reforming and cracking efficiency have been correlated with higher surface area and iodine number in biochar catalysts (Yang et al., 2023). The PKS-OP1 physicochemical properties highlight its potential as a catalyst or catalyst support in biomass gasification processes. However, compared to physically activated biochar (PKS-Akt) with higher iodine numbers and engineered porosity, PKS-OP1 may offer moderate catalytic performance. Its catalytic efficiency could be enhanced further by activation or doping with transition metals, as seen in this study and some studies with Ni-doped biochar showing superior syngas and hydrogen yields (Marques et al., 2023).

In summary, PKS-OP1 biochar is promising as a biomass gasification catalyst based on its physicochemical properties, particularly for tar reforming applications and syngas quality improvement. Additional modifications or activation could further elevate its catalytic effectiveness and durability in industrial-scale gasification.

Comparison with Traditional Catalysts

An investigation comparing PKS-OP1, a biochar-based catalyst, to traditional catalysts for thermochemical hydrogen production reveals emerging advantages and challenges associated with biochar utilization in the field of catalysis. Traditional catalysts, such as nickel, platinum, and other metal-based materials, are well-established for their high catalytic activity in processes like SMR, biogas reforming, and WGS reactions (Akhtar et al., 2025). However, their drawbacks include high cost, susceptibility to sintering and poisoning, and limited sustainability (Akhtar et al., 2025; Niu et al., 2023). On the other hand, PKS-OP1 biochar as a catalyst leverages its high fixed carbon content and moderate surface area to facilitate catalytic activity

primarily by providing adsorption sites for tar and gas-phase molecules, thereby aiding tar cracking and reforming. It offers sustainability advantages due to its renewable origin and low production cost derived from palm kernel shells. The low ash content in PKS-OP1 reduces catalyst fouling, contributing to longevity and stability during operation.

3.3.5.9 Study of PKS-Akt as catalyst for biomass gasification

The properties of the PKS-Akt 280, as described in the presented data, suggest its promising potential as a catalyst or catalyst support for biomass gasification processes. The elevated iodine numbers (885 mg/g) indicate a highly developed porous structure and substantial surface area, which are essential for catalytic activity. This high surface area facilitates effective contact with reactions intermediates (Figueiredo et al., 2025), promotes tar cracking (Han et al., 2008), and enhances catalytic conversion efficiencies during gasification (Pérez et al., 2014).

The low volatile matter (~ 4 wt%) and high fixed carbon percentage (~ 90 wt%) in PKS-Akt 280 sample further strengthen its thermal stability and durability at elevated temperatures typical of gasification processes. Additionally, the presence of mineral constituents such as Ca, K potentially stemming from the biomass source (Afrane et al., 2008) and retained during activation as seen through its high ash content (5.24 wt%), can act as natural catalysts or promoters, aiding in key reactions such as hydrocarbon reforming and tar decomposition (Ravenni et al., 2018). The high pH (10.1) of the PKS-Akt 280 implies a predominantly basic surface, which can be advantageous in catalyzing conversion reactions involving acidic components and in reducing tar formation.

Moreover, the high density and favorable physical characteristics suggest that PKS-Akt 280 can withstand the high operational conditions of gasification reactors without significant degradation which is a common problem due to pollutants (Olivier et al., 2025). Its porous structure, combined with chemical stability, offers an active platform for catalytic reactions, possibly reducing the need for external catalysts and lowering operational costs.

Comparison with Traditional Catalysts

Compared to traditional catalysts such as nickel-based or alkali metal catalysts commonly used in biomass gasification (Chaiprasert et al., 2009), PKS-Akt 280 exhibits a comparable surface area and microporosity, as evidenced by its high iodine numbers (up to 885 mg/g), which facilitate increased active sites for catalytic reactions (Reinoso-Rodriguez, 2013). Additionally, its natural mineral content and high fixed carbon content contribute to intrinsic catalytic activity and thermal stability, potentially reducing the reliance on external catalytic agents. Unlike traditional metal-based catalysts (Fe and Ni) prone to sintering and deactivation at high temperatures (Liu et al., 2023), PKS-Akt 280 offers enhanced durability and resistance to deactivation due to its carbonaceous and mineral-rich structure. Therefore, PKS-Akt 280 not only matches the catalytic efficiency of conventional catalysts but also provides a cost-effective,

sustainable, and thermally stable alternative for biomass gasification processes, enabling effective tar cracking and syngas enhancement without extensive catalyst regeneration.
Notwithstanding, comparative analysis with dolomite which is a cost effective catalyst and interesting for tar cracking, suffers from mechanical degradation and attrition, requiring frequent replenishment (Varjani, 2022). Though Nickel-based catalysts slightly outperformed activated carbon in catalytic gasification, in terms of syngas yield but their high cost and susceptibility to sulfur poisoning restrict large-scale application (Guil-Lopez et al., 2011). The PKS-Akt 280 produced in this study not only economically viable but also a cost-effective material from biomass residue which aligns with circular economic principles (Tibor & Grande, 2022). Although experimental validation remains essential to this study, the physicochemical features of PKS-Akt 280 support the hypothesis that it could serve effectively as a catalyst or catalyst support in biomass gasification. Its intrinsic properties may enhance gas yields, improve syngas purity, and facilitate tar reduction, contributing to more efficient and cleaner biomass conversion processes.

3.4 Conclusion

The results demonstrate that pyrolysis process conditions particularly temperature have significant influence on PKS-biochar yield and quality. Lower pyrolysis temperatures (300°C) result in higher biochar yields and greater volatile retention, whereas higher temperatures (500°C) lead to lower yields but yield more carbonized and stable materials with higher fixed carbon content. The ANOVA and Pareto analyses robustly confirm the statistical significance of temperature on yield, with heating rate exerting a secondary, lesser effect and residence time having no significant influence. Steam activation at elevated temperatures (800-900°C) further modifies material properties, enhancing microporosity indicative of increased iodine numbers but reducing yield due to progressive devolatilization and carbon burn-off. The optimum activated carbon (PKS-Akt 280; 850°C, 120min) was identified as achieving a favorable balance of high yield (~57 wt%), substantial micropore capacity (iodine number 885mg/g), and strong fixed carbon content (90.3 wt%), making it a robust precursor for catalytic hydrogen production. Further, the materials demonstrated high pH and low volatile content, supporting their use in environmental remediation, such as gas cleaning and water treatment.

Conclusion and perspective

This study demonstrated the successful conversion of PKS into high quality biochar and a highly microporous activated carbon through a two-stage optimization process for catalytic applications. The first stage employed a BBD to optimize pyrolysis conditions, revealing that temperature and heating rate were the most critical factors in producing high-quality biochar. Comprehensive experimental design and characterization allowed clear identification of the optimal process parameters that balance economic yield and physicochemical quality, pivotal for large-scale applications. Subsequent steam activation significantly enhanced the physicochemical properties, transforming the biochar into optimized PKS-activated carbon exhibiting high microporosity, rich fixed carbon content, and favorable surface chemistry (alkaline pH, low ash and volatile matter), properties that are essential for tar reduction, syngas upgrading, and contaminant adsorption in catalytic biomass gasification or steam reforming systems. Importantly, the work demonstrates that with suitable pre-treatment and process control, PKS, an abundant agricultural residue, can be transformed into a high-performance catalyst or catalyst support without reliance on expensive or hazardous chemicals. This contributes directly to the circular economy and valorization of agricultural residues, reinforcing the sustainability of hydrogen production pathways.

Perspectives and Future Work:

Future work should focus on:

I. Scaling up the process to pilot and industrial reactors to validate operational robustness and catalyst recyclability under real-world conditions.

II. Investigating the effect of PKS-activated carbon modification, such as metallic impregnation on catalytic activity, hydrogen yield, and tar removal.

III. Co-activation of PKS-biochar with other soft biomass material (e.g., wood sawdust) to generate hybrid activated carbon with enhanced porosity and adsorption/catalytic properties.

IV. Capturing and depositing volatile compounds generated during PKS pyrolysis onto PKS-activated carbon to enhance its surface functionality, pore structure, and catalytic activity.

V. Performing comprehensive techno-economic analysis and life cycle assessment to benchmark PKS-derived catalysts against commercial alternatives.

VI. Exploring the synergy of PKS-derived catalyst with other biomass feedstocks to extend the range of bioenergy applications.

VII. Examining long-term catalyst stability, sintering resistance, and regeneration strategies during repeated gasification cycles.

VIII. Testing experimentally to validate the catalytic efficiency of PKS-Akt 280 in a bench-scale or pilot-scale gasification unit. Testing its performance in terms of tar cracking efficiency, hydrogen yield.

In conclusion, the work establishes palm kernel shell as a valuable feedstock for high-quality biochar/activated carbon catalyst production and signals a promising avenue for further research and deployment within green hydrogen technologies and sustainable bioenergy systems.

References

Abioye, K. J., Harun, N. Y., Sufian, S., Yusuf, M., Jagaba, A. H., Ekeoma, B. C., Kamyab, H., Sikiru, S., Waqas, S., & Ibrahim, H. (2024). A review of biomass ash related problems: Mechanism, solution, and outlook. *Journal of the Energy Institute*, *112*(October 2023), 101490. https://doi.org/10.1016/j.joei.2023.101490

Adhikari, S., Timms, W., & Mahmud, M. A. P. (2022). Optimising water holding capacity and hydrophobicity of biochar for soil amendment – A review. *Science of the Total Environment*, *851*(July), 158043. https://doi.org/10.1016/j.scitotenv.2022.158043

Afrane, G., & Achaw, O. W. (2008). Effect of the concentration of inherent mineral elements on the adsorption capacity of coconut shell-based activated carbons. *Bioresource Technology*, *99*(14), 6678–6682. https://doi.org/10.1016/j.biortech.2007.11.071

Ahiekpor, J. C., Mensah, I., Bensah, E. C., Narra, S., Amponsem, B., & Antwi, E. (2023). Modeling the behavior of Celtis mildbraedii sawdust and polyethylene terephthalate co-pyrolysis for syngas production. *Scientific African*, *19*(December), e01450. https://doi.org/10.1016/j.sciaf.2022.e01450

Akhtar, M. S., Naseem, M. T., Ali, S., & Zaman, W. (2025). Metal-Based Catalysts in Biomass Transformation: From Plant Feedstocks to Renewable Fuels and Chemicals. *Catalysts*, *15*(1). https://doi.org/10.3390/catal15010040

Akila, E., Pugalendhi, S., Subramanian, P., Duraisamy, M. R., & Surendrakumar, A. (2019). Production and characterization of activated carbon from date stones by single step steam activation. *Environment and Ecology*, *37*(October 2018), 194–197. https://www.cabdirect.org/cabdirect/abstract/20193125725

Akpasi, S. O. (2016). Biochar Development as a Catalyst and Its Application. *Intech*, *11*(tourism), 13. https://www.intechopen.com/books/advanced-biometric-technologies/liveness-detection-in-biometrics

Amalina, F., Razak, A. S. A., Krishnan, S., Sulaiman, H., Zularisam, A. W., & Nasrullah, M. (2022). Biochar production techniques utilizing biomass waste-derived materials and environmental applications – A review. *Journal of Hazardous Materials Advances*, *7*(June), 100134. https://doi.org/10.1016/j.hazadv.2022.100134

Aman, A. M. N., Selvarajoo, A., Laua, T. L., & Chen, W. H. (2024). Comparison of Optimized Production of Palm Oil Waste Biochar with Response Surface Methodology for Cement Replacement Application. *E3S Web of Conferences*, *589*, 1–12. https://doi.org/10.1051/e3sconf/202458903007

Ammar, M., Mutalib, M. I. A., Yusup, S., Inayat, A., Shahbaz, M., & Ali, B. (2016). Influence of Effective Parameters on Product Gas Ratios in Sorption Enhanced Gasification. *Procedia Engineering*, *148*, 735–741. https://doi.org/10.1016/j.proeng.2016.06.605

ASTM D4607-94. (2006). *Determination of Iodine number*.

Babatunde, E. O., Enomah, S., Akwenuke, O. M., Ibeh, M. A., Okwelum, C. O., Mundu, M.

M., Adepoju, P. O., Aki, A. O., Oghenejabor, O. D., Adepoju, T. F., Ifedora, C. O., & Mabel, K. (2025). Preparation and characterization of Palm Kernel Shell (PKS) based biocatalyst for the transformation of kernel oil to biodiesel. *South African Journal of Chemical Engineering*, *52*(February), 200–210. https://doi.org/10.1016/j.sajce.2025.02.008

Baffour-Awuah, E., Akinlabi, S. A., Jen, T. C., Hassan, S., Okokpujie, I. P., & Ishola, F. (2021). Characteristics of Palm Kernel Shell and Palm Kernel Shell-Polymer Composites: A Review. *IOP Conference Series: Materials Science and Engineering*, *1107*(1), 012090. https://doi.org/10.1088/1757-899x/1107/1/012090

Bahari, M. B., Mamat, C. R., Jalil, A. A., Siang, T. J., Hassan, N. S., Khusnun, N. F., Nabgan, W., Roslan, N. A., Abidin, S. Z., Setiabudi, H. D., & Vo, D. V. N. (2022). Cobalt-based catalysts for hydrogen production by thermochemical valorization of glycerol: a review. *Environmental Chemistry Letters*, *20*(4), 2361–2384. https://doi.org/10.1007/s10311-022-01423-y

Balat, M. (2008). Mechanisms of Thermochemical Biomass Conversion Processes. Part 1: Reactions of Pyrolysis. *Energy Sources Part A-Recovery Utilization and Environmental Effects*, *30*, 620–635. https://doi.org/10.1080/15567030600817258

Biedermann, F., & Obernberger, I. (2005). Ash-related Problems during Biomass Combustion and Possibilities for a Sustainable Ash Utilisation Friedrich Biedermann. *Proceeddings of the Internacional Conference "World Renewable Energy Congress" (WREC)*, *x*, 8. www.bios-bioenergy.at

Bitter, J. H. (2023). Dark material with a bright future: Carbon as support in future heterogeneous catalysis – A short personal perspective. *Catalysis Today*, *423*(January), 114015. https://doi.org/10.1016/j.cattod.2023.01.022

Boonsombuti, A., Phinichkha, N., Supansomboon, S., & Luengnaruemitchai, A. (2023). The use of lignin from palm kernel shell (PKS) to fabricate oil palm mesocarp fiber (OPMF) particleboards. *International Journal of Adhesion and Adhesives*, *125*(July 2022), 103425. https://doi.org/10.1016/j.ijadhadh.2023.103425

Brewer, C. E., Chuang, V. J., Masiello, C. A., Gonnermann, H., Gao, X., Dugan, B., Driver, L. E., Panzacchi, P., Zygourakis, K., & Davies, C. A. (2014). New approaches to measuring biochar density and porosity. *Biomass and Bioenergy*, *66*, 176–185. https://doi.org/10.1016/j.biombioe.2014.03.059

Britovsek, G. (2012). Homogeneous Catalysts. Activity—Stability—Deactivation. By Piet W. N. M. van Leeuwen and John C. Chadwick. *Angewandte Chemie International Edition*, *51*. https://doi.org/10.1002/anie.201108293

Cai, N., Zhang, H., Nie, J., Deng, Y., & Baeyens, J. (2020). Biochar from Biomass Slow Pyrolysis. *IOP Conference Series: Earth and Environmental Science*, *586*(1). https://doi.org/10.1088/1755-1315/586/1/012001

Cao, X., Sun, S., & Sun, R. (2017). Application of biochar-based catalysts in biomass

upgrading: A review. *RSC Advances*, *7*(77), 48793–48805. https://doi.org/10.1039/c7ra09307a

Çapa, T., Bahç, B., & Abdeljelil, B. Ben. (2023). *Assessment of Homogeneous and Heterogeneous Catalysts in Transesterification Reaction : A Mini Review*. *4*, 412–422. https://doi.org/10.1002/cben.202200021

Carrere, R. (2013). Oil palm in Africa: past, present, and future scenarios. *World Rainforest Movement*, *15*, 79. http://wrm.org.uy/wp-content/uploads/2014/08/Oil_Palm_in_Africa_2013.pdf

Chaiprasert, P., & Vitidsant, T. (2009). Effects of promoters on biomass gasification using nickel/dolomite catalyst. *Korean Journal of Chemical Engineering*, *26*(6), 1545–1549. https://doi.org/10.1007/s11814-009-0259-7

Chang, C. F., Chang, C. Y., & Tsai, W. T. (2000). Effects of burn-off and activation temperature on preparation of activated carbon from corn cob agrowaste by CO2 and steam. *Journal of Colloid and Interface Science*, *232*(1), 45–49. https://doi.org/10.1006/jcis.2000.7171

Chatterjee, R., Sajjadi, B., Chen, W. Y., Mattern, D. L., Hammer, N., Raman, V., & Dorris, A. (2020). Effect of Pyrolysis Temperature on PhysicoChemical Properties and Acoustic-Based Amination of Biochar for Efficient CO2 Adsorption. *Frontiers in Energy Research*, *8*(May), 1–18. https://doi.org/10.3389/fenrg.2020.00085

Chaudhary, M. L., Al-Fatesh, A. S., Kumar, R., Lanre, M. S., Frusteri, F., AlReshaidan, S. B., Ibrahim, A. A., Abasaeed, A. E., & Fakeeha, A. H. (2022). Promotional effect of addition of ceria over yttria-zirconia supported Ni based catalyst system for hydrogen production through dry reforming of methane. *International Journal of Hydrogen Energy*, *47*(48), 20838–20850. https://doi.org/10.1016/j.ijhydene.2022.04.199

Chen, B. (2020). *Pyrolytic biochar stability assessed by chemical accelerating aging method SCHOOL OF INDUSTRIAL ENGINEERING AND MANAGEMENT*.

Chen, D., Cen, K., Zhuang, X., Gan, Z., Zhou, J., Zhang, Y., & Zhang, H. (2022). Insight into biomass pyrolysis mechanism based on cellulose, hemicellulose, and lignin: Evolution of volatiles and kinetics, elucidation of reaction pathways, and characterization of gas, biochar and bio-oil. *Combustion and Flame*, *242*. https://doi.org/10.1016/j.combustflame.2022.112142

Chen, J., Zhou, J., Zheng, W., Leng, S., Ai, Z., Zhang, W., Yang, Z., Yang, J., Xu, Z., Cao, J., Zhang, M., Leng, L., & Li, H. (2024). A complete review on the oxygen-containing functional groups of biochar: Formation mechanisms, detection methods, engineering, and applications. *Science of the Total Environment*, *946*(March), 174081. https://doi.org/10.1016/j.scitotenv.2024.174081

Chen, T., Peng, Y., Qiu, M., Yi, C., & Xu, Z. (2023). Heterogenization of homogeneous catalysts in polymer nanoparticles : From easier recovery and reuse to more efficient catalysis. *Coordination Chemistry Reviews*, *489*(May), 215195. https://doi.org/10.1016/j.ccr.2023.215195

Chen, W., Huang, M., Chang, J., & Chen, C. (2015). Torrefaction operation and optimization of microalga residue for energy densification and utilization. *Applied Energy*, *154*, 622–630. https://doi.org/10.1016/j.apenergy.2015.05.068

Cheng, F., & Li, X. (2018). Preparation and application of biochar-based catalysts for biofuel production. *Catalysts*, *8*(9), 1–35. https://doi.org/10.3390/catal8090346

Cheng, X., Lei, A., Mei, T., Xu, H., Xu, K., & Zeng, C. (2022). *Recent Applications of Homogeneous Catalysis in Electrochemical Organic Synthesis*. 1120–1152. https://doi.org/10.31635/ccschem.021.202101451

Chiaramonti, D., Prussi, M., Nistri, R., Pettorali, M., & Rizzo, A. M. (2014). Biomass carbonization: Process options and economics for small scale forestry farms. *Energy Procedia*, *61*(June 2015), 1515–1518. https://doi.org/10.1016/j.egypro.2014.12.159

Choi, Y. J., Choi, J. Bin, Im, J. S., & Kim, J. H. (2023). Effect of Porosity in Activated Carbon Supports for Silicon-Based Lithium-Ion Batteries (LIBs). *ACS Omega*, *8*(22), 19772–19780. https://doi.org/10.1021/acsomega.3c01506

Ciftci, A., Ligthart, D., & Hensen, E. (2014). Aqueous phase reforming of glycerol over Re-promoted Pt and Rh catalysts. *Green Chem.*, *16*. https://doi.org/10.1039/C3GC42046A

Cole-Hamilton, D. (2003). Homogeneous Catalysis--New Approaches to Catalyst Separation, Recovery, and Recycling. *Science (New York, N.Y.)*, *299*, 1702–1706. https://doi.org/10.1126/science.1081881

Conceicao, K. (2024). *Journal of Chemical Engineering & Catalytic Strategies for Environmental Remediation and Pollution Control*. *15*(1000496), 1–2. https://doi.org/10.35248/2157-7048.25.16.531

Crabtree, R. (2014). ChemInform Abstract: Deactivation in Homogeneous Transition Metal Catalysis: Causes, Avoidance, and Cure. *Chemical Reviews*, *115*. https://doi.org/10.1021/cr5004375

Crabtree, R. H. (2005). *CHEMISTRY OF THE TRANSITION METALS THE ORGANOMETALLIC CHEMISTRY OF THE*.

D. Phadtare, P., & R. Kalbande, S. (2022). Biochar Production Technologies from Agricultural Waste, Its Utilization in Agriculture and Current Global Biochar Market: A Comprehensive Review. *International Journal of Environment and Climate Change*, *August*, 1010–1031. https://doi.org/10.9734/ijecc/2022/v12i1131078

D2652-11, A. (2015). *Determination of Bulk Density*.

Daabo, A. M., Saeed, L. I., Altamer, M. H., Fadhil, A. B., & Badawy, T. (2022). The production of bio-based fuels and carbon catalysts from chicken waste. *Renewable Energy*, *201*(P1), 21–34. https://doi.org/10.1016/j.renene.2022.10.088

Debbache, H., Amor, A. A., Amor, F. Z. A., Khiari, R., Moussaoui, Y., Belfar, M. L., Moussaoui, Y., & Zerrouki, H. (2024). a Comprehensive Analysis of the Use of Chemical Activation Technology To Produce Activated Carbon From Agricultural Residues. *Cellulose Chemistry and Technology*, *58*(9–10), 1149–1161.

https://doi.org/10.35812/CelluloseChemTechnol.2024.58.98

Debe, M. K. (2012). Electrocatalyst approaches and challenges for automotive fuel cells. *Nature*, *486*(7401), 43–51. https://doi.org/10.1038/nature11115

Della, N., & Mohallem, S. (2011). *Automotive Catalysts : Performance , Characterization and Development*. *January*. https://doi.org/10.5772/13303

Demirel, E., Erkey, C., & Ayas, N. (2021). The Journal of Supercritical Fluids Supercritical water gasification of fruit pulp for hydrogen production : Effect of reaction parameters. *The Journal of Supercritical Fluids*, *177*(January), 105329. https://doi.org/10.1016/j.supflu.2021.105329

Deshmukh, A., & Deshmukh, K. (2023). *Biochar: A Sustainable Approach for Enhancing Soil Fertility*. *December*, 1–16.

Devi, L., Ptasinski, K. J., & Janssen, F. J. J. G. (2003). A review of the primary measures for tar elimination in biomass gasification processes. *Biomass and Bioenergy*, *24*(2), 125–140. https://doi.org/https://doi.org/10.1016/S0961-9534(02)00102-2

Diallo, I., Thiam, A., Diop, B., Mbow, B., & Fofana, M. (2025). *Brief Review on the Evolution of Catalysis in Chemistry*. *15*(2), 25–42. https://doi.org/10.5923/j.chemistry.20251502.01

Dong, A., Li, Z., Ma, Y., Liao, W., Zhao, F., Zhang, X., & Gao, H. (2025). Recent Advances in Non-Noble Metal Electrocatalysts for Hydrogen Evolution Reaction in Water Splitting. *Nanomaterials*, *15*(14), 1–35. https://doi.org/10.3390/nano15141106

Dong, W., Xing, J., Huang, Y., Wu, M., Yi, P., Pan, B., & Xing, B. (2024). Hydrogen bonds between the oxygen-containing functional groups of biochar and organic contaminants significantly enhance sorption affinity. *Chemical Engineering Journal*, *499*, 156654. https://doi.org/10.1016/j.cej.2024.156654

Dong, X., Chu, Y., Tong, Z., Sun, M., Meng, D., Yi, X., Gao, T., Wang, M., & Duan, J. (2024). Mechanisms of adsorption and functionalization of biochar for pesticides: A review. *Ecotoxicology and Environmental Safety*, *272*(40), 116019. https://doi.org/10.1016/j.ecoenv.2024.116019

Drobíková, K., Martynková, G. S., Dvořáček, J., Seidlerová, J., Tomášek, V., & Matějka, V. (2012). Characterization of carbon prepared from crop-plant. *NANOCON 2012 - Conference Proceedings, 4th International Conference*, 757–762.

Faris, L. N., & Mustafa, B. I. N. (2023). *Catalytic co-pyrolysis of palm kernel shell and polypropylene*. *January*.

Fidel, R. B., Laird, D. A., Thompson, M. L., & Lawrinenko, M. (2017). Characterization and quantification of biochar alkalinity. *Chemosphere*, *167*, 367–373. https://doi.org/10.1016/j.chemosphere.2016.09.151

Foong, S. Y., Abdul Latiff, N. S., Liew, R. K., Yek, P. N. Y., & Lam, S. S. (2020). Production of biochar for potential catalytic and energy applications via microwave vacuum pyrolysis conversion of cassava stem. *Materials Science for Energy Technologies*, *3*, 728–733. https://doi.org/10.1016/j.mset.2020.08.002

Fornasiero, P. (2021). *and Chemicals*. *2019*, 5915–5951.

Frainetti, A. J., & Klinghoffer, N. B. (2024). Engineering biochar-supported nickel catalysts for efficient CO2 methanation. *Biomass and Bioenergy*, *184*(March), 107179. https://doi.org/10.1016/j.biombioe.2024.107179

Franz, R., Pinto, D., Uslamin, E., Urakawa, A., & Pidko, E. (2021). Impact of Promoter Addition on the Regeneration of Ni/Al2O3 Dry Reforming Catalysts. *ChemCatChem*, *13*. https://doi.org/10.1002/cctc.202101080

Frilund, C., Kurkela, E., & Hiltunen, I. (2023). Development of a simplified gas ultracleaning process: experiments in biomass residue-based fixed-bed gasification syngas. *Biomass Conversion and Biorefinery*, *13*(17), 15673–15684. https://doi.org/10.1007/s13399-021-01680-x

Fu, J., Zhang, J., Jin, C., Wang, Z., Wang, T., Cheng, X., & Ma, C. (2020). Effects of temperature, oxygen and steam on pore structure characteristics of coconut husk activated carbon powders prepared by one-step rapid pyrolysis activation process. *Bioresource Technology*, *310*(April), 123413. https://doi.org/10.1016/j.biortech.2020.123413

Gross, E., Shu, X.-Z., Alayoglu, S., Bechtel, H. A., Martin, M. C., Toste, F. D., & Somorjai, G. A. (2014). In Situ IR and X-ray High Spatial-Resolution Microspectroscopy Measurements of Multistep Organic Transformation in Flow Microreactor Catalyzed by Au Nanoclusters. *Journal of the American Chemical Society*, *136*(9), 3624–3629. https://doi.org/10.1021/ja412740p

Gui, X., Xu, X., Zhang, Z., Hu, L., Huang, W., Zhao, L., & Cao, X. (2025). Biochar-amended soil can further sorb atmospheric CO2 for more carbon sequestration. *Communications Earth and Environment*, *6*(1). https://doi.org/10.1038/s43247-024-01985-5

Guil-Lopez, R., Botas, J. A., Fierro, J. L. G., & Serrano, D. P. (2011). Comparison of metal and carbon catalysts for hydrogen production by methane decomposition. *Applied Catalysis A: General*, *396*(1–2), 40–51. https://doi.org/10.1016/j.apcata.2011.01.036

Han, J., & Kim, H. (2008). The reduction and control technology of tar during biomass gasification/pyrolysis: An overview. *Renewable and Sustainable Energy Reviews*, *12*(2), 397–416. https://doi.org/10.1016/j.rser.2006.07.015

Haryati, Z., Loh, S. K., Kong, S. H., & Bachmann, R. T. (2018). Pilot scale biochar production from palm kernel shell (PKS) in a fixed bed allothermal reactor. *Journal of Oil Palm Research*, *30*(3), 485–494. https://doi.org/10.21894/jopr.2018.0043

Helena, P., & Sanchez, B. (2014). *NICKEL BASED CATALYSTS FOR HYDROGEN PRODUCTION FROM THE PYROLYSIS / GASIFICATION OF REFUSE DERIVED FUEL (RDF) By*. *June*.

Hernandez, J. R., Aquino, F. L., & Capareda, S. C. (2007). Activated carbon production from pyrolysis and steam activation of cotton gin trash. *2007 ASABE Annual International Meeting, Technical Papers*, *12 BOOK*(07). https://doi.org/10.13031/2013.23322

Hosseini, S. E., Wahid, M. A., & Ganjehkaviri, A. (2015). An overview of renewable hydrogen

production from thermochemical process of oil palm solid waste in Malaysia. *Energy Conversion and Management*, *94*, 415–429. https://doi.org/10.1016/j.enconman.2015.02.012

Hrbek, J., Pfeifer, C., Barisano, D., Vreugdenhil, B., Lundgren, J., Rauch, R., Koroveshi, X., & Catizzone, E. (2021). *Gasification Applications in Existing Infrastructures for Production of Sustainable Value-Added Products*. *December*, 1–34.

Huang, K., Chang, M., Zhang, J., Luo, Z., Zhang, Y., Zhao, K., Wang, W., & Chen, D. (2023). Exploring the Impact of Ni Doping on Bagasse Biochar and Its Efficient Hydrogen Production via Assisted Water Electrolysis. *Energy Technology*, *11*. https://doi.org/10.1002/ente.202201450

Huber, G. W., Iborra, S., & Corma, A. (2006). Synthesis of Transportation Fuels from Biomass: Chemistry, Catalysts, and Engineering. *Chemical Reviews*, *106*(9), 4044–4098. https://doi.org/10.1021/cr068360d

Hussain, M., Zabiri, H., Uddin, F., Yusup, S., & Tufa, L. D. (2023). Pilot-scale biomass gasification system for hydrogen production from palm kernel shell (part A): steady-state simulation. *Biomass Conversion and Biorefinery*, *13*(5), 3849–3862. https://doi.org/10.1007/s13399-021-01474-1

Hutchings, G. (2001). Promotion in Heterogeneous Catalysis: A Topic Requiring a New Approach? *Catalysis Letters*, *75*, 1–12. https://doi.org/10.1023/A:1016784122682

Ilić, M., Haegel, F. H., Lolić, A., Nedić, Z., Tosti, T., Ignjatović, I. S., Linden, A., Jablonowski, N. D., & Hartmann, H. (2022). Surface functional groups and degree of carbonization of selected chars from different processes and feedstock. In *PLoS ONE* (Vol. 17, Issue 11 November). https://doi.org/10.1371/journal.pone.0277365

Iwuozor, K. O., Emenike, E. C., Omonayin, E. O., Bamigbola, J. O., Ojo, H. T., Awoyale, A. A., Eletta, O. A. A., & Adeniyi, A. G. (2023). Unlocking the hidden value of pods: A review of thermochemical conversion processes for biochar production. *Bioresource Technology Reports*, *22*(March), 101488. https://doi.org/10.1016/j.biteb.2023.101488

Jafri, Y., Waldheim, L., & Lundgren, J. (2020). Emerging Gasification Technologies for Waste & Biomass. In *IEA Bioenergy* (Issue December).

Jagadale, M., Sarangi, P. K., Jose, N., Ray, D. P., Jadhav, M., Shrivastava, P., T, N. K., Debnath, S., & Shakyawar, D. B. (2025). A comprehensive review on biochar catalyst for advancement of pyrolytic conversion of biomass into valuable biofuels. *Journal of the Taiwan Institute of Chemical Engineers*, *April*, 106232. https://doi.org/10.1016/j.jtice.2025.106232

Janu, R., Mrlik, V., Ribitsch, D., Hofman, J., Sedláček, P., Bielská, L., & Soja, G. (2021). Biochar surface functional groups as affected by biomass feedstock, biochar composition and pyrolysis temperature. *Carbon Resources Conversion*, *4*(November 2020), 36–46. https://doi.org/10.1016/j.crcon.2021.01.003

Kakaei, K., Esrafili, M. D., & Ehsani, A. (2019). Introduction to Catalysis. *Interface Science*

and Technology, *27*, 1–21. https://doi.org/10.1016/B978-0-12-814523-4.00001-0

Kalivodová, M., Baláš, M., Milčák, P., Lisá, H., Lisý, M., Lachman, J., Kracík, P., Križan, P., & Vejražka, K. (2022). the Determination of Higher Heating Value By Calculation Based on Elemental Analysis. *Paliva*, *14*(1), 8–20. https://doi.org/10.35933/paliva.2022.01.02

Karume, I., Bbumba, S., Tewolde, S., Mukasa, I. Z. T., & Ntale, M. (2023). Impact of carbonization conditions and adsorbate nature on the performance of activated carbon in water treatment. *BMC Chemistry*, *17*(1), 1–12. https://doi.org/10.1186/s13065-023-01091-1

King, D. L., Zhang, L., Xia, G., Karim, A. M., Heldebrant, D. J., Wang, X., Peterson, T., & Wang, Y. (2010). Aqueous phase reforming of glycerol for hydrogen production over Pt–Re supported on carbon. *Applied Catalysis B: Environmental*, *99*(1), 206–213. https://doi.org/https://doi.org/10.1016/j.apcatb.2010.06.021

Köhler, T., Pursche, F., Burscheidt, P., Seide, G., & Gries, T. (2017). Optimization of process parameters during carbonization for improved carbon fibre strength. *IOP Conference Series: Materials Science and Engineering*, *254*(4). https://doi.org/10.1088/1757-899X/254/4/042018

Kok, M. V., & Ozgur, E. (2017). Characterization of lignocellulose biomass and model compounds by thermogravimetry. *Energy Sources, Part A: Recovery, Utilization and Environmental Effects*, *39*(2), 134–139. https://doi.org/10.1080/15567036.2016.1214643

Kong, S. H., Chin, C. Y. J., Yek, P. N. Y., Wong, C. C., Wong, C. S., Cheong, K. Y., Liew, R. K., & Lam, S. S. (2022). Removal of heavy metals using activated carbon from microwave steam activation of palm kernel shell. *Environmental Advances*, *9*(July), 100272. https://doi.org/10.1016/j.envadv.2022.100272

Kong, S. H., Loh, S. K., Bachmann, R. T., Zainal, H., & Cheong, K. Y. (2019). Palm kernel shell biochar production, characteristics and carbon sequestration potential. *Journal of Oil Palm Research*, *31*(3), 508–520. https://doi.org/10.21894/jopr.2019.0041

Kongto, P., Palamanit, A., Pattiya, A., Promsampao, N., Sonsupap, S., Phusunti, N., Theapparat, Y., Chanakaewsomboon, I., & Tippayawong, N. (2024). Yields and characteristics of bio-oil and biochar from fast pyrolysis and co-pyrolysis of oil palm biomass using innovative twin screw reactor for bio-circular-green economy approach. *Biomass Conversion and Biorefinery*, *0123456789*. https://doi.org/10.1007/s13399-024-06460-x

Koppejan, J., Cremers, M., & Gl, D. (2019). *Biomass pre-treatment for bioenergy Policy report*.

Kostić, M. D., Bazargan, A., Stamenković, O. S., Veljković, V. B., & McKay, G. (2016). Optimization and kinetics of sunflower oil methanolysis catalyzed by calcium oxide-based catalyst derived from palm kernel shell biochar. *Fuel*, *163*, 304–313. https://doi.org/10.1016/j.fuel.2015.09.042

Kpelou, P., Sodoga, K., Kongnine, D. M., & Napo, K. (2018). Evaluation of Some Combustion Characteristics of Biochar produced from Coconut Husks, Corn Cobs and Palm Kernel

Shells. *Article in International Journal of Innovation and Applied Studies*, *24*(3), 1124–1130. http://www.ijias.issr-journals.org/

Kumar, A., Daw, P., & Milstein, D. (2022). *Homogeneous Catalysis for Sustainable Energy : Hydrogen and Methanol Economies , Fuels from Biomass , and Related Topics*. https://doi.org/10.1021/acs.chemrev.1c00412

Kumar, N., Aepuru, R., Lee, S.-Y., & Park, S.-J. (2025). Advances in Catalysts for Hydrogen Production: A Comprehensive Review of Materials and Mechanisms. *Nanomaterials*, *15*, 256. https://doi.org/10.3390/nano15040256

Kumar, P., Ramesh, P., & Karthikeyan, S. (2022). *Steam Activation of Coconut Husk for Porous Carbon Production: Effect of Temperature and Time on Pore Characteristics*.

Lakhtaria, P., Ribeirinha, P., Huhtinen, W., Sousa, J., Mendes, A., & Viik, S. (2023). *Hydrogen production via aqueous-phase reforming for high-temperature proton exchange membrane fuel cells - a review [version 3 ; peer review : 2 approved]*.

Lam, E., & Luong, J. H. T. (2014). Carbon Materials as Catalyst Supports and Catalysts in the Transformation of Biomass to Fuels and Chemicals. *ACS Catalysis*, *4*(10), 3393–3410. https://doi.org/10.1021/cs5008393

Lebendig, F., & Müller, M. (2022). Effect of pre-treatment of herbaceous feedstocks on behavior of inorganic constituents under chemical looping gasification (CLG) conditions. *Green Chemistry*, *24*(24), 9643–9658. https://doi.org/10.1039/d2gc02906e

Leng, L., Xiong, Q., Yang, L., Li, H., Zhou, Y., Zhang, W., Jiang, S., Li, H., & Huang, H. (2021). An overview on engineering the surface area and porosity of biochar. *Science of The Total Environment*, 144204. https://doi.org/10.1016/j.scitotenv.2020.144204

Lesaoana, M., Mlaba, R. P. V., Mtunzi, F. M., Klink, M. J., Edijike, P., & Pakade, V. E. (2019). Influence of inorganic acid modification on Cr(VI) adsorption performance and the physicochemical properties of activated carbon. *South African Journal of Chemical Engineering*, *28*(November 2018), 8–18. https://doi.org/10.1016/j.sajce.2019.01.001

Levin, O. V. (2023). Catalysts in Energy Applications. *Catalysts*, *13*(12). https://doi.org/10.3390/catal13121484

Li, G., Iakunkov, A., Boulanger, N., Lazar, O. A., Enachescu, M., Grimm, A., & Talyzin, A. V. (2023). Activated carbons with extremely high surface area produced from cones, bark and wood using the same procedure. *RSC Advances*, *13*(21), 14543–14553. https://doi.org/10.1039/d3ra00820g

Li, J., Xu, K., Yao, X., & Liu, J. (2024). Investigation of biomass slow pyrolysis mechanisms based on the generation trends in pyrolysis products. *Process Safety and Environmental Protection*, *183*(December 2023), 327–338. https://doi.org/10.1016/j.psep.2024.01.027

Li, S., & Skelly, S. (2023). Physicochemical properties and applications of biochars derived from municipal solid waste: A review. *Environmental Advances*, *13*(May), 100395. https://doi.org/10.1016/j.envadv.2023.100395

Lille-uccs, C., & Lille, C. (2022). *Heterogenization of homogenous catalysts using Covalent*

Organic Frameworks materials. *33*(0).

Lin, C., Zuo, W., Yuan, S., Zhao, P., & Zhou, H. (2023). EEffect of moisture on gasification of hydrochar derived from real-MSW. *Biomass and Bioenergy*, *178*(October), 106976. https://doi.org/10.1016/j.biombioe.2023.106976

Lin, F., Xu, M., Ramasamy, K., Li, Z., Klinger, J., Schaidle, J., & Wang, H. (2022). Catalyst Deactivation and Its Mitigation during Catalytic Conversions of Biomass. *ACS Catalysis*, *12*, 13555–13599. https://doi.org/10.1021/acscatal.2c02074

Liu, H., Ye, C., Ye, Z., Zhu, Z., Wang, Q., Tang, Y., Luo, G., Guo, W., Dong, C., Li, G., Xu, Y., & Wang, Q. (2023). Catalytic cracking and catalyst deactivation/regeneration characteristics of Fe-loaded biochar catalysts for tar model compound. *Fuel*, *334*(P2), 126810. https://doi.org/10.1016/j.fuel.2022.126810

Loviat, F., Czekaj, I., Wambach, J., & Wokaun, A. (2009). Nickel deposition on γ-Al 2O 3 model catalysts: An experimental and theoretical investigation. *Surface Science - SURFACE SCI*, *603*, 2210–2217. https://doi.org/10.1016/j.susc.2009.04.032

Lu, X., & Berge, N. (2014). Influence of feedstock chemical composition on product formation and characteristics derived from the hydrothermal carbonization of mixed feedstocks. *Bioresource Technology*, *166C*, 120–131. https://doi.org/10.1016/j.biortech.2014.05.015

Manfro, R. L., & Souza, M. M. V. M. (2023). Overview of Ni-Based Catalysts for Hydrogen Production from Biogas Reforming. *Catalysts*, *13*(9). https://doi.org/10.3390/catal13091296

Mariyam, S., Alherbawi, M., Pradhan, S., Al-Ansari, T., & McKay, G. (2024). Biochar yield prediction using response surface methodology: effect of fixed carbon and pyrolysis operating conditions. *Biomass Conversion and Biorefinery*, *14*(22), 28879–28892. https://doi.org/10.1007/s13399-023-03825-6

Marques, I. S., Jarrais, B., Ramos, R., Abdelkader-Fernandez, V. K., Yaremchenko, A., Freire, C., Fernandes, D. M., & Peixoto, A. F. (2023). Nitrogen-doped biochar-supported metal catalysts: High efficiency in both catalytic transfer hydrogenation of furfural and electrocatalytic oxygen reactions. *Catalysis Today*, *418*(December 2022). https://doi.org/10.1016/j.cattod.2023.114080

Marras, F. (2010). *Recovery and recycling of homogeneous catalysts: silica as temporary or permanent support*. 26.

McLaughlin, H., & Shields, F. (2012). *Analytical Options for Biochar Adsorption and Surface Area*. 43 ,□□□□ □□□□□.

Miguel, C., Cássia, A. De, Carneiro, O., Rocha, B., Gusmão, C., Freitas, L. De, Alves, M., Magalhães, D., Guimarães, A., & Lelis, W. (2018). Biomass torrefaction for energy purposes – De fi nitions and an overview of challenges and opportunities in Brazil. *Renewable and Sustainable Energy Reviews*, *82*(August 2017), 2426–2432. https://doi.org/10.1016/j.rser.2017.08.095

Minitab. (2025). *G Getting Started with Minitab Solution Center rted with Minitab Solution*.

Moccia, F., Rigamonti, L., Messori, A., & Zanotti, V. (2021). *Bringing Homogeneous Iron Catalysts on the Heterogeneous Side : Solutions for Immobilization*. 1–26.

Mohammad, Z., Moghaddam, A., & Mehdi, A. (2010). The influence of nickel loading on reducibility of NiO/Al2O3 catalysts synthesized by sol-gel method. *Chemical Engineering Research Bulletin*, *14*. https://doi.org/10.3329/cerb.v14i2.5052

Mohammed Saleh, A., Bahari Alias, A., Azil Bahari Alias, Hamdi Mahdi, H., H. Jawad, A., Shatir A. Syed-Hassan, S., Mohammed Saleh, N., & Khalil Ahmed, O. (2024). Characterizing Biochar Derived from Palm Kernel Shell Biomass via Slow Pyrolysis for Adsorption Applications. *NTU Journal of Renewable Energy*, *6*(1), 10–20. https://doi.org/10.56286/ntujre.v6i1.729

Mohd Hasan, M. H., Bachmann, R. T., Loh, S. K., Manroshan, S., & Ong, S. K. (2019). Effect of Pyrolysis Temperature and Time on Properties of Palm Kernel Shell-Based Biochar. *IOP Conference Series: Materials Science and Engineering*, *548*(1). https://doi.org/10.1088/1757-899X/548/1/012020

Moilanen, A., & Nasrullah, M. (2011). Gasification reactivity and ash sintering behaviour of biomass feedstocks. In *VTT Publications*. http://www.vtt.fi/inf/pdf/publications/2011/P769.pdf

Molina-Sabio, M., & Rodríguez-Reinoso, F. (2004). Role of chemical activation in the development of carbon porosity. *Colloids and Surfaces A: Physicochemical and Engineering Aspects*, *241*(1–3), 15–25. https://doi.org/10.1016/j.colsurfa.2004.04.007

Müller, B. R. (2021). Preparation and characterization of K2CO3-doped powdered activated carbon for effective in-vitro adsorption of deoxynivalenol. *Bioresource Technology Reports*, *15*(April), 100703. https://doi.org/10.1016/j.biteb.2021.100703

Muzyka, R., Misztal, E., Hrabak, J., Banks, S. W., & Sajdak, M. (2023). Various biomass pyrolysis conditions influence the porosity and pore size distribution of biochar. *Energy*, *263*(PE), 126128. https://doi.org/10.1016/j.energy.2022.126128

Nabila, R., Hidayat, W., Haryanto, A., Hasanudin, U., Iryani, D. A., Lee, S., Kim, S., Kim, S., Chun, D., Choi, H., Im, H., Lim, J., Kim, K., Jun, D., Moon, J., & Yoo, J. (2023). Oil palm biomass in Indonesia: Thermochemical upgrading and its utilization. *Renewable and Sustainable Energy Reviews*, *176*(June 2022), 113193. https://doi.org/10.1016/j.rser.2023.113193

Naji, S., & Tye, C. (2021). *Heterogeneous catalyst deactivation causes and mechanisms: Overview*.

Navarro, R. M., Peña, M. A., & Fierro, J. L. G. (2007). Hydrogen Production Reactions from Carbon Feedstocks: Fossil Fuels and Biomass. *Chemical Reviews*, *107*(10), 3952–3991. https://doi.org/10.1021/cr0501994

Neagu, D., Tsekouras, G., Miller, D. N., Ménard, H., & Irvine, J. T. S. (2013). In situ growth of nanoparticles through control of non-stoichiometry. *Nature Chemistry*, *5*(11), 916–923. https://doi.org/10.1038/nchem.1773

Niu, H., Wang, Q., Huang, C., Zhang, M., Yan, Y., Liu, T., & Zhou, W. (2023). Noble Metal-Based Heterogeneous Catalysts for Electrochemical Hydrogen Evolution Reaction. *Applied Sciences (Switzerland)*, *13*(4). https://doi.org/10.3390/app13042177

Niu, Y. hong, Chi, Z. yang, Li, M., Du, J. zheng, & Han, F. tao. (2024). Advancements in biomass gasification and catalytic tar-cracking technologies. *Materials Reports: Energy*, *4*(4), 100295. https://doi.org/10.1016/j.matre.2024.100295

Noor, N. M., Shariff, A., Abdullah, N., & Aziz, N. S. M. (2019). Temperature effect on biochar properties from slow pyrolysis of coconut flesh waste. *Malaysian Journal of Fundamental and Applied Sciences*, *15*(2), 153–158. https://doi.org/10.11113/mjfas.v15n2.1015

Nor, W., & Wan, N. (2015). *Design Of Experiment (DOE) Response Surface IF ??*

Nwachukwu, C. F. (2024). *A Review An Overview of Catalysts Application in Energy Conversion and Environmental Protection*. *October*.

Ochoa, A., Arregi, A., Amutio, M., Gayubo, A. G., Olazar, M., Bilbao, J., & Castaño, P. (2018). Coking and sintering progress of a Ni supported catalyst in the steam reforming of biomass pyrolysis volatiles. *Applied Catalysis B: Environmental*, *233*, 289–300. https://doi.org/10.1016/j.apcatb.2018.04.002

Ocsachoque, M., Bengoa, J., Gazzoli, D., & González, M. G. (2011). Role of CeO 2 in Rh/α-Al 2O 3 catalysts for CO 2 reforming of methane. *Catalysis Letters*, *141*(11), 1643–1650. https://doi.org/10.1007/s10562-011-0685-0

Ogungbenro, A. E., Quang, D. V., Al-Ali, K. A., Vega, L. F., & Abu-Zahra, M. R. M. (2018). Physical synthesis and characterization of activated carbon from date seeds for CO2 capture. *Journal of Environmental Chemical Engineering*, *6*(4), 4245–4252. https://doi.org/10.1016/j.jece.2018.06.030

Olivier, F., Schaefer, S., Maiga, K., Roulet, M., Laidin, I., Ania, C. O., & Cagnon, B. (2025). Understanding the role of pollutant confinement during the thermal regeneration of activated carbons. *Carbon*, *234*(October 2024), 120003. https://doi.org/10.1016/j.carbon.2025.120003

Ong, H. C., Chen, W. H., Farooq, A., Gan, Y. Y., Lee, K. T., & Ashokkumar, V. (2019). Catalytic thermochemical conversion of biomass for biofuel production: A comprehensive review. *Renewable and Sustainable Energy Reviews*, *113*(July), 109266. https://doi.org/10.1016/j.rser.2019.109266

Orang, N., & Tran, H. (2015). Effect of feedstock moisture content on biomass boiler operation. *Tappi Journal*, *14*, 629–637. https://doi.org/10.32964/TJ14.10.629

Ozdemir, I., Şahin, M., Orhan, R., & Erdem, M. (2014). Preparation and characterization of activated carbon from grape stalk by zinc chloride activation. *Fuel Processing Technology*, *125*, 200–206. https://doi.org/10.1016/j.fuproc.2014.04.002

Pastor-Pérez, L., Buitrago-Sierra, R., & Sepúlveda-Escribano, A. (2014). CeO2-promoted Ni/activated carbon catalysts for the water-gas shift (WGS) reaction. *International Journal of Hydrogen Energy*, *39*(31), 17589–17599.

https://doi.org/10.1016/j.ijhydene.2014.08.089

Pelkmans, A. L., Cowie, A., & Berndes, G. (2024). *The role of bioenergy in the energy transition , and implications on the global use of biomass*.

Pfeifer, C., Rauch, R., & Hofbauer, H. (2004). In-Bed Catalytic Tar Reduction in a Dual Fluidized Bed Biomass Steam Gasifier. *Industrial and Engineering Chemistry Research*, *43*(7), 1634–1640. https://doi.org/10.1021/ie030742b

Pinilla, J. L., Utrilla, R., Karn, R. K., Suelves, I., Lázaro, M. J., Moliner, R., García, A. B., & Rouzaud, J. N. (2011). High temperature iron-based catalysts for hydrogen and nanostructured carbon production by methane decomposition. *International Journal of Hydrogen Energy*, *36*(13), 7832–7843. https://doi.org/10.1016/j.ijhydene.2011.01.184

Pinkard, B. R., Gorman, D. J., Tiwari, K., & Rasmussen, E. G. (2019). Supercritical water gasi fi cation : practical design strategies and operational challenges for lab-scale , continuous fl ow reactors. *Heliyon*, *February*, e01269. https://doi.org/10.1016/j.heliyon.2019.e01269

Pranolo, S. H., Waluyo, J., Putro, F. A., Adnan, M. A., & Kibria, M. G. (2023). Gasification process of palm kernel shell to fuel gas: Pilot-scale experiment and life cycle analysis. *International Journal of Hydrogen Energy*, *48*(7), 2835–2848. https://doi.org/10.1016/j.ijhydene.2022.10.066

Preetha Devi, R., Kamaraj, S., Angeeswaran, R., & Pugalendhi, S. (2017). Tar and Particulate Removal Methods for the Producer Gas Obtained from Biomass Gasification. *International Journal of Current Microbiology and Applied Sciences*, *6*(10), 269–284. https://doi.org/10.20546/ijcmas.2017.610.034

Puri, L., Hu, Y., & Naterer, G. (2024). Critical review of the role of ash content and composition in biomass pyrolysis. *Frontiers in Fuels*, *2*(March), 1–19. https://doi.org/10.3389/ffuel.2024.1378361

Qureshi, K. M., Lup, A. N. K., Khan, S., Abnisa, F., & Daud, W. M. A. W. (2021). Effect of temperature and feed rate on pyrolysis oil produced via helical screw fluidized bed reactor. *Korean Journal of Chemical Engineering*, *38*(9), 1797–1809. https://doi.org/10.1007/s11814-021-0842-0

Rahayu, D. E., Nasarani, D., Hadi, W., & Wrjodirjo, B. (2018). Potential of biomass residues from oil palm agroindustry in Indonesia. *MATEC Web of Conferences*, *197*, 1–4. https://doi.org/10.1051/matecconf/201819713008

Rashid, T., Gnanasundaram, N., Appusamy, A., Kait, C. F., & Thanabalan, M. (2018). Enhanced lignin extraction from different species of oil palm biomass: Kinetics and optimization of extraction conditions. *Industrial Crops and Products*, *116*(August 2017), 122–136. https://doi.org/10.1016/j.indcrop.2018.02.056

Ravenni, G., Sárossy, Z., Ahrenfeldt, J., & Henriksen, U. B. (2018). Activity of chars and activated carbons for removal and decomposition of tar model compounds – A review. *Renewable and Sustainable Energy Reviews*, *94*, 1044–1056. https://doi.org/10.1016/j.rser.2018.07.001

Reinoso-Rodriguez, F. (2013). THE ROLE OF CARBON MATERIALS IN HETEROGENEOUS CATALYSIS* FRANCISCO. *2013 International Conference on Localization and GNSS, ICL-GNSS 2013*, *36*(3), 159–175. https://doi.org/10.1109/ICL-GNSS.2013.6577279

Rima, J., Assaker, K., Roques-carmes, T., Mouneimne, A. H., & El Ali, F. (2013). Developing a new carbonization process using high pressure and temperature to treat medical and municipality wastes for coal production. *Journal of Applied Sciences Research*, *9*(3), 1666–1674.

Rocha, R. P., & Figueiredo, J. L. (2025). Active Sites in Carbocatalysis: Tuning Their Activity. *Catalysts*, *15*(5). https://doi.org/10.3390/catal15050443

Roncancio, R., & Gore, J. P. (2021). CO2 char gasification: A systematic review from 2014 to 2020. *Energy Conversion and Management: X*, *10*(December 2020), 100060. https://doi.org/10.1016/j.ecmx.2020.100060

Rostamian, R., Heidarpour, M., Mousavi, S. F., & Afyuni, M. (2015). Characterization and sodium sorption capacity of biochar and activated carbon prepared from rice husk. *Journal of Agricultural Science and Technology*, *17*(4), 1057–1069.

Roychowdhury, S., Mukthar Ali, M., Dhua, S., Sundararajan, T., & Ranga Rao, G. (2021). Thermochemical hydrogen production using Rh/CeO2/γ-Al2O3 catalyst by steam reforming of ethanol and water splitting in a packed bed reactor. *International Journal of Hydrogen Energy*, *46*(37), 19254–19269. https://doi.org/https://doi.org/10.1016/j.ijhydene.2021.03.079

Rubinsin, N. J., Karim, N. A., Timmiati, S. N., Lim, K. L., Isahak, W. N. R. W., & Pudukudy, M. (2024). An overview of the enhanced biomass gasification for hydrogen production. *International Journal of Hydrogen Energy*, *49*, 1139–1164. https://doi.org/10.1016/j.ijhydene.2023.09.043

Ruocco, C., Palma, V., Cortese, M., & Martino, M. (2020). *Noble Metals-Based Catalysts for Hydrogen Production via Bioethanol Reforming in a Fluidized Bed Reactor*. 1. https://doi.org/10.3390/eccs2020-07543

Sabitha, M., Pavithran, R., C. V, S., R. S., A., & Prasad K, A. (2025). Effect of Degassing Temperature on the Specific Surface Area of Some Metal Chelates. *Oriental Journal Of Chemistry*, *41*(3), 831–838. https://doi.org/10.13005/ojc/410315

Sadeghbeigi, R. (2020). *Fluid catalytic cracking handbook an expert guide to the practical operation, design, and optimization of FCC units* (4th ed.). Kidlington. http://lib.ugent.be/catalog/ebk01:4100000011049682

Sajjadi, B., Chen, W. Y., & Egiebor, N. O. (2019). A comprehensive review on physical activation of biochar for energy and environmental applications. *Reviews in Chemical Engineering*, *35*(6), 735–776. https://doi.org/10.1515/revce-2017-0113

Sakhiya, A. K., Anand, A., & Kaushal, P. (2020). Production, activation, and applications of biochar in recent times. In *Biochar* (Vol. 2, Issue 3). Springer Singapore.

https://doi.org/10.1007/s42773-020-00047-1

Sakhiya, A. K., Baghel, P., Pathak, S., Vijay, V. K., & Kaushal, P. (2020). Effect of Process Parameters on Slow Pyrolysis of Rice Straw: Product Yield and Energy Analysis. *Proceedings of the 2020 International Conference and Utility Exhibition on Energy, Environment and Climate Change, ICUE 2020*, *January*. https://doi.org/10.1109/ICUE49301.2020.9306945

Saleh, Mohammed; Ali, B., & Alias, A. (2024). Characterizing Biochar Derived from Palm Kernel Shell Biomass via Slow Pyrolysis for Adsorption Applications. *NTU Journal of Renewable Energy*, *6*(1), 10–20. https://doi.org/10.56286/ntujre.v6i1.729

Salehi, E., Abedi, J., & Harding, T. (2009). Bio-oil from sawdust: Pyrolysis of sawdust in a fixed-bed system. *Energy and Fuels*, *23*(7), 3767–3772. https://doi.org/10.1021/ef900112b

Santamaria, L., Lopez, G., Fernandez, E., Cortazar, M., Arregi, A., & Olazar, M. (2021). *Progress on Catalyst Development for the Steam Reforming of Biomass and Waste Plastics Pyrolysis Volatiles : A Review*. https://doi.org/10.1021/acs.energyfuels.1c01666

Santana Maldonado, C., Weir, A., & Rumbeiha, W. K. (2023). A comprehensive review of treatments for hydrogen sulfide poisoning: past, present, and future. *Toxicology Mechanisms and Methods*, *33*(3), 183–196. https://doi.org/10.1080/15376516.2022.2121192

Schure, J., Pinta, F., Cerutti, P. O., & Kasereka-Muvatsi, L. (2019). Efficiency of charcoal production in sub-Saharan Africa: Solutions beyond the kiln. *Bois et Forets Des Tropiques*, *340*, 57–70. https://doi.org/10.19182/bft2019.340.a31691

Şentorun-Shalaby, Ç., Uçak-Astarlioğlu, M. G., Artok, L., & Sarici, Ç. (2006). Preparation and characterization of activated carbons by one-step steam pyrolysis/activation from apricot stones. *Microporous and Mesoporous Materials*, *88*(1–3), 126–134. https://doi.org/10.1016/j.micromeso.2005.09.003

Serra, V., Saracco, G., Badini, C., & Specchia, V. (1997). Combustion of carbonaceous materials by CuKV based catalysts: II. Reaction mechanism. *Applied Catalysis B: Environmental*, *11*(3), 329–346. https://doi.org/https://doi.org/10.1016/S0926-3373(96)00054-9

Setiawan, N. M., Sella Stephanie, Aziz, A. N., & Berliana Yusfinda. (2025). Recycling Palm Shell Waste into Biochar Using Biomass-Based Pyrolysis Method for Sustainable Energy Transition: A Review. *Journal of Clean Technology*, *2*(2), 61–75. https://doi.org/10.15294/joct.v2i2.28865

Shahcheragh, S. K., Bagheri Mohagheghi, M. M., & Shirpay, A. (2023). Effect of physical and chemical activation methods on the structure, optical absorbance, band gap and urbach energy of porous activated carbon. *SN Applied Sciences*, *5*(12). https://doi.org/10.1007/s42452-023-05559-6

Shakir, M. A., Ahmad, M. I., Mansur, F. Z., & Abdul Khalil, H. P. S. (2024). Biomass to

biofuel: Palm kernel shells as catalyst supports for enhanced biodiesel production. *Biofuels, Bioproducts and Biorefining*, *18*(6), 2038–2052. https://doi.org/10.1002/bbb.2683

Sharma, T., Hakeem, I. G., Gupta, A. B., Joshi, J., Shah, K., Vuppaladadiyam, A. K., & Sharma, A. (2024). Parametric influence of process conditions on thermochemical techniques for biochar production: A state-of-the-art review. *Journal of the Energy Institute*, *113*(August 2023), 101559. https://doi.org/10.1016/j.joei.2024.101559

Shen, W., Zheng, J. T., Zhang, Y. L., Wang, J., & Qin, Z. F. (2003). The effect of pore structure of activated carbon on the adsorption of Congo red and vitamin B12. *Studies in Surface Science and Catalysis*, *146*, 779–782. https://doi.org/10.1016/S0167-2991(03)80499-8

Shen, Y., & Fu, Y. (2018). Advances in: In situ and ex situ tar reforming with biochar catalysts for clean energy production. *Sustainable Energy and Fuels*, *2*(2), 326–344. https://doi.org/10.1039/c7se00553a

Shyam, S., Ahmed, S., Joshi, S. J., & Sarma, H. (2025). Biochar as a Soil amendment: implications for soil health, carbon sequestration, and climate resilience. *Discover Soil*, *2*(1). https://doi.org/10.1007/s44378-025-00041-8

Siakavelas, G. I., Charisiou, N. D., AlKhoori, S., AlKhoori, A. A., Sebastian, V., Hinder, S. J., Baker, M. A., Yentekakis, I. V., Polychronopoulou, K., & Goula, M. A. (2021). Highly selective and stable nickel catalysts supported on ceria promoted with Sm2O3, Pr2O3 and MgO for the CO2 methanation reaction. *Applied Catalysis B: Environmental*, *282*(July 2020), 119562. https://doi.org/10.1016/j.apcatb.2020.119562

Skoczko, I., Szatyłowicz, E., Tabor, A., & Gumiński, R. (2024). Manufacturing Options for Activated Carbons with Selected Synthetic Polymers as Binders. *Materials*, *17*(8). https://doi.org/10.3390/ma17081753

Sopandi, T. P., Sulianto, A. A., Anugroho, F., Yusoff, M. Z. M., Mohamed, M. S., Farid, M. A. A., & Setyawan, H. Y. (2025). RSM-optimized biochar production from young coconut waste (Cocos nucifera): Multivariate analysis of non-linear interactions between temperature, time, and activator concentration. *Industrial Crops and Products*, *223*(October 2024), 120157. https://doi.org/10.1016/j.indcrop.2024.120157

Su, Z., Guan, J., Liu, Y., Shi, D., Wu, Q., Chen, K., Zhang, Y., & Li, H. (2024). Research progress of ruthenium-based catalysts for hydrogen production from ammonia decomposition. *International Journal of Hydrogen Energy*, *51*, 1019–1043. https://doi.org/https://doi.org/10.1016/j.ijhydene.2023.09.107

Sun, K., & Jiang, J. chun. (2010). Preparation and characterization of activated carbon from rubber-seed shell by physical activation with steam. *Biomass and Bioenergy*, *34*(4), 539–544. https://doi.org/10.1016/j.biombioe.2009.12.020

Sutton, D., Kelleher, B., & Ross, J. (2001). Review of Literature on Catalysts for Biomass Gasification. *Fuel Processing Technology*, *73*, 155–173. https://doi.org/10.1016/S0378-3820(01)00208-9

Szablowski, L., Wojcik, M., & Dybinski, O. (2025). Review of steam methane reforming as a method of hydrogen production. *Energy*, *316*(April 2024), 134540. https://doi.org/10.1016/j.energy.2025.134540

Szpisják-Gulyás, N., Al-Tayawi, A. N., Horváth, Z. H., László, Z., Kertész, S., & Hodúr, C. (2023). Methods for experimental design, central composite design and the Box–Behnken design, to optimise operational parameters: A review. *Acta Alimentaria*, *52*(4), 521–537. https://doi.org/10.1556/066.2023.00235

Tibor, S. T., & Grande, C. A. (2022). Industrial production of activated carbon using circular bioeconomy principles: Case study from a Romanian company. *Cleaner Engineering and Technology*, *7*(January), 100443. https://doi.org/10.1016/j.clet.2022.100443

Uchegbulam, I., Momoh, E. O., & Agan, S. A. (2022). Potentials of palm kernel shell derivatives: a critical review on waste recovery for environmental sustainability. *Cleaner Materials*, *6*(July), 100154. https://doi.org/10.1016/j.clema.2022.100154

van Leeuwen, P. W. N. M. (2003). *Catalysis, Homogeneous* (R. A. B. T.-E. of P. S. and T. (Third E. Meyers (ed.); pp. 457–490). Academic Press. https://doi.org/https://doi.org/10.1016/B0-12-227410-5/00085-5

Varjani, S. (2022). Efficient removal of tar employing dolomite catalyst in gasification: Challenges and opportunities. *Science of the Total Environment*, *836*(February). https://doi.org/10.1016/j.scitotenv.2022.155721

Vassilev, S. V., Baxter, D., Andersen, L. K., & Vassileva, C. G. (2013). An overview of the composition and application of biomass ash. Part 1. Phase-mineral and chemical composition and classification. *Fuel*, *105*, 40–76. https://doi.org/10.1016/j.fuel.2012.09.041

Venezia, V., Pota, G., Silvestri, B., Costantini, A., Vitiello, G., & Luciani, G. (2022). Tailoring Structure: Current Design Strategies and Emerging Trends to Hierarchical Catalysts. In *Catalysts* (Vol. 12, Issue 10). https://doi.org/10.3390/catal12101152

Vitidsant, T., Suravattanasakul, T., & Damronglerd, S. (1999). Production of Activated Carbon from Palm-oil Shell by Pyrolysis and Steam Activation in a Fixed Bed Reactor. *ScienceAsia*, *25*(4), 211–222. https://doi.org/10.2306/scienceasia1513-1874.1999.25.211

Walters, R. D., & White, J. G. (2018). Biochar in situ decreased bulk density and improved soil-water relations and indicators in southeastern US coastal plain Ultisols. *Soil Science*, *183*(3), 99–111. https://doi.org/10.1097/SS.0000000000000235

Wang, Q., Zhang, X., Cui, D., Sun, S., Wang, Z., Wang, Y., Xu, F., Wang, Z., & Zhang, J. (2023). Effect of pressure on the pyrolysis and gasification mechanism of corn stovers from kinetics. *Journal of Analytical and Applied Pyrolysis*, *176*(October), 106267. https://doi.org/10.1016/j.jaap.2023.106267

Wang, Y., & Wu, J. J. (2023). Thermochemical conversion of biomass: Potential future prospects. *Renewable and Sustainable Energy Reviews*, *187*(September), 113754. https://doi.org/10.1016/j.rser.2023.113754

Wang, Z., Belli, J., & Jensen, C. (2011). Homogeneous dehydrogenation of liquid organic hydrogen carriers catalyzed by an iridium PCP complex. *Faraday Discussions*, *151*, 297–305; discussion 385. https://doi.org/10.1039/C1FD00002K

Wei, Z., Colin, F., Jens, K., & Thomas, F. (2017). *Combining theory and experiment in electrocatalysis : Insights into materials design Combining Theory and Experiment in Electrocatalysis : Insights into Materials Design*. https://doi.org/10.1126/science.aad4998

Wu, J., Yan, Y., Zhang, L., Qin, Z., & Tao, S. (2019). Enhanced Mass Transfer and Improved Catalyst Recovery in a Stirred Reactor by Polymeric Ionic Liquids Modified 3D Printed Devices. In *Advanced Materials Technologies* (Vol. 4, Issue 2). https://doi.org/10.1002/admt.201800515

Yalçin, N., & Sevinç, V. (2000). Studies of the surface area and porosity of activated carbons prepared from rice husks. *Carbon*, *38*(14), 1943–1945. https://doi.org/10.1016/S0008-6223(00)00029-4

Yang, H., Cui, Y., Jin, Y., Lu, X., Han, T., Sandström, L., Jönsson, P. G., & Yang, W. (2023). Evaluation of Engineered Biochar-Based Catalysts for Syngas Production in a Biomass Pyrolysis and Catalytic Reforming Process. *Energy and Fuels*, *37*(8), 5942–5952. https://doi.org/10.1021/acs.energyfuels.3c00410

Yao, D., Hu, Q., Wang, D., Yang, H., Wu, C., Wang, X., & Chen, H. (2016). Hydrogen production from biomass gasification using biochar as a catalyst/support. *Bioresource Technology*, *216*, 159–164. https://doi.org/10.1016/j.biortech.2016.05.011

Yeboah, M. L., Li, X., & Zhou, S. (2020). Facile fabrication of biochar from palm kernel shell waste and its novel application to magnesium-based materials for hydrogen storage. *Materials*, *13*(3). https://doi.org/10.3390/ma13030625

Yuliusman, & Afifah, T. M. (2021). Production of palm shell based activated carbon by two stage phosphoric acid impregnation and physical activation. *IOP Conference Series: Materials Science and Engineering*, *1173*(1), 012019. https://doi.org/10.1088/1757-899x/1173/1/012019

Zeng, K. (2015). *Parametric study and process optimization for solar pyrolysis of beech wood*.

Zhang, M., Zhu, H., Xi, B., Tian, Y., Sun, X., Zhang, H., & Wu, B. (2022). Surface Hydrophobic Modification of Biochar by Silane Coupling Agent KH-570. *Processes*, *10*(2). https://doi.org/10.3390/pr10020301

Zhang, S., Wang, L., Zhang, Y., Cao, F., Sun, Q., Ren, X., & Wennersten, R. (2022). Effect of hydroxyl functional groups on SO2adsorption by activated carbon. *Journal of Environmental Chemical Engineering*, *10*(6), 108727. https://doi.org/10.1016/j.jece.2022.108727

Zhang, Y., Pan, J., Gong, G., Song, R., Yuan, Y., Li, M., Hu, W., Fan, P., Yuan, L., & Wang, L. (2023). In Situ Surface Reconstruction of Catalysts for Enhanced Hydrogen Evolution. *Catalysts*, *13*(1). https://doi.org/10.3390/catal13010120

Zhao, C., Ge, L., Li, X., Zuo, M., Xu, C., Chen, S., Li, Q., Wang, Y., & Xu, C. (2023). Effects

of the carbonization temperature and intermediate cooling mode on the properties of coal-based activated carbon. *Energy*, *273*(December 2022). https://doi.org/10.1016/j.energy.2023.127177

Zhao, Y., Tian, C., Chen, H., Zhai, Y., Li, X., Li, J., Zhang, R., Mao, Y., Shan, T., Zheng, K., & Dai, P. (2025). Carbon-supported nickel–molybdenum alloy/tungsten carbide nanoparticles as efficient bifunctional catalysts for hydrogen evolution and oxidation reactions in alkaline media. *International Journal of Hydrogen Energy*, *114*, 229–238. https://doi.org/https://doi.org/10.1016/j.ijhydene.2025.03.019

Zheng, Z., Xia, H., Srinivasakannan, C., Peng, J., & Zhang, L. (2014). Steam activation of Eupatorium adenophorum for the production of porous carbon and hydrogen rich fuel gas. *Journal of Analytical and Applied Pyrolysis*, *110*(1), 113–121. https://doi.org/10.1016/j.jaap.2014.08.007

Zhu, H., Babkoor, M., Coppens, M. O., & Materazzi, M. (2025). Thermochemical technologies for conversion of biomass and waste into light olefins (C2-C4). *Fuel Processing Technology*, *267*(July 2024), 108174. https://doi.org/10.1016/j.fuproc.2024.108174

Zulkania, A., Hanum, G. F., & Sri Rezki, A. (2018). The potential of activated carbon derived from bio-char waste of bio-oil pyrolysis as adsorbent. *MATEC Web of Conferences*, *154*, 1–6. https://doi.org/10.1051/matecconf/201815401029

Zulkornain, M. F., Shamsuddin, A. H., Normanbhay, S., Md Saad, J., Zhang, Y. S., Samsuri, S., & Wan Ab Karim Ghani, W. A. (2021). Microwave-assisted Hydrothermal Carbonization for Solid Biofuel Application: A Brief Review. *Carbon Capture Science and Technology*, *1*(October), 100014. https://doi.org/10.1016/j.ccst.2021.100014

Appendix

Table A: Rate of water consumption during activation

Sample	Duration (h)	Amount of H_2O (ml)	H_2O in bottle (g)	Rate of H_2O consumption (g/g/h)
PKS-Akt 274	1	180.1	115.91	0.321
PKS-Akt 275	1	180.1	102.19	0.390
PKS-Akt 278	1	180.1	85.41	0.473
PKS-Akt 279	2	360. 2	251.33	0.272
PKS-Akt 280	2	360.1	231.33	0.322
PKS-Akt 281	2	360.1	218.15	0.310

Table B: Yield of PKS-activated carbon

Sample	Duration (min)	Yield (%)
PKS-Akt 274	60	70.15
PKS-Akt 275	60	67.93
PKS-Akt 278	60	61.08
PKS-Akt 279	120	61.59
PKS-Akt 280	120	56.73
PKS-Akt 281	120	48.54

Picture 1

Researcher at AdFIS Product GmbH, Teterow - Germany. Right to left: Dipl.-Ing. Stifft - Managing Director; Dr. Miersch - Head R&D; Whuling, III - Researcher; & Dr. Nakagawa - R&D

Picture 2 (a)

(a) Pretreatment (Washing of PKS with deionized water)

(b) PKS undergoing pyrolysis with visible tar and volatile in reactor wall

(c) A carbonized sample in quartz tube

(d) Stored carbonized samples in air-tight bottles

(e) Measurement of bulk and compact densities using a mass balance

(f) Measurement of compact density using a Jolting Volumeter STAV II

Picture 2 (b)

(a) Researcher: feeding of biochar in rotary kiln for direct activation (steam activation)
(b) Sample undergoing steam activation in a horizontal tube furnace (Xerion)
(c) PKS-activated carbon
(d) Powdered samples for further analysis

Picture 3

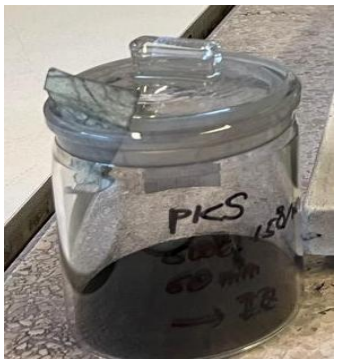

Step 1 : Powdered PKS-activated

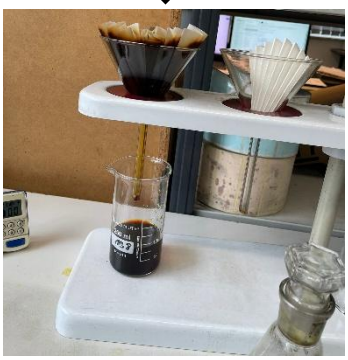

Step 2 : Filtered aliquote part of iodine solution

Step 3 : Titration with $Na_2S_2O_3$ using starch as indicator

Step 4 : Colorless solution

Flow diagram for determining iodine number